Technische Universität München

Fakultät für Medizin

Exploring the role of telomerase and adipose tissue serine racemase in modulating obesity and metabolic homeostasis

Ahmed Elagamy Mohamed Mahmoud Khalil

Vollständiger Abdruck der von der Fakultät für Medizin der Technischen Universität München zur Erlangung des akademischen Grades eines

Doktors der Naturwissenschaften (Dr. rer. nat.)

genehmigten Dissertation.

Vorsitz: Prof. Dr. Heiko Lickert

Prüfer*innen der Dissertation: 1. TUM Junior Fellow Dr. Siegfried Ussar

2. Prof. Dr. Nina Henriette Uhlenhaut

Die Dissertation wurde am 15.09.2022 bei der Technischen Universität München eingereicht und durch die Fakultät für Medizin am 03.01.2023 angenommen.

Abstract

Obesity and aging are two risk factors for many debilitating diseases like diabetes, cardiovascular diseases and cancer. Both obesity and aging are associated with decreased life expectancy. Obesity is characterized by excessive fat accumulation that can lead to glucose intolerance and insulin resistance, thus predisposing individuals to become diabetics. Chronic low-grade inflammation, mitochondrial dysfunction and cellular senescence are hallmarks of obesity, diabetes and aging. White adipose tissue is the main organ for fat storage. When the amount of fat exceeds the storage capacity of white adipose tissue, it is deposited in other organs like muscle and liver leading to insulin resistance. Brown adipose tissue, on the other hand, burns fat to produce heat. Specific stimuli like cold exposure and β-adrenergic receptor stimulation induce the appearance of brown-like cells, termed beige or brite adipocytes, in the adipose tissue. Induction of beige adipocytes or activation of brown adipocytes have been shown to protect against diet-induced obesity and metabolic abnormalities. Therefore, factors modulating beige adipocytes are under investigation.

Amino acids are known to modulate energy homeostasis. For instance, Serine levels are positively associated with improved insulin sensitivity and glucose tolerance in men. D-serine is produced from L-serine via the action of serine racemase. D-serine supplementation impairs glucose tolerance in mice. Moreover, D-serine modulates diabetic retinopathy. Furthermore, D-serine is thought to play a role in beiging. So, I studied the role of D-serine in beiging and energy homeostasis. Especially that the effects of Serine could be due to D-serine biosynthesis and not solely from L-serine. Therefore, we generated mice with adipose tissue-specific deletion of serine racemase ($SRR^{Adipo\text{-}KO}$). The neurotransmitter D-serine functions as a co-agonist of the N-methyl-D-aspartate receptor. Therefore, we aimed to explore if this receptor is expressed in the adipose tissue and if fat depots use D-serine to communicate with the nervous system.

Aging and obesity both lead to telomere shortening. Obese adults and children show shorter telomeres than non-obese counterparts and telomere length is inversely correlated with body mass index. Telomere shortening is one of the mechanisms contributing to aging. However, study of the direct effect of short telomeres on metabolic parameters in aged individuals is hampered by existing co-morbidities, like obesity, that is associated with aging. Telomeres are nucleoprotein structures found at the end of the chromosomes to protect them from degradation and interchromosomal fusion. Telomeres become shorter with each cell cycle and when telomeres become critically short, cells go into apoptosis or senescence. However, this will pose a problem for cells which proliferate extensively like stem cells. Therefore, telomeres can be extended via the action of telomerase. Telomerase are ribonucleoprotein enzyme complex. The two main players in telomerase are telomerase reverse transcriptase and telomerase RNA component (Terc). The study of the effect of telomere shortening can be done *in vivo* in mice via deletion of Terc. Breeding of Terc knockout (KO) mice results in progressive decline in telomere length with each generation. Interestingly, previous studies used high generation number, third or fourth generation, which show physiological impairments in several tissues, thus, impeding the attribution of observed phenotypes to telomere shortening alone. Moreover, they only focused on male mice. Therefore, I used second generation Terc KO mice to study the effects of telomerase shortening on body weight, energy intake, energy absorption, and energy expenditure in both sexes.

Abstract

In this thesis, I show that SRR$^{Adipo\text{-}KO}$ mice show normal body weight and composition. However, they show adipose tissue hypertrophy that is exacerbated by high fat diet feeding. Moreover, SRR$^{Adipo\text{-}KO}$ mice exhibit increased expression of beiging markers in subcutaneous white adipose tissue only under room temperature and, surprisingly, not under cold exposure. SRR$^{Adipo\text{-}KO}$ mice also show lower energy expenditure and differences in adipose tissues gene expression under chow diet in comparison to controls. Furthermore, I show that *Grin1* is expressed at low levels in the adipose tissue and not in mature adipocytes. However, paradoxically, mice with specific deletion of *Grin1* in adipocytes (Grin1$^{Adipo\text{-}KO}$ mice) show lower body weight in comparison to controls due to a reduction in lean mass. Meanwhile, Terc KO mice show reduced body fat and lean mass that could be due to reduced intestinal fatty acid uptake that is validated by reduced expression of fatty acid uptake genes in small intestine enterocytes. Furthermore, Terc KO mice show sexual dimorphism with female mice exhibiting increased dark phase respiratory exchange ratio and a trend toward reduced locomotor activity. Additionally, female mice display increased fecal caloric content. Our data show that adipose tissue-specific deletion of serine racemase modulates whole body energy expenditure, adipose tissue hypertrophy, beiging and adipose tissue gene expression and that *Grin1* is expressed in fat depots. We also demonstrate, that telomere shortening reduces body weight and this could be due to reduction in fatty acid uptake. Moreover, for the first time, we show sexual dimorphism in Terc KO mice.

Zusammenfassung

Adipositas und Alterung sind zwei Risikofaktoren für viele schwächende Krankheiten wie Diabetes, Herz-Kreislauf-Erkrankungen und Krebs. Sowohl Adipositas als auch das Altern sind mit einer verringerten Lebenserwartung verbunden. Adipositas ist durch übermäßige Fettansammlung gekennzeichnet, die zu Glukoseintoleranz und Insulinresistenz führen und dadurch die Entwicklung von Diabetes begünstigen kann. Chronische leichte Entzündung, mitochondriale Dysfunktion und zelluläre Seneszenz sind gemeinsame Kennzeichen von Fettleibigkeit, Diabetes und Alterung. Weißes Fettgewebe ist das Hauptorgan für die Fettspeicherung. Wenn die Lipidmenge die Speicherkapazität des weißen Fettgewebes übersteigt, wird es in anderen Organen wie Muskeln und Leber abgelagert, was zu einer Insulinresistenz führt. Braunes Fettgewebe hingegen verbrennt Fett, um Wärme zu erzeugen. Spezifische Reize wie Kälteeinwirkung und Stimulation des β-adrenergen Rezeptors induzieren das Auftreten von braunen Fettzellen, die als beige oder brite-Fettzellen bezeichnet werden, im Fettgewebe. Es wurde gezeigt, dass die Induktion beiger Fettzellen oder die Aktivierung brauner Fettzellen vor ernährungsbedingter Fettleibigkeit und Stoffwechselanomalien schützt. Daher werden Faktoren untersucht, die beige Fettzellen modulieren.

Aminosäuren sind dafür bekannt, die Energiehomöostase zu modulieren. Zum Beispiel sind Serinspiegel positiv mit einer verbesserten Insulinsensitivität und Glukosetoleranz bei Männern verbunden. D-Serin wird aus L-Serin durch die Wirkung von Serinracemase hergestellt. D-Serin-Supplementierung beeinträchtigt die Glukosetoleranz bei Mäusen. Darüber hinaus moduliert D-Serin die diabetische Retinopathie. Zusätzlich wird angenommen, dass D-Serin eine Rolle beim Beiging spielt. Also habe ich die Rolle von D-Serin beim Beiging und der Energiehomöostase untersucht. Insbesondere, dass die Wirkungen von Serin auf die D-Serin-Biosynthese zurückzuführen sein könnten und nicht nur auf L-Serin. Daher haben wir Mäuse mit fettgewebespezifischer Deletion von Serinracemase ($SRR^{Adipo\text{-}KO}$) erzeugt. Der Neurotransmitter D-Serin fungiert als Co-Agonist des N-Methyl-D-Aspartat-Rezeptors. Daher wollten wir untersuchen, ob dieser Rezeptor im Fettgewebe exprimiert wird und ob Fettdepots D-Serin verwenden, um mit dem Nervensystem zu kommunizieren.

Alterung und Fettleibigkeit führen beide zu einer Verkürzung der Telomere. Übergewichtige Erwachsene und Kinder weisen verkürzte Telomere auf, und die Telomerlänge korreliert negativ mit dem Body-Mass-Index. Die Verkürzung der Telomere ist einer der Mechanismen, die zum Altern beitragen. Die Untersuchung der direkten Wirkung kurzer Telomere auf metabolische Parameter bei älteren Personen wird jedoch durch bestehende Komorbiditäten wie Fettleibigkeit behindert, die ebenfalls mit dem Altern einhergehen. Telomere sind Nukleoproteinstrukturen an den Enden der Chromosome, die dazu dienen sie vor Abbau und interchromosomaler Fusion zu schützen. Telomere werden mit jedem Zellzyklus kürzer und wenn Telomere zu kurz werden, gehen Zellen in Apoptose oder Seneszenz über. Dies stellt jedoch ein Problem für Zellen dar, die sich wie Stammzellen stark teilen. Daher können Telomere durch die Wirkung von Telomerase verlängert werden. Telomerase ist ein Ribonukleoprotein-Enzymkomplex. Die beiden Hauptkomponenten der Telomerase sind die Telomerase-Reverse-Transkriptase und die Telomerase-RNA-Komponente (Terc). Die Untersuchung der Wirkung der Telomerverkürzung kann *in vivo* an Mäusen durch Deletion von Terc erfolgen. Die Zucht von Terc-Knockout-Mäusen (KO) führt mit jeder Generation zu einer fortschreitenden Abnahme der Telomerlänge. Interessanterweise verwendeten frühere Studien eine hohe Generationszahl, dritte oder vierte Generation, die physiologische Beeinträchtigungen in mehreren Geweben zeigten, wodurch die Zuordnung der beobachteten Phänotypen allein zur

Telomerverkürzung behindert wurde. Außerdem konzentrierten sie sich nur auf männliche Mäuse. Daher habe ich Terc KO-Mäuse der zweiten Generation verwendet, um die Auswirkungen der Telomerase-Verkürzung auf das Körpergewicht, die Energieaufnahme, die Energieabsorption und den Energieverbrauch bei beiden Geschlechtern zu untersuchen.

In dieser Arbeit zeige ich, dass $SRR^{Adipo\text{-}KO}$ Mäuse normales Körpergewicht und Zusammensetzung aufweisen. Sie zeigen jedoch eine Fettgewebshypertrophie, die durch eine fettreiche Ernährung verschlimmert wird. Darüber hinaus zeigen $SRR^{Adipo\text{-}KO}$ Mäuse nur unter Raumtemperatur und überraschenderweise nicht unter Kälteeinwirkung eine erhöhte Expression von Beiging-Markern im subkutanen weißen Fettgewebe. $SRR^{Adipo\text{-}KO}$ Mäuse zeigen auch einen geringeren Energieverbrauch und Unterschiede in der Genexpression des Fettgewebes unter Chow-Diät im Vergleich zu Kontrollen. Außerdem zeige ich, dass *Grin1* in geringen Mengen im Fettgewebe und nicht in reifen Adipozyten exprimiert wird. Paradoxerweise weisen Mäuse mit spezifischer Deletion von *Grin1* in Adipozyten ($Grin1^{Adipo\text{-}KO}$ Mäuse) jedoch ein geringeres Körpergewicht im Vergleich zu Kontrollen auf, was auf eine Verringerung der Magermasse zurückzuführen ist. Unterdessen zeigt Terc KO Mäuse reduziertes Körperfett und reduzierte Magermasse, was auf eine reduzierte Fettsäureaufnahme im Darm zurückzuführen sein könnte, was durch eine reduzierte Expression von Fettsäureaufnahmegenen in Dünndarm-Enterozyten bestätigt wird. Darüber hinaus zeigen Terc KO-Mäuse sexuellen Dimorphismus, wobei weibliche Mäuse ein erhöhtes Atmungsaustauschverhältnis in der Dunkelphase und einen Trend zu einer verringerten lokomotorischen Aktivität aufweisen. Zusätzlich weisen weibliche Mäuse einen erhöhten Kaloriengehalt im Stuhl auf. Unsere Daten zeigen, dass die fettgewebespezifische Deletion von Serinracemase den Energieverbrauch des gesamten Körpers, die Fettgewebehypertrophie, Beiging und die Genexpression des Fettgewebes moduliert und dass *Grin1* in Fettdepots exprimiert wird. Wir zeigen auch, dass die Verkürzung der Telomere das Körpergewicht reduziert und dies auf eine Verringerung der Aufnahme von Fettsäuren zurückzuführen sein könnte. Darüber hinaus zeigen wir zum ersten Mal sexuellen Dimorphismus in Terc KO-Mäusen.

Table of contents

List of figures

List of figures

List of tables

Abbreviations

Acaca	Acetyl-coA carboxylase
Actb	Beta actin
Adipoq	Adiponectin
Adrb1	Adrenoceptor beta 1
Adrb2	Adrenoceptor beta 2
Adrb3	Adrenoceptor beta 3
APS	Ammonium persulfate
ASC1/SLC7A10	Alanine-serine-cysteine transporter 1
Asct1	solute carrier family 1 (glutamate/neutral amino acid transporter) member 4
Asct2	solute carrier family 1 (glutamate/neutral amino acid transporter) member 5
ATGL	Adipose tissue triglyceride lipase
ATP	Adenosine triphosphate
BAT	Brown adipose tissue
BCAA	Branched chain amino acids
BMI	Body mass index
BSA	Bovine serum albumin
Cd36	Cluster of differentiation 36
cDNA	Complementary DNA
Cebpa	CCAA enhancer binding protein alpha
Cebpb	CCAA enhancer binding protein beta
DGAT	diacylglycerol acyltransferase
DMSO	Dimethyl sulfoxide
DNA	Deoxyribonucleic acid
DTT	Dithiothreitol
EDTA	ethylenediaminetetraacetic acid
EE	Energy expenditure
Fabp4	Fatty acid binding protein 4
FABPpm/GOT2	Plasma membrane-associated fatty acid-binding protein
Fasn	Fatty acid synthase
FATP	Fatty acid transport protein
FBS	Fetal bovine serum
FFA	Free fatty acids
FGF21	Fibroblast growth factor 21
G2	Second generation
G3	Third generation
G4	Fourth generation
Gamt	guanidinoacetate methyltransferase
Gatm	glycine amidinotransferase
Glut1	Sodium-independent glucose transporter 1
Glut2	Sodium-independent glucose transporter 1

Grin1	Glutamate Ionotropic receptor NMDA type subunit 1
GTT	Glucose tolerance test
H&E	Hematoxylin and Eosin
HbA1c	Glycosylated hemoglobin
HFD	High fat diet
HPLC/MS	Ultra high performance liquid chromatography coupled with mass spectrometry
Hprt	hypoxanthine guanine phosphoribosyl transferase
HSL	Hormone sensitive lipase
HSP70	Heat shock protein 70
IL-1β	Interleukin 1 beta
IL-6	Interleukin 6
ITT	Insulin tolerance test
LPL	Lipoprotein lipase
MGAT	Monoacylglycerol acyltransferase
mRNA	Messenger RNA
NCD	Non-communicable disease
NMDAR	N-methyl-D-aspartate receptors
oGTT	Oral glucose tolerance test
P/S	Penicillin/Streptomycin
P2rx5	purinergic receptor P2X, ligand-gated ion channel, 5
Pat2	Protein assistant amino acid transporter 2
PBS	Phosphate-buffered saline
pgWAT	Perigonadal white adipose tissue
PHGDH	Phosphoglycerate dehydrogenase
Pparg	Peroxisome proliferator activated receptor gamma
Ppargc1a	Peroxisome proliferator-activated receptor gamma coactivator 1-alpha
Prdm16	PR domain containing 16
Pref-1	Pre-adipocyte factor 1
PSAT	Phosphoserine aminotransferase
PSPH	Phosphoserine phosphatase
PVDF	polyvinylidendifluorid
qPCR	Real-Time PCR
RER	Respiratory exchange ratio
RIN	RNA integrity number
scWAT	Subcutaneous white adipose tissue
SDS	sodium dodecyl sulfate
SDS-PAGE	Sodium dodecyl sulfate-poly acrylamide gel electrophoresis
Slc27a2	Fatty acid transport protein 2
Slc27a4	Fatty acid transport protein 4

SLC2A4/GLUT4	Sodium-independent glucose transporter 4
Slc5a1	Sodium/glucose cotransporter 1
Slc5a2	Sodium/glucose cotransporter 2
Srr	Serine racemase
Tbp	TATA binding protein
TEMED	Tetramethylethylenediamine
TERC	Telomerase RNA component
TERT	Telomerase reverse transcriptase
TNF-α	Tumor necrosis factor alpha
UCP-1	Uncoupling protein 1
UK	United kingdom
US	United states
vWAT	Visceral white adipose tissue
WAT	White adipose tissue
WHO	World health organization

1 Introduction

1.1 Obesity, its prevalence and its associated co-morbidities

Non-communicable diseases (NCDs) are diseases that are not transmitted from one person to another. NCDs including cardiovascular diseases, cancer and diabetes are responsible for almost 70% of deaths worldwide and count for more than 40 million cases of mortality annually (Collaborators 2016). Obesity is a major NCDs and is a major risk factor for cardiovascular diseases (including hypertension, myocardial infarction and stroke), cancer (for example, prostate, ovarian, liver and colon) and diabetes (Blüher 2019). Thus, obesity is a major contributor to NCDs incidence. Obesity incidence has increased dramatically in the last 40 years, now reaching pandemic proportions. Obesity is a complex multifactorial disease and is defined by the world health organization (WHO), as abnormal or excessive fat accumulation that presents a risk to health. In order to combat obesity, a thorough knowledge of its etiology, its progression and consequences is warranted. Obesity is defined by a body mass index (BMI) equal to or above 30 and BMI equal to or above 25 being overweight. BMI is a simple, fast and inexpensive measurement to assess your weight group that is calculated as follows: body weight in kilograms divided by square of height in meters (WHO 2021). However, even something that is as widely used as BMI is not completely accurate on its own and these cutoff values may not be appropriate for all ethnicities. Therefore, some Asian countries have a lower BMI cutoff value for being overweight and obese (Consultation 2004; Low et al. 2009; Misra et al. 2009). The reason for this is that at the same BMI as Whites, Asians have double the risk to develop type 2 diabetes and for every 11 pounds gained, the risk to develop type 2 diabetes increases by 84% for Asians. The risk to develop type 2 diabetes increases with body weight in other ethnicities as well but to a lesser degree than in Asians (Shai et al. 2006). Asians also have a higher risk to develop hypertension and cardiovascular disorders when compared to other ethnicities with the same BMI (Deurenberg-Yap et al. 2000; Pan et al. 2004; Wen et al. 2009). One reason for this is that at the same BMI, Asians have higher body fat percentage than other ethnicities (Deurenberg, Deurenberg-Yap, and Guricci 2002). These data demonstrate one facet of the complexity of defining obesity.

Obesity is increasing rapidly and has reached pandemic proportions. In 2016, 1.9 billion people were overweight and out of those 650 million were obese. Obesity rates have almost tripled since 1975 and now almost 40% of all adults are overweight and 13% obese. Obesity is also on the rise in children and adolescents. It is now estimated that, in 2016, 340 million children and adolescents aged 5 to 16 are either overweight or obese. Moreover, in 2020, 39 million children below the age of 5 years were either overweight or obese (WHO 2021). Thus, there is an alarming increase in obesity in children and adolescents as cases increased in boys from 0.7% to 5.6% and in girls from 0.9% to 7.8% between 1975 and 2016 (Abarca-Gómez et al. 2017). In a study where anthropometric data were taken during childhood and adolescence, it was found that 90% of children who were obese at three years old, were either obese or overweight at adolescence (Geserick et al. 2018). In Adulthood, obesity rates increased from 3.2% to 10.8% in men and from 6.4% to 14.9% in women between 1975 and 2016 (Abarca-Gómez et al. 2017). Obesity rates have increased in most countries except for North Korea and some countries in sub-Saharan Africa and Nauru. Interestingly, the rate of BMI increase has slowed, since 2000, in high income countries and some middle income countries in comparison to the previous century in both adults and children (Abarca-Gómez et al. 2017; Collaboration 2016). Moreover, childhood obesity and overweight seem to

plateau (or even decrease) in some high income countries like Norway, Sweden, Japan and Australia (Abarca-Gómez et al. 2017; Rokholm, Baker, and Sørensen 2010).

1.2 Factors modulating obesity

Obesity is characterized by excessive weight gain that is due to an imbalance between energy intake and energy expenditure. In the United States (US), this increase in energy intake (food intake) can be attributed to an increase in portion size and an increase in food accessibility (Rolls 2003). Not only is our food much more accessible than before but also highly processed, pre-packaged and non-perishable. This fat-laden and energy-rich food is consumed by millions of families and is marketed not only towards adults but also children (Wright and Aronne 2012), thereby, contributing to obesity. However, another arm of the increase in obesity is the decrease in physical activity. In the US, physical activity has been decreasing steadily for the past few decades. For example, in 2005, less than half of US adults engaged in the recommended level of physical activity (Kruger, Kohl III, and Miles 2007). This decrease in physical activity is also seen in adolescents (Kimm et al. 2002). Moreover, there is less access to physical activity and less physical education in schools (Gabbard 2001). Furthermore, there is a culture shift to more sedentary leisure activities like surfing the internet or playing video games. However, the decrease in physical activity and the increase in energy intake are not the only causes of obesity. For example, some of the widely prescribed medications are known to cause significant weight gain. For instance, in the case of some psychotropic medications, antihypertensives, steroid hormones, contraceptives and antihistamines (Aronne and Segal 2003). Sleep debt or deprivation has also been linked to obesity. BMI negatively correlates with the number of sleeping hours (Gangwisch et al. 2005). Moreover, sleep reduction is associated with increased ghrelin (hunger hormone) and decreased leptin (satiety hormone) thereby leading to increased hunger and appetite (Spiegel et al. 2004). Furthermore, endocrine function disruption via certain chemicals like dichlorodiphenyltrichloroethane, some alkylphenols and polychlorinated biphenols that may disrupt endogenous hormonal regulation, promotes obesity (Keith et al. 2006). Social connections also play a role in modulating obesity. For example, the probability of a person to develop obesity increases by 37% increase if his/her spouse develops obesity. Furthermore, in adults, there is a 40% increase in obesity risk if your sibling becomes obese (Wright and Aronne 2012). Moreover, a person´s chance to develop obesity increases by 57% if he or she knows a friend who became obese in a given interval (Christakis and Fowler 2007).

Two main factors that greatly affect obesity are genetics and epigenetics. The landmark study of Stunkard and colleagues demonstrated that in adopted Danish twins the body weight of the adult twins was closely related to the biological parents despite being raised with another family (Stunkard et al. 1986). Furthermore, they examined the BMI of twins reared together or apart and concluded a heritability of around 70% (Stunkard et al. 1990). A systemic review of twin studies later demonstrated that genetic factors had a robust effect on BMI and showed a heritability between 45-90% (Silventoinen et al. 2010). Also, genetics play a clear role in obesity, one could not attribute the drastic increase in obesity in the last 50 years solely to genetics (Blüher 2019). Furthermore, monogenetic mutations (caused by a single gene mutation) are very rare (Thaker 2017). However, epigenetics changes can, in part, explain this increase in obesity incidence. Epigenetics is the study of heritable regulatory changes that is not due to changes in deoxyribonucleic acid (DNA) sequence but due to epigenetic modifications that can either allow or suppress the expression of certain genes. These epigenetic modifications include DNA methylation, histone modification and micro-RNAs (Thaker 2017). For example. Exposure to famine during gestation

period can alter DNA methylation of genes involved in growth and metabolism compared to unexposed same sex siblings (Tobi et al. 2009) and lead to glucose intolerance due to a deficit in insulin secretion (De Rooij et al. 2006). Furthermore, the expression of several genes involved in adipogenesis namely Pre-adipocyte factor 1 (*Pref1*), CCAA enhancer binding protein alpha (*Cebpa*), *Cebpb* and peroxisome proliferator activated receptor γ (*Pparg*) is regulated by histone modifications during differentiation of adipocytes (Zhang et al. 2012). Moreover, micro-RNAs play a role in proliferation and differentiation of adipocytes and obese individuals show alterations in micro-RNAs profile and these alterations can be reversed by weight loss (Cruz et al. 2017). Additionally, several micro-RNAs are deregulated in prepubertal obese children and are significantly associated with BMI. Therefore, micro-RNAs could be used as a marker to identify obese individuals with metabolic abnormalities (Prats-Puig et al. 2013). These data elucidate the role of genetics and epigenetics in the development of obesity.

A major player in the regulation of body weight and has received attention in the field of obesity is microbiota. Microbiota are the microorganisms residing in the gastrointestinal tract and exert several beneficial effects for the host like providing additional energy for the host that is otherwise inaccessible by breaking down soluble fibers, producing vitamins like folate, biotin and vitamin K, preventing colonization of the gut by pathogens thereby protecting the host and helping in the development of the immune system (Davis 2016). The role of the gut microbiota in body weight control became clear while studying germ-free mice. These mice do not have microorganisms in their gut. Interestingly, germ-free mice are leaner than conventionally reared mice even though they have higher food intake (Bäckhed et al. 2004). Moreover, transplantation of distal gut microbiota from normal mice into gnotobiotic mice led to an increase in body weight with no apparent changes in food intake or energy expenditure (Bäckhed et al. 2004). Furthermore, germ-free mice are also protected from diet induced obesity when placed under a westernized high fat sugar rich diet. This is due an increase in muscle and liver adenosine monophosphate (AMP) activated protein kinase and its downstream targets which are involved in fatty acid oxidation (Bäckhed et al. 2007; Bajzer and Seeley 2006). Obesity is also associated with changes in gut microbiota composition. For example, obese (*ob/ob*) mice show higher proportion of intestinal *Firmicutes* and 50% less *Bacteroidetes* and, in comparison to their lean siblings, show higher enrichment of microbial genes involved in polysaccharide degradation (Ley et al. 2005). Interestingly, germ-free mice which received microbiota from obese (*ob/ob*) mice showed higher fat mass than germ-free mice which received microbiota from lean controls (Turnbaugh et al. 2006). Thus, differences in microbiota composition can modulate the amount of energy extracted from food. Additionally, mice receiving microbiota from lean and obese human twins show similar phenotype to the donor. This means that mice receiving microbiota from lean human remain lean while mice receiving microbiota from the obese twin have increased fat mass (Ridaura et al. 2013). These data demonstrate the effects of microbiota on energy acquisition and demonstrate the ability of microbiota to modulate body weight. Taken together, obesity is a complex multifactorial disease that is a result of interactions between socioeconomic, environmental and individual factors that has now reached pandemic proportions.

1.3 Consequences of obesity

Obesity is regarded as a chronic disease affecting millions worldwide (Rosen 2014). Additionally, obesity is associated with several dilapidating diseases and increased mortality. In the year 2000, 15% of mortality cases in the US could be attributed to obesity and overweight due to physical inactivity and poor diet (Mokdad et al. 2004). Moreover, it is known that obesity and overweight in adults shorten life expectancy

by 4 to 7 years and lead to early mortality (Peeters et al. 2003). Many studies have demonstrated that obesity/overweight increase the risk of overall mortality, death from cardiovascular disorders, diabetes, cancer and accidental death (Hruby and Hu 2015). Therefore, obesity is a major cause for mortality that is currently rampant worldwide. Excess weight can lead to insulin resistance (Kolterman et al. 1980) and insulin resistance predisposes to diabetes (Reaven 1988). Diabetes is a chronic illness characterized by elevated levels of blood glucose and perturbed metabolism of nutrients. Blood glucose level rises because it cannot be metabolized by the cells either due to reduced ability of cells to respond to insulin (insulin resistance) or due to insufficient insulin production from pancreatic β-cells (Roglic 2016). Many cross sectional and longitudinal studies have demonstrated a strong association between excess weight and glucose intolerance, insulin resistance and diabetes (PI-SUNYER 1999). In fact the association between excess weight and diabetes is very clear that the American Diabetes association recommends testing for diabetes in individuals who are ≥45 years old if they are overweight/obese and regardless of age if they are severely obese (Association 2012). Being overweight raises the risk of developing diabetes three fold and obesity raises the risk seven fold (Abdullah et al. 2010). Excess weight in childhood and adolescence and weight gain through early to mid-adulthood are strong risk factors for diabetes (Kodama et al. 2014; Narayan et al. 2007; Reilly and Kelly 2011). It is true that not every obese person is diabetic. However, 80% of diabetic individuals are obese or overweight (Hruby and Hu 2015). Furthermore, even in the absence of metabolic abnormalities like hypertension, poor glycemic control and dyslipidemia, obesity itself raises the risk to develop diabetes. An example of this is metabolically healthy obese individuals which have half the risk to develop diabetes in comparison to unhealthy obese individuals. However, they still have four times the risk to develop diabetes in comparison to lean individuals who are metabolically healthy (Bell, Kivimaki, and Hamer 2014).

The association between obesity/overweight and hypertension has been demonstrated in many longitudinal and cross sectional studies. The prevalence of hypertension is much higher in obese individuals than in the general population (PI-SUNYER 1999). This increase in hypertension incidence with obesity can be seen in populations with high prevalence of hypertension (African-Americans) (Stamler et al. 1978) as well as in populations with low prevalence of hypertension (Mexican-Americans) (Haffner et al. 1992). The Framingham study demonstrated that weight gain leads to an increase, among others, in blood pressure (Kannel, Gordon, and Offutt 1969). Several studies have demonstrated that obesity is also associated with an increase in triglyceride levels as well as a decrease in high density lipoprotein cholesterol (PI-SUNYER 1999). Both these abnormalities are considered independent risk factors for cardiovascular disorders (Assmann and Schulte 1992; Austin 1991; Gordon et al. 1977). Therefore, it is no wonder that obesity and overweight are risk factors for heart disease and stroke. Thus, benign obesity appears to be a myth as excess weight clearly adds to the risk of heart disease and stroke beyond its implications in hypertension, dysglycemia and dyslipidemia (Flint et al. 2010; Kramer, Zinman, and Retnakaran 2013; Lu et al. 2014). Given the rising incidence in obesity in children and adolescents, research examined the effect of excess weight in early life on subsequent adulthood disease. It has been demonstrated that obesity in childhood or adolescence increases the risk for coronary heart disease, hypertension and stroke by two fold or more during adulthood (Reilly and Kelly 2011). These data highlight the burden of obesity especially given that Ischemic heart disease and stroke are the leading causes of death globally (Lozano et al. 2012).

Obesity is a risk factor for the development of several types of cancer. It is also a risk factor for diabetes which is a risk factor for many types of cancer (PI-SUNYER 1999). Moreover, insulin resistance is a feature

of obesity and is also associated with increased cancer risk (Goodwin et al. 2002; Hsing et al. 2001; Kim, Abbasi, and Reaven 2004). Being overweight increases the risk for cancers of the gastrointestinal tract by 1.5 to 2.4 fold (Moore, Wilson, and Campleman 2005). It has been estimated that 5.5% of all cancer cases are related to obesity or overweight in the United Kingdom (UK) (Parkin and Boyd 2011) while it is was estimated that around 6% (4% in men, 7% in women) of all cancer cases in the US in 2007 were due to obesity (Polednak 2008). However, some estimate that the incidence of cancer due to obesity is much higher than that (Calle et al. 2003; Wolin, Carson, and Colditz 2010). Nonetheless, obesity is associated with increased risk of esophageal, pancreatic, renal, postmenopausal breast, endometrial, prostate, liver, leukemia and ovarian cancer (Discacciati, Orsini, and Wolk 2012; Larsson and Wolk 2007b; Larsson and Wolk 2007a; Larsson and Wolk 2008; Vainio and Bianchini 2002).

In a study of patients admitted to a trauma center, it was found that severely obese individuals have 30% higher chance of mortality and double the risk of developing major complications in comparison to non-obese patients. Severely obese patients have at least double the risk of non-obese controls for acute renal failure. Moreover, severely obese females have much higher risk to develop wound complications and decubiti (bedsores) than non-obese controls (Glance et al. 2014). Another meta-analysis study of obese patients admitted to intensive care has concluded that obesity increases the risk of mortality by 45%. Furthermore, obese patients stay longer in the intensive care unit and have higher risk of developing major complications in comparison to non-obese patients with equivalent injury severity (Liu et al. 2013). Additionally, obese individuals seem to have impaired immune response. A study demonstrated that obese individuals are more likely to be non-responders to two doses of vaccination against hepatitis B virus (Young, Gray, and Bekker 2013). Therefore, obesity aggravates the risk of trauma and could impair vaccination immune response.

Excess weight has a clear effect on the brain. Brain volume inversely correlates with BMI. Moreover, old obese individuals show atrophy in the frontal lobes, hippocampus, hypothalamus and anterior cingulate gyrus in comparison to individuals with normal weight (Raji et al. 2010). Obese children and adolescence perform significantly worse than healthy controls in executive functions (inhibitory controls). Furthermore, obese adolescents show neurostructural deficits in the orbitofrontal cortices (Reinert, Po'e, and Barkin 2013). Moreover, overweight individuals have increased risk for Alzheimer's disease and dementia and this risk increases even further in obese individuals (Anstey et al. 2011). Therefore, excess weight alters brain morphology and increases the risk for brain disorders.

Given the deleterious health effects of obesity, tremendous costs are paid by health care systems and governments across the world due to excess weight. It is estimated that in the US obese men incur an additional $1.152 per year in health care spending primarily due to hospitalization and drugs prescription in comparison to non-obese individuals and for obese women the amount is even higher ($3.613 per year). The authors concluded that obesity and obesity-related conditions cost the US government $190 billion per year amounting to 21% of health care expenditures (Cawley and Meyerhoefer 2012). The cost incurred due to obesity is expected to increase as obesity rates increase worldwide. For example, it is estimated in 2060 that the costs of obesity will increase to 2.4% of gross domestic product (GDP) in Spain and 4.9% in Thailand (Okunogbe et al. 2021). Beside direct health costs, obesity also imposes costs due lost economic growth as a result of lower productivity, lost work days, mortality and permanent disability (Tremmel et al. 2017). All these data point that excess weight is an alarming issue with disastrous consequences that needs the full attention of policy makers around the world.

1.4 Adipose tissue and its role in health and disease

Obesity is due to surplus of energy. This surplus of energy is stored in the form of fat (triglycerides) and these triglycerides are stored in designated cells (adipocytes) in designated compartments (adipose tissues) (Koenen et al. 2021). Upon consumption of fat, its digestion begins in the mouse via the action of lingual lipase secreted from the tongue. After that, fat reaches the stomach where it is emulsified by peristalsis and hydrolyzed by the action of gastric and lingual lipases. The stomach empties in the small intestine where most of fat hydrolysis occurs. In the small intestine, fat is further emulsified and hydrolyzed through the action of bile acids and pancreatic lipases. The resulting free fatty acids (FFA) and monoglycerides are transported in the form of micelles that enter the enterocytes (epithelial cells lining the intestine) (Mu and Høy 2004; Phan and Tso 2001). Several proteins are responsible for the uptake and transport of FFA from the intestinal lumen into the enterocytes. These proteins include CD36, plasma membrane-associated fatty acid-binding protein (FABPpm, also known as GOT2) and a family of fatty acid transport proteins (FATP) 1-6. Once inside the enterocyte, the monoglycerides and FFA will be re-esterified to form diglycerides via the action of monoacylglycerol acyltransferases (MGAT) and then further re-esterified to form triglycerides via the action of diacylglycerol acyltransferases (DGAT). The triglycerides are then packaged into chylomicron and released into the lymphatic system, bypassing the liver, and later joining the blood stream. When chylomicrons reach adipose tissues, they are hydrolyzed by lipoprotein lipase (LPL), generating FFA. FFA are taken up by adipocytes and stored as triglycerides (Iqbal and Hussain 2009; Phan and Tso 2001). During starvation or exercise, when there is increased energy demand, adipose tissue can hydrolyze its triglycerides storage providing FFA and glycerol for others organs to be used as an energy source. Breaking down of triglyceride into FFA and glycerol involves the sequential action of several proteins. Firstly, adipose tissue triglyceride lipase (ATGL) hydrolyzes triglyceride into digylcerides and release one fatty acid then hormone sensitive lipase (HSL) hydrolyzes diglycerides into monoglycerides releasing one more fatty acid then, lastly, monoacylglycerol lipase hydrolyzes monoglyceride, releasing the last fatty acid and glycerol. Some of these FFA are released into the circulation to be taken up by tissues for energy (Langin 2006).

Adipose tissue is classically divided into white and brown adipose tissue. White adipose tissue (WAT) stores energy in the form of triglycerides to be used in times of energy demand while brown adipose tissue (BAT) utilizes energy to produce heat via the action of the inner mitochondrial membrane protein uncoupling protein 1 (UCP-1) which uncouples the proton motive force from adenosine triphosphate (ATP) production thus producing heat. This is of special importance for infants lacking shivering thermogenesis or hibernating animals to defend their body temperature against cold challenge (Zoico et al. 2019). Both WAT and BAT consist of white or brown adipocytes and stromal vascular fraction cells including immune cells, endothelial cells, pericytes, fibroblasts and progenitor cells (Schoettl, Fischer, and Ussar 2018). Both white adipocytes and brown adipocytes are morphologically, functionally and developmentally different. For instance, white adipocytes are classically spherical in shape with size ranging from 25μm^2 to 200μm^2 and have one large lipid droplet occupying 90% of the cell volume, a peripheral flat nucleus and small smooth and rough endoplasmic reticulum. WAT is a poorly vascularized and innervated tissue (Gómez-Hernández et al. 2016). On the other hand, brown adipocytes have a polygonal shape and contain an oval centered nucleus, large cytoplasm and underdeveloped endoplasmic reticulum. Furthermore, brown adipocytes contain a large number of mitochondria and multiple lipid droplets and are usually smaller in size than white adipocytes. BAT is a highly vascularized and innervated organ. WAT is mainly divided into subcutaneous WAT (scWAT) which is under the skin and comprises 80%

of WAT and the second is visceral WAT (vWAT) which is divided into mesenteric and omental with omental fat being the one widely used for the study of visceral fat (Gómez-Hernández et al. 2016). Surprisingly, there are lean individuals which are metabolically unhealthy (Ruderman, Schneider, and Berchtold 1981). These individuals favor accumulation of fat viscerally (Dvorak et al. 1999; Ruderman et al. 1998). On the other hand, there are obese individuals who are metabolically healthy and favor fat accumulation subcutaneously (Primeau et al. 2011; Stefan et al. 2008). In general, men tend to accumulate fat viscerally giving them the apple-shaped appearance while women tend to accumulate fat subcutaneously given them the pear-shaped appearance (Gesta, Tseng, and Kahn 2007). Visceral fat accumulation has been consistently associated, in epidemiological studies, with metabolic disorders while subcutaneous fat does not (Fox et al. 2007). An explanation for this is that the two depots (subcutaneous and visceral fat) are morphologically, molecularly and anatomically different (Gómez-Hernández et al. 2016; Wajchenberg 2000). For instance, subcutaneous adipocytes are larger in size than visceral adipocytes in humans and in mice it is the other way around (mice visceral adipocytes are larger than subcutaneous adipocytes) (Schoettl, Fischer, and Ussar 2018). Moreover, messenger RNA (mRNA) expression of leptin is higher in subcutaneous than omental fat especially in women (Montague et al. 1997). Furthermore, the amount of protein released also differs according to the depot tested (Fain et al. 2004; Motoshima et al. 2002). For example, smaller adipocytes secrete more adiponectin (insulin-sensitizing hormone) than larger ones and as mentioned omental adipocytes are small than subcutaneous one. Therefore, omental adipocytes secrete more adiponectin than subcutaneous adipocytes. However, since subcutaneous fat is much larger than visceral fat, subcutaneous fat contributes more to adiponectin secretion (Reynisdottir et al. 1997). Furthermore, omental fat is more responsive to catecholamine stimulation and less responsive to insulin action in comparison to subcutaneous fat (Montague and O'Rahilly 2000). Additionally, omental adipocytes secrete cytokines (adipokines) and metabolites into the portal vein, thus, facilitating delivery to the liver. These differences could, at least partially, explain the differences in the metabolic outcomes associated with fat accumulation in different depots.

Adipose tissue can modulate insulin sensitivity and glucose tolerance and cause insulin resistance and metabolic abnormalities. FFA released by adipose tissues play a major role in insulin sensitivity. FFA levels are increased in obesity and diabetes and are positively correlated with insulin resistance (Boden 1997; Reaven et al. 1988). Insulin resistance develops hours after an increase in FFA levels (Roden et al. 1996). Moreover, reduction of FFA by the antilipolytic drug Acipimox improved glucose tolerance and reduced insulin resistance in both lean and obese individuals without diabetes and in obese diabetic individuals (Santomauro et al. 1999). Furthermore, adipose tissue is only responsible for a small percentage of glucose clearance *in vivo*. However, deletion of the sodium-independent glucose transporter 4 (SLC2A4 also known as GLUT4) specifically in the adipose tissue results in glucose intolerance and insulin resistance. The insulin resistance is even seen in muscles and liver which have intact GLUT4 expression (Minokoshi, Kahn, and Kahn 2003). Another example of how adipose tissue can cause metabolic abnormalities is through adipokines. For instance, leptin is a hormone that regulates appetite via its action on certain brain regions and regulates energy expenditure in the periphery (Marti, Berraondo, and Martinez 1999). Leptin is mainly produced by adipose tissues and is positively correlated with fat mass (Nakata et al. 1999). However, when leptin concentration rises for prolonged period of times, leptin resistance ensues. Hyperleptinaemia is associated with insulin resistance in obese subjects through modulation of insulin receptor phosphorylation (Balland et al. 2019; Obradovic et al. 2021; Paz-Filho et al. 2012; Pérez et al. 2004; Thon, Hosoi, and Ozawa 2016). Another prominent adipokine is adiponectin. Adiponectin is known for its insulin sensitizing and anti-inflammatory effect. Thus, adiponectin is

negatively associated with BMI and is reduced in obesity and type 2 diabetes (Nguyen 2020; Ryo et al. 2004; Snehalatha et al. 2003; Yamamoto et al. 2004). Obesity also causes excessive lipid accumulation in the adipose tissue. This leads to cellular stress and activation of inflammatory pathways resulting in the production of several pro-inflammatory molecules like IL-6, IL-1β and TNF-α. This process leads to the recruitment and activation of macrophages which augments the inflammatory response (Gómez-Hernández et al. 2016). TNF-α levels are positively correlated with adipocyte cell volume (Winkler et al. 2003) that´s why it´s expression is upregulated in obese mouse models and in obese and diabetic humans linking this increase in TNF-α levels with insulin resistance (Hotamisligil 2006; Hotamisligil et al. 1995). Moreover, TNF-α activates lipolysis in adipose tissue and reduces expression of GLUT4 and LPL to circumvent further increase in adipocyte size. Therefore, TNF-α increases FFA levels thus contributing to insulin resistance and in the liver it reduces the action of insulin thus promoting hepatic glucose production (Hotamisligil et al. 1994). Hence, treatment with anti-TNF-α neutralizing antibodies reduces blood glucose levels in diabetic KKAy mice (Takano et al. 2010) and could improve insulin sensitivity in insulin resistant subjects (Yazdani-Biuki et al. 2004). These data demonstrate that WAT acts not only as a storage organ but also modulates whole body energy homeostasis.

When rodents are exposed to cold, transient receptor potential channels located on sensory neurons on the body surface sense the temperature. This information is conveyed to the brain which increases the activity of sympathetic nerves entering BAT (Nakamura 2011). Noradrenaline released from nerve terminals activate β-adrenergic receptors. This leads to an increase in cyclic AMP which leads to increased lipolysis. The liberated FFA enter the mitochondria where it will be used to produce heat, instead of ATP, via the action of UCP-1. Sympathetic activation also induces lipolysis in WAT thus supplying FFA to the peripheral organs including BAT (Saito et al. 2020). When animals are exposed to cold for prolonged periods, they increase the number of brown adipocytes and the amount of UCP-1. Interestingly, this leads to the recruitment of brown-like adipocytes in scWAT. These cells are termed beige or brite adipocytes (Saito et al. 2020). Beige cells express UCP-1 and participate in thermogenesis, although, they have different developmental origin than brown adipocytes. Beige adipocytes either arise from progenitor cells or from transdifferentiation of white adipocytes into beige adipocytes (Fenzl and Kiefer 2014). Promoting BAT function and Induction of beige adipocytes have been show to improve glucose tolerance and insulin sensitivity and protect against diet induced obesity and metabolic abnormalities in rodents (Klingenspor 2003; Lim et al. 2012; Qiang, Wang, Kon, Zhao, Lee, Zhang, Rosenbaum, Zhao, and Gu 2012; Vitali et al. 2012; Wu, Cohen, and Spiegelman 2013). For decades, it was thought that adults humans do not have BAT. However, in 2009, using ^{18}fluor-deoxy-glucose positron emission tomography coupled with computed tomography, several groups demonstrated that humans have functional BAT (Cypess et al. 2009; Saito et al. 2009; van Marken Lichtenbelt et al. 2009; Virtanen et al. 2009). In humans, BAT function and quantity is inversely associated with body fat and aging (Ouellet et al. 2011; Persichetti et al. 2013; Pfannenberg et al. 2010; Zhang et al. 2013). At the same time, the decline in BAT is associated with visceral fat accumulation (Yoneshiro et al. 2011). Moreover, prolonged cold exposure recruits and activates BAT in humans, increases energy expenditure and reduces body fat content (Blondin et al. 2014; van der Lans et al. 2013; Yoneshiro et al. 2013). Furthermore, exposure to cold improves glucose tolerance and insulin sensitivity (Chondronikola et al. 2014; Matsushita et al. 2014). Thus, BAT and beige adipocytes activation is a promising therapeutic target for increasing energy expenditure, reducing fat mass and ameliorating metabolic abnormalities (Chechi, Nedergaard, and Richard 2014; Lidell, Betz, and Enerbäck 2014).

1.5 Aging, telomeres and metabolic abnormalities

Elderly are the fastest growing segment of the human population. Therefore, it is expected by 2050 that there will two billion people above 60 years old, thus, exceeding the number of children (Glatt et al. 2007). Aging is characterized by impairment in cells and tissues integrity which leads to reduced functionality and increased risk of mortality (Tam, Morais, and Santosa 2020). Aging is associated with a decline in lean mass and an increase in fat mass (Jiang et al. 2015). Moreover, aging results in redistribution of fat from the subcutaneous depot to the visceral depot which is associated with increased risk of metabolic abnormalities (Kuk et al. 2009). Furthermore, Aging is the leading risk factor for several debilitating diseases like diabetes, cardiovascular diseases and cancer (Jura and Kozak 2016). Interestingly, Obesity and aging increase the risk for many of the same diseases and cause similar impairment in tissue functionality. For instance, both conditions lead to increased reactive oxygen species, increased senescence, mitochondrial dysfunction, increased apoptosis, insufficient autophagy, and increased inflammation (Vijg and Campisi 2008). That´s why it has been proposed that obesity and aging are two sides of the same coin (Tam, Morais, and Santosa 2020). One of the mechanisms that lead to aging is telomere shortening. Telomeres are nucleoprotein structures found at the end of chromosomes that protect them from degradation and interchromosomal fusion. Telomeres consist of a highly conserved hexamer repetitive (TTAGGG) tandem repeat of DNA sequences with a 50 – 400 nucleotide single-stranded 3´ overhang (Turner, Vasu, and Griffin 2019). The presence of telomeres is essential due the to the end replication problem of linear chromosomes. It is known that during DNA replication, DNA polymerase can only replicate from 5´ to 3´ end which is the same direction as the replication fork. RNA primers attach to the strand providing 3´ OH group for the addition of free nucleotides. So, the synthesis of a new 5´ to 3´ DNA strand is made continuously with one primer. However, for the synthesis of the new 3´ to 5´ DNA strand several RNA primers are needed that anneal to the strand and are then elongated into Okazaki fragments that are later ligated. Therefore, at least a piece of DNA the size of the RNA primer is lost. However, in reality much more DNA is lost (Turner, Vasu, and Griffin 2019). That´s why the presence of telomere is essential so that no crucial information is lost during DNA replication. But that also means that cells will continuously lose telomeres during each replication cycle (cells lose 50 – 100 base pair per replication cycle) (Levy et al. 1992; Saretzki 2018). After several replication cycles, when the telomere length becomes very short, the cells will go into senescence or apoptosis. However, this will pose a serious problem for cells which replicate extensively like stem cells or germ cells. Therefore, there is a natural system for the elongation of telomeres known as telomerase (Turner, Vasu, and Griffin 2019). Telomerase is a ribonucleoprotein enzyme complex that can elongate telomeres. The two main players in telomerase are telomerase reverse transcriptase (TERT) which is the enzyme which uses telomerase RNA component (TERC) as a template for the elongation of telomeres (Turner, Vasu, and Griffin 2019). Nonetheless, telomeres shorten with aging. This can be seen in young adults who show longer telomeres than the elderly (LaRocca, Seals, and Pierce 2010). Moreover, telomere length is inversely correlated with BMI. For example, obese women show shorter telomeres in comparison to women with normal weight (Valdes et al. 2005). Additionally, obese children show shorter telomeres in comparison to non-obese children (Buxton et al. 2011). Furthermore, obesity is associated with decreased telomere length in both subcutaneous and visceral fat. Additionally, visceral adipocyte size is negatively associated with telomere length in visceral and subcutaneous adipocytes (Monickaraj et al. 2012). It has been demonstrated clearly that the ability of the elderly to utilize glucose is reduced and that their glucose tolerance is impaired (DeFronzo 1981). Moreover, aging is the strongest risk factor for diabetes. In the US, 12 million of the 30

million estimated diabetes cases, in 2015, are 65 years old or older (CDC 2017). This number represents more than quarter of all the people in this age group. If this trend continues, in 2050, out of the projected 48 million cases, 27 million will be 65 years or older which is more than half of all diabetes cases (CDC 2017; Chia, Egan, and Ferrucci 2018). Obesity, as discussed above, is also a risk factor for glucose intolerance and diabetes. All these data demonstrate that obesity and aging share common phenotypes and that obesity increases telomere attrition. Interestingly, many disease-associated mutations in the telomerase components, TERT and TERC, have been identified (Kam, Nguyen, and Ngeow 2021; Podlevsky et al. 2007). Moreover, single nucleotide polymorphisms in TERC significantly increase the risk of diabetes (Al Khaldi et al. 2015). In order to study the role of telomere shortening, several mice models with deletion in either *Tert* or *Terc* were developed. These mice show progressive shortening of telomere length with each generation. Fourth generation (G4) Terc KO mice showed impairment in glucose tolerance. This was to due impaired insulin secretion capacity as a result of a reduction in islet size (Kuhlow et al. 2010). On the other hand, third generation (G3) Terc KO mice showed enhancement in glucose metabolism under normal diet (Missios et al. 2014). All these data show that telomere length and aging modulate energy homeostasis.

1.6 Amino acids and metabolism

Amino acids consist of an amino group and a carboxylic acid group. They play crucial functions in the human body as they are the building blocks of all proteins in the human body. Moreover, amino acids are precursor to neurotransmitters, enzymes and hormones (Wu 2009). Furthermore, during starvation, amino acids can be used to produce energy (Giesecke et al. 1989). Additionally, amino acids, like branched chain amino acids (BCAA), can participate in cell signaling and mammalian target of rapamycin (mTOR) activation (Wu 2009). However, apart from these prominent roles in physiology, several studies demonstrated crucial roles of amino acid in glucose and energy homeostasis. For instance, higher circulating levels of BCAA are observed with obesity (Felig, Marliss, and Cahill Jr 1969). Moreover, in old individuals (62-75 years old), higher BCAA levels are associated with higher fat and lean mass (Mikkola et al. 2020). Furthermore, in a prospective study that followed 2422 individuals for 12 years, it was that found that increased BCAA levels, as well as phenylalanine and tyrosine, are associated with a 5-fold increase in the risk of developing type 2 diabetes (Wang et al. 2011). Additionally, in the Framingham study, high BCAA levels were associated with high risk of developing diabetes 10 years in the future (Biswas, Duffley, and Pulinilkunnil 2019). This finding is also corroborated by observational studies in humans showing that a positive association between dietary BCAA and type 2 diabetes (Isanejad et al. 2017; Zheng et al. 2016). Also in rodents, BCAA contribute to the development of obesity induced insulin resistance (Newgard et al. 2009). Another amino acid that places a role in energy homeostasis is methionine. Methionine restriction improves glucose tolerance and insulin sensitivity (Orgeron et al. 2014; Xu et al. 2019). Furthermore, it reduces body weight and increases energy expenditure in rodents (Green and Lamming 2019; Spring et al. 2019). In addition, Methionine restriction improves lipid profile and decrease hepatosteatosis in diet-induced obese mice (Castaño-Martinez et al. 2019; Sharma et al. 2019; Wu et al. 2019). Interestingly, these metabolic benefits of methionine restriction could be partly explained by fibroblast growth factor 21 (FGF21) which is an adipokine secreted by BAT (Green and Lamming 2019). Moreover, diet-induced obese mice show increased adiponectin levels upon methionine restriction which is in line with the improvement in metabolic parameters (Ables et al. 2012; Castaño-Martinez et al. 2019). Another neglected amino acid that demonstrates a role in energy homeostasis is Serine. Serine is a polar amino acid and was first discovered by Cramer in 1865 as a component of raw silk

(Cramer 1865). Serine is classified as a non-essential amino acid. However, it was found that vertebrates cannot synthesize enough Serine under certain circumstances (De Koning et al. 2003; Metcalf et al. 2018). Serine can be derived from 4 sources namely dietary intake, biosynthesis from glycolytic intermediate 3-phosphoglycerate, glycine and turnover of proteins (El-Hattab 2016). Biosynthesis of Serine from 3-phosphglycerate is catalyzed by phosphoglycerate dehydrogenase (PHGDH), phosphoserine aminotransferase (PSAT) and phosphoserine phosphatase (PSP) (Holm and Buschard 2019). Inhibition of PSP causes insulin resistance in rat adipocytes due to inappropriate serine phosphorylation (Begum, Sussman, and Draznin 1992). Moreover, overexpression of PSAT improves insulin sensitivity in mice (Yu et al. 2014). A study examining non-diabetic Finnish men (45-73 years old) showed that serine levels are positively correlated with insulin secretion and sensitivity and improved glucose tolerance after two hours glucose tolerance test (Vangipurapu et al. 2019). Furthermore, a study comparing type 1 diabetic children to non-diabetic controls found that Serine is decreased in plasma of type 1 diabetic children (Bervoets et al. 2017). Additionally, type 2 diabetic individuals show a reduction of Serine in blood (Bertea et al. 2010; Drábková et al. 2015). In line with this, Serine supplementation in non-obese diabetic mice, a type 1 diabetic mouse model, reduces insulitis and diabetes incidence and improves glucose tolerance (Holm et al. 2018). Recently, our group demonstrated that Serine supplementation blunts fasting-induced weight regain especially in diet-induced obese mice. This could be attributed to increased energy expenditure due to elevated BAT activity (López-Gonzales et al. 2022). These data demonstrate that amino acids regulate body weight, glucose tolerance and insulin sensitivity and therefore should be further tested for therapeutic applications.

1.7 D-serine, serine racemase and N-methyl-D-aspartate receptor in the periphery

All the above studies examined the effect of the L-isoform of the amino acids. However, the D-isoform of amino acids play a physiologically relevant role as well. D-aspartate and D-serine are the only two canonical D-amino acids in the human body and play a role in the nervous system and several endocrine organs (Fuchs et al. 2005; Sasabe and Suzuki 2018). D-serine has been shown to play a role in metabolism and energy homeostasis. D-serine supplementation blunts high fat diet induced weight gain. It also impairs glucose tolerance. This impairment in metabolic parameters was due to lower insulin secretion due to an effect on the sympathetic nervous system (Suwandhi et al. 2018). Moreover, D-serine is linked to the development of diabetic retinopathy (Ozaki et al. 2018). Additionally, D-serine could be involved in the beiging process as deletion of the alanine-serine-cysteine (ASC1, also known as SLC7A10) transporter, which transports, among others, D-serine, leads to induction of beiging in subcutaneous pre-adipocytes upon differentiation (Suwandhi et al. 2021). D-serine can be acquired through the diet, microbiota or through the action of serine racemase which is the only enzyme known to synthesize D-serine *in vivo* in humans and rodents (Wolosker and Mori 2012). Serine racemase was first isolated and cloned from rat brains in 1999, thus solving the mystery of the origin of D-serine in the brain *in vivo* (Wolosker, Blackshaw, and Snyder 1999; Wolosker et al. 1999). Serine racemase catalyzes the conversion of L-serine to D-serine. However, it also catalyzes α,β-elimination of water from L-serine, D-serine and L-threonine leading to the production of pyruvate and ammonium. So, it is hypothesized that serine racemase could regulate D-serine levels in areas of the brain lacking D-amino acid oxidase, which is an enzyme that degrades D-amino acids. Interestingly, 4 molecules of pyruvate are produced for each molecule of D-serine formed and both Mg^{2+} and ATP stimulate the action of serine racemase (Wolosker and Mori 2012). Serine racemase also

regulates glucose homeostasis. This is demonstrated in serine racemase whole body knockout mice that have improved glucose tolerance (Lockridge et al. 2016). This improvement in glucose homeostasis is attributed to improved insulin sensitivity and insulin secretion capacity (Lockridge et al. 2016).

The main function of D-serine *in vivo* is as a co-agonist for the activation of N-methyl-D-aspartate receptors (NMDAR). NMDAR are ionotropic glutamate receptors which are ligand-gated non-selective cation channels. NMDAR are hetero tetrameric receptors consisting of two subunits of GluN1 (encoded by GRIN1), and two subunits of GluN2A-2D (encoded by GRIN2A-2D) or GluN3A-B (encoded by GRIN3A-3B) (Kumar 2015). The channel pore is blocked, in a voltage-dependent manner, by extracellular Mg^{2+}. This block can be released by membrane depolarization. Therefore, for NMDAR activation, both membrane depolarization and binding of the agonist, glutamate, and the co-agonist D-serine (or Glycine) are required. Upon NMDAR activation, Ca^{2+} influx ensues. In the brain, NMDAR are involved in synaptic plasticity and memory and learning (Hansen et al. 2018). However, NMDAR also play a role in the periphery (Hogan-Cann and Anderson 2016). For example, NMDAR activity in the stomach regulate gastric acid secretion and inhibition (Golovynska et al. 2018). In the kidney, NMDAR have an effect on glomerular vasodilation, thereby, modulating renal blood flow, filtration and absorption in the renal proximal tube (Deng and Thomson 2009). Interestingly, D-serine shows acute antidiabetic effects through potentiation of insulin secretion by co-agonism of excitatory β-cells NMDAR (Lockridge et al. 2021). These data highlight the role of D-serine and its target, NMDAR, in the metabolic homeostasis and in peripheral organs function.

1.8 Aims of the work

D-serine supplementation impaired glucose tolerance due to a reduction in insulin secretion based on effects on the sympathetic nervous system. Moreover, D-serine is suspected to play a role in the beiging phenotypes seen when ASC1 is knocked down in subcutaneous pre-adipocytes. These pre-adipocytes show augmented beiging upon differentiation when ASC1 is knocked down. Furthermore, deletion of the enzyme producing D-serine, serine racemase, in mice show improvement in glucose tolerance and insulin sensitivity. Adipose tissue is known to be able to modulate glucose tolerance and insulin sensitivity and is responsible for a part of the post-prandial glucose uptake and could, therefore, play a part in this observed improvement in glucose homeostasis in serine racemase knockout mice. Additionally, Serine levels are decreased in both type 1 and type 2 diabetic individuals and Serine supplementation blunts fasting-induced weight regain through activation of brown fat and increasing energy expenditure. One would wonder if these observations are due to L-serine or simply due to D-serine produced via serine racemase action. Therefore, to elucidate the role of serine racemase and D-serine in adipose tissues, I studied mice with adipose tissue specific deletion of serine racemase. Adipose tissue was histologically and functionally examined. Moreover, the effect of adipose tissue specific deletion of serine racemase on glucose tolerance and insulin sensitivity was studied. Furthermore, one important aspect is to study the beiging effect in fat tissues and if deletion of serine racemase modulates adipose tissue or blood D-serine levels, thus, altering whole-body D-serine availability. As BAT is a major site for non-shivering thermogenesis, I tested if the deletion of serine racemase in adipose tissues could alter whole body energy expenditure and cold temperature tolerance.

The main role of D-serine *in vivo* is to act as a co-agonist of the NMDAR. It is well known that the sympathetic nervous system controls adipose tissue function. But, it is not known if adipose tissues can communicate with the nervous system via neurotransmitters like D-serine. Therefore, I examined if NMDAR are present and functional in the adipose tissue. NMDAR were deleted specifically in the adipose tissue via mating of $Grin1^{flox/flox}$ mice with adiponectin-Cre^{+} mice. The aim was to see if deletion of NMDAR in adipose tissues have an effect on whole body glucose homeostasis, energy expenditure and adipose tissue function and if adipose tissue D-serine communicates with the nervous system and modulate its function.

Aging and obesity are both risk factors for type 2 diabetes and increased mortality. Aging is associated with reduction in telomeres length and it is thought that several of the aging phenotypes are caused by telomere shortening. However, in aged individuals, several co-morbidities, like obesity, exist that make it hard to attribute a given phenotype solely to telomere shortening. Luckily, the effect of telomere shortening can be studied in mice. This can be achieved through telomerase deletion. Thus, no elongation of telomeres will occur and telomere length will gradually decrease with each cell division and with each generation in mice (Blasco 2005; Samper, Flores, and Blasco 2001). Impaired glucose tolerance is seen in G4 Terc KO mice due to diminished insulin secretion as a result of reduced pancreatic islets size (Kuhlow et al. 2010). Meanwhile, G3 Terc KO mice show augmented glucose metabolism under normal diet. However, this improvement in glucose metabolism is abolished when mice are fed high-sugar diet (Missios et al. 2014). Nonetheless, one caveat of these papers is that higher generational numbers (G4 or G3) of Terc KO mice show physiological pathologies and impairments (Samper, Flores, and Blasco 2001), thus, mimicking the situation in aged humans where the observed phenotype could not be attributed solely to shortened telomeres due to the presence of other physiological impairments. Therefore, I studied

telomere function in G2 Terc KO mice. The effect of telomeres shortening on adipose tissues function and morphology was examined. Moreover, energy intake, absorption and expenditure were examined. Furthermore, differences exist between males and females in fat distribution and females tend to have higher body fat than males. Moreover, female rats gain less weight than males when challenged with high fat diet (Palmer and Clegg 2015). An effect that is dependent on estrogen. That´s why I studied both male and female G2 Terc KO. Especially given that males tend to have shorter telomeres than females although both sexes are born with similar telomeres length, indicating a difference in telomerase action (Gardner et al. 2014; Öngel et al. 2021). By studying G2 Terc KO male and female mice, one would be able to elucidate the effects of telomerase deficiency (telomere shortening) on adipose tissue and energy intake and expenditure in both sexes.

2 Materials and Methods

2.1 Materials

2.1.1 Laboratory equipment

Table 1: List of laboratory equipments.

Equipment	Supplier
ACQUITY UPLC system	Waters, Milford, USA
Agilent 2100 Bioanalyzer	Agilent, Santa Clara, California, USA
BenchRocker 2D	Benchmark Scientific, Sayreville, New Jersey, USA
C1000 Touch Thermal Cycler	Biorad, Hercules, California, USA
C7000 calorimeter	Ika, Staufen, Germany
Cell culture hood (Herasafe KS)	ThermoFisher scientific, Waltham, Massachusetts, USA
Cell culture incubator (Heracell 240i)	ThermoFisher scientific, Waltham, Massachusetts, USA
Centrifuge 5430R	Eppendorf, Hamburg, Germany
CFX384 Touch Real-Time PCR Detection System	Biorad, Hercules, California, USA
Cold plate EG 1150 C	Leica, Wetzlar, Germany
DCA Vantage Analyzer	Siemens, Munich, Germany
ECLIPSE Ci microscope	Nikon, Minato city, Tokyo, Japan
Glucometer	Abbott, Wiesbaden, Germany
Heating magnetic stirrer	VELP scientifica, Usmate, Italy
Heraeus Multifuge X3 FR	ThermoFisher scientific, Waltham, Massachusetts, USA
Mice weighing scale (Ranger 4000)	OHAUS Europe, Greifensee, Switzerland
Nanodrop 2000 UV-Vis spectrophotometer	ThermoFisher scientific, Waltham, Massachusetts, USA
NanoPhotometer N60	ThermoFisher scientific, Waltham, Massachusetts, USA
Neubauer counting chamber	Hecht Assistent, Sondheim, Germany
Paraffin embedding station EG 1150 H	Leica, Wetzlar, Germany
PerfectBlue Horizontal Maxi Gel Systems	VWR, Radnor, Pennsylvania, USA
PerfectBlue Power supply	VWR, Radnor, Pennsylvania, USA
Proflex PCR System	ThermoFisher scientific, Waltham, Massachusetts, USA
QuantStudio 7 Flex Real-Time PCR System	ThermoFisher scientific, Waltham, Massachusetts, USA
Savant DNA SpeedVac Concentrator	ThermoFisher scientific, Waltham, Massachusetts, USA
Scale M-prove	Sartorius, Goettingen, Germany
Semi-automated microtome	Leica, Wetzlar, Germany
Shake ´n´ Stack Hybridization Incubator	ThermoFisher scientific, Waltham, Massachusetts, USA

Shaking Incubator	ThermoFisher scientific, Waltham, Massachusetts, USA
Table centrifuge perfect spin mini	PeQ Lab, Erlangen, Germany
Thermomixer C	Eppendorf, Hamburg, Germany
TissueLyser II	Qiagen, Hilden, Germany
TSE PhenoMaster (indirect calorimetry)	TSE systems, Berlin, Germany
Water bath	ThermoFisher scientific, Waltham, Massachusetts, USA
Whole body composition analyzer	EchoMRI, Houston, Texas, USA

Table 2: List of consumables

Consumable	**Supplier**
100µm cell strainer	Corning, Corning, New York, USA
3-piece single use syringe 1ml	B Braun, Melsungen, Germany
Adhesion slides Superfrost Plus	Carl Roth, Karlsruhe, Germany
Cell culture plate, 12 well	Sarstedt, Nümbrecht, Germany
Cell culture plate, 6 well	Sarstedt, Nümbrecht, Germany
Cell scraper	Sarstedt, Nümbrecht, Germany
FilterTips TipOne 0.1-10	Starlab, Hamburg, Germany
FilterTips TipOne 0.5-20	Starlab, Hamburg, Germany
FilterTips TipOne 100-1000	Starlab, Hamburg, Germany
FilterTips TipOne 1-200	Starlab, Hamburg, Germany
Flat bottom 96-well microtiter plate	Greiner, Frickenhausen, Germany
FreeStyle Lite glucose stripes	Abbott, Chicago, Illinois, USA
Goldenrod Animal Lancet	Medipoint, New York, USA
Hard-Shell 384-Well PCR Plates	Biorad, Hercules, California, USA
Histological cassettes	Carl Roth, Karlsruhe, Germany
Microseal `B` PCR Plate Sealing Film	Biorad, Hercules, California, USA
Microvette 500 Serum Gel tubes	Sarstedt, Nümbrecht, Germany
Microvette CB 300 K2 EDTA tubes	Sarstedt, Nümbrecht, Germany
Optical adhesive covers	ThermoFisher scientific, Waltham, Massachusetts, USA
PCR strip	Sarstedt, Nümbrecht, Germany
PCR strip of lids	Sarstedt, Nümbrecht, Germany
Pipettes 10ml	Greiner, Frickenhausen, Germany
Pipettes 25ml	Greiner, Frickenhausen, Germany
Pipettes 5ml	Greiner, Frickenhausen, Germany
Reaction tubes 1ml	Sarstedt, Nümbrecht, Germany
Reaction tubes 2ml	Sarstedt, Nümbrecht, Germany
Single use syringe 1ml (Injekt-H Solo)	B Braun, Melsungen, Germany

2.1.2 Chemicals

Table 3: List of chemicals

Product	Supplier
3-Isobutyl-1-methylxanthin	Sigma-Aldrich, St. Louis, Missouri, USA
Acetic acid	AppliChem, Council Bluffs, Iowa, USA
Agarose	Sigma-Aldrich, St. Louis, Missouri, USA
Ammonium persulfate (APS)	Serva, Heidelberg, Germany
Beta-mercaptoethanol	Carl Roth, Karlsruhe, Germany
Bovine serum albumin (BSA) fraction V	Carl Roth, Karlsruhe, Germany
Bovine serum albumin essentially fatty acid free	Sigma-Aldrich, St. Louis, Missouri, USA
Chloroform	Carl Roth, Karlsruhe, Germany
Chromotrope II R (Eosin)	Alfa Aesar. Ward Hill, Massachusetts, USA
Collagenase type IV	Life Technologies, Carlsbad, California, USA
Dexamethasone	Sigma-Aldrich, St. Louis, Missouri, USA
Dimethyl sulfoxide (DMSO)	Carl Roth, Karlsruhe, Germany
Dithiothreitol (DTT)	VWR, Radnor, Pennsylvania, USA
DMEM, high glucose, GlutaMAX, pyruvate	Life Technologies, Carlsbad, California, USA
DMEM, low glucose, pyruvate, no glutamine, no phenol red	ThermoFisher scientific, Waltham, Massachusetts, USA
DNA/RNA staining dye (peqGREEN)	VWR, Radnor, Pennsylvania, USA
EDTA disodium salt dihydrate	Carl Roth, Karlsruhe, Germany
Ethanol (absolute)	Merck Millipore, Burlington, Massachusetts, USA
Ethanol (denatured)	Brenntag, Essen, Germany
EZ-RUN Recombinant Protein Ladder	ThermoFisher scientific, Waltham, Massachusetts, USA
FastLoad 100bp DNA Ladder	Serva, Heidelberg, Germany
FastLoad 1kb DNA Ladder	Serva, Heidelberg, Germany
Fetal Bovine Serum (FBS)	Life Technologies, Carlsbad, California, USA
Glucose solution 20%	B Braun, Melsungen, Germany
Glycine	Carl Roth, Karlsruhe, Germany
Immobilon Western Chemiluminescent HRP substrate	Merck Millipore, Burlington, Massachusetts, USA
Insulin (Actrapid Pendill)	Novo Nordisk, Bagsværd, Denmark
Insulin (cell culture)	Sigma-Aldrich, St. Louis, Missouri, USA
Isoproterenol hydrochloride	Sigma-Aldrich, St. Louis, Missouri, USA
iTaq Universal SYBR Green Supermix	Biorad, Hercules, California, USA
Ketamine	Pharmanovo, Garbsen, Germany
Mayer´s solution (Hematoxylin)	Merck, Darmstadt, Germany
Methanol	Merck Millipore, Burlington, Massachusetts, USA
Normocin	InvivoGen, San Diego, California, Germany
NP-40	Abcam, Cambridge, United Kingdom
Nuclease-free water	Qiagen, Hilden, Germany
Paraffin	Leica, Wetzlar, Germany
Paraformaldehyde	Carl Roth, Karlsruhe, Germany
Penicillin/Streptomycin (P/S) (10,000 U/ml)	Life Technologies, Carlsbad, California, USA
Phosphatase inhibitor cocktail II	Sigma-Aldrich, St. Louis, Missouri, USA

Phosphatase inhibitor cocktail III	Sigma-Aldrich, St. Louis, Missouri, USA
Phosphate-buffered saline (PBS)	Life Technologies, Carlsbad, California, USA
Platinum Green Hot Start PCR Master Mix (2X)	ThermoFisher scientific, Waltham, Massachusetts, USA
Potassium chloride (KCl)	Carl Roth, Karlsruhe, Germany
Potassium dihydrogen phosphate (KH_2PO_4)	Carl Roth, Karlsruhe, Germany
Protease inhibitor cocktail	Sigma-Aldrich, St. Louis, Missouri, USA
QIAzol	Qiagen, Hilden, Germany
Restore PLUS Western Blot Stripping Buffer	ThermoFisher scientific, Waltham, Massachusetts, USA
Roti-Histokitt II	Carl Roth, Karlsruhe, Germany
Rotiphorese Gel 30	Carl Roth, Karlsruhe, Germany
Sample buffer 4X	Life Technologies, Carlsbad, California, USA
Sodium chloride (NaCl)	Carl Roth, Karlsruhe, Germany
Sodium chloride solution (0.9%)	Fresenius, Bad Homburg, Germany
Sodium dodecyl sulfate (SDS)	Carl Roth, Karlsruhe, Germany
Sodium hydroxide (NaOH)	Carl Roth, Karlsruhe, Germany
Sodium Phosphate (Na_2HPO_4)	Acros Organics, Geel, Belgium
SuperSignal West Femto Maximum Sensitivity Substrate	ThermoFisher scientific, Waltham, Massachusetts, USA
Tetramethylethylenediamine (TEMED)	AppliChem, Council Bluffs, Iowa, USA
Tris	Carl Roth, Karlsruhe, Germany
Triton X-100	Sigma-Aldrich, St. Louis, Missouri, USA
Trypan blue solution	Sigma-Aldrich, St. Louis, Missouri, USA
Trypsin, 0.05% EDTA, phenol red	Life Technologies, Carlsbad, California, USA
Tween-20	Santa Cruz, Santa Cruz, California, USA
Xylazine hydrochloride (20mg/ml)	Prodivet pharmaceuticals, Raeren, Belgium
Xylol	Carl Roth, Karlsruhe, Germany

2.1.3 Primers

Table 4: List of primers

Gene name	Forward (5´ - 3´)	Reverse (3´ - 5´)
Acaca	TGGGCGGGATGGTCTCTTT	AGTCGCAGAAGCAGCCCATT
Actb	TTGCTGACAGGATGCAGAAG	ACATCTGCTGGAAGGTGGAC
Adipoq	GATGGCACTCCTGGAGAGAA	TCTCCAGGCTCTCCTTTCCT
Adrb1	CCGTCGTCTCCTTCTACGTG	CTCGCAGCTGTCGATCTTCT
Adrb2	TCGTGCACGTTATCAGGGAC	AAGGCAGAGTTGACGTAGCC
Adrb3	CCTTCCGTCGTCTTCTGTGT	GCCATCAAACCTGTTGAGCG
Asc1	AGTGTTCCAGGACACCCTTG	GGGTGGCACTCAAGAAAGAG
Asct1	CCTGTTCCCTTCCAATCTTGT	GAGCTGGTGTTATGGGTCAC
Asct2	ACGACTCTGTTGTAGACCCC	AAGGCAGCAGACACCAGATT
Cd36	AATTTGTCCTATTGGCCAAGCT	AGCGTAGATAGACCTGCAAATG
Cebpa	AGGTGCTGGAGTTGACCAGT	CAGCCTAGAGATCCAGCGAC
Cebpb	CCAAGAAGACGGTGGACAA	CAAGTTCCGCAGGGTGCT
Fabp4	GATGCCTTTGTGGGAACCT	CTGTCGTCTGCGGTGATTT

Fasn	GAGGACACTCAAGTGGCTGA	GTGAGGTTGCTGTCGTCTGT
Gamt	GCAGCCACATAAGGTTGTTCC	CTCTTCAGACAGCGGGTACG
Gatm	GACCTGGTCTTGTGCTCTCC	GGGATGACTGGTGTTGGAGG
Glut1	AACTGGGCAAGTCCTTTG	TTCTTCTCCCGCATCATCTG
Glut2	GACATCGGTGTGATCAATGC	ATCCAGTGGAACACCCAAAA
Got2	TGACTTCTCCAGACTTGCGG	TCATGCTGATGATGCGGTCA
Grin1	ATCAAGAATGTGACTCCCGC	AAGATCCCAGCTACGATGCC
Hprt	AAGCTTGCTGGTGAAAAGGA	TTGCGCTCATCTTAGGCTTT
Il1b	CTGAAAGCTCTCCACCTCAA	CCCAAGGCCACAGGTATTTT
P2rx5	CTGCAGCTCACCATCCTGT	CACTCTGCAGGGAAGTGTCA
Pat2	GTGCCAAGAAGCTGCAGAG	TGTTGCCTTTGACCAGATGA
Phgdh	GAGCTCACCTGTGGGATGAT	GCCATCTTTCATCGAAGCTGTT
Pparg	CCCTGGCAAAGCATTTGTAT	GAAACTGGCACCCTTGAAAA
Ppargc1a	AGCCGTGACCACTGACAACGAG	GCTGCATGGTTCTGAGTGCTAAG
Prdm16	CCGCTGTGATGAGTGTGATG	GGACGATCATGTGTTGCTCC
Psat	CAGAGGACTCGGCATCAGTG	AGCAATTCCCTCACAAGATTCTCT
Psph	GGCCAAATTCTGTGGTGTGG	GCCTCTGGACTTGATCCCTG
Slc27a2	TGAATGTGTATGGCGTGCCT	AGGTACTCCGCGATGTGTTG
Slc27a4	CGTTTCGACGGGTACCTCAA	ACATTCTCCCCTTTCCAGCG
Slc5a1	TTTCCGTTCTGTCCCTGCTC	TATCCAGGCCCAAGGCTAGA
Slc5a2	ACCGTATTCGCCTCTACCTGT	GTGTACATCAGTGCCGCCAG
Srr	AACTACGGCTTTGGGCTTCT	GGCGCAATCTTTTCTTCAAA
Tbp	ACCCTTCACCAATGACTCCTATG	TGACTGCAGCAAATCGCTTGG
Tnfa	CCCACGTCGTAGCAAACCA	GTCTTTGAGATCCATGCCGTTG
Ucp1	AGCCATCTGCATGGGATCAAA	GGGTCGTCCCTTTCCAAAGTG

2.1.4 Antibodies

Table 5: List of primary and secondary antibodies

Antibody	**Company**	**Catalog number**
Beta-actin (β-actin-HRP)	Santa Cruz, Santa Cruz, California, USA	Sc-47778
Glutamate Ionotropic receptor NMDA type subunit 1 (GluN1)	ThermoFisher scientific, Waltham, Massachusetts, USA	32-0500
Heat shock protein 70 (HSP70)	Cell signaling, Danvers, Massachusetts, USA	4872
Mouse IgG-HRP	Santa Cruz, Santa Cruz, California, USA	Sc-2005
Phosphoglycerate dehydrogenase (PHGDH)	Cell signaling, Danvers, Massachusetts, USA	13428S
Rabbit IgG-HRP	Cell signaling, Danvers, Massachusetts, USA	7074
Serine racemase (SRR)	Cell signaling, Danvers, Massachusetts, USA	29798
Uncoupling protein 1 (UCP1)	Cell signaling, Danvers, Massachusetts, USA	14670

2.1.5 Kits

Table 6: List of kits

Product	Company	Catalog number
DCA HbA1c Reagent Kit	Siemens, Munich, Germany	10698915
Free Fatty Acid Quantification Colorimetric/Fluorometric Kit	Biovision, Milpitas, California, USA	K612
Free Glycerol Colorimetric/Fluorometric Assay Kit	Biovision, Milpitas, California, USA	K630
High-Capacity cDNA Reverse Transcription Kit	ThermoFisher scientific, Waltham, Massachusetts, USA	4368813
Pierce BCA Protein Assay	ThermoFisher scientific, Waltham, Massachusetts, USA	23225
RNeasy Mini Kit	Qiagen, Hilden, Germany	74106
Triglyceride Quantification Colorimetric/Fluorometric Kit	Biovision, Milpitas, California, USA	K622
Ultrasensitive Mouse Insulin ELISA Kit	CrystalChem, Elk Grove Village, Illinois, USA	90080

2.1.6 Mouse diets

Table 7: List of diets

Type of diet	Chow	High Fat
Name	Altromin 1318	Research Diet D12331
Protein (kcal%)	27	17
Fat (kcal%)	14	58
Carbohydrate (kcal%)	59	25
Total (kcal%)	100	100
Energy density (kcal/g)	3.47	5.56

2.2 Methods

2.2.1 *In vivo* experiments

2.2.1.1 Mouse strains

In $SRR^{fl/fl}$ mice, the first coding exon of the *Srr* gene is flanked by loxP sites enabling excision upon Cre recombinase expression. The $SRR^{fl/fl}$ mice are already characterized (Basu et al. 2009; Benneyworth et al. 2012). $SRR^{fl/fl}$ mice were mated to Adiponectin-Cre mice (mice expressing Cre recombinase under the control of the adiponectin promoter) (Jackson stock No.:010803). The resulting $SRR^{fl/fl}$ mice Adiponectin-Cre^{+} mice ($SRR^{Adipo\text{-}KO}$) have specific deletion of serine racemase in adiponectin expressing cells (fat cells). The $SRR^{fl/fl}$ mice Adiponectin-Cre^{-} littermate mice were used as controls. $Grin^{fl/fl}$ mice were purchased from Jackson laboratory (Stock No.:005246). A loxP site was inserted between exons 9 and 10 and the other loxP site was inserted at the 3´end (Tsien, Huerta, and Tonegawa 1996). Therefore, upon Cre recombinase

expression the entire transmembrane domain and C-terminal region will be excised. $Grin^{fl/fl}$ mice were mated to Adiponectin-Cre mice to generate $Grin^{fl/fl}$ Adiponectin-Cre^{+} ($Grin1^{Adipo\text{-}KO}$) mice and $Grin^{fl/fl}$ Adiponectin-Cre^{-} mice (controls). The Terc KO mice have the entire *Terc* gene disrupted (Blasco et al. 1997). The Terc KO mice were purchased from Jackson laboratory (Stock No.:004132). Heterozygous mice $Terc^{+/-}$ mice were mated to each other to generate first generation (G1) Terc KO mice and WT mice. G1 Terc KO mice were mated to generate second generation (G2) Terc KO mice and WT mice were mated to generate G2 WT mice (controls). G2 Terc KO mice and controls were used for further analysis. $SRR^{Adipo\text{-}KO}$ and $Grin1^{Adipo\text{-}KO}$ mice and their controls were on a C57BL/6J background while G2 Terc KO and WT were on a C57BL/6J&6N mixed background.

2.2.1.2 Housing conditions

Mice were housed in individually ventilated cages in specific pathogen free animal facility at Helmholtz Munich (Neuherberg, Germany). The mice were kept at ambient room temperature of 22±2°C and 45-65% humidity. Mice were kept in 12 hours day and night cycle. Day cycle started from 6 am to 6 pm and the night cycle started from 6 pm to 6 am. All mice had free access (*ad libitum*) to standard chow diet (Altromin 1318, Lage, Germany) and water until further dietary interventions or death. Animal experiments were approved and conducted according to the German animal welfare law and further guidelines and regulations of the government of upper Bavaria (ROB-55.2-2532. Vet_02-17-232 and ROB-55.2-2532. Vet_02-18-188)

2.2.1.3 Glucose tolerance test

Mice were separated and single housed in new, clean cages without food but with *ad libitum* access to water for 4 hours. Thus, mice were fasted for 4 hours during the light phase. After that, mice tails were pierced with a needle and blood glucose levels were measured (fasting glycemia) using a FreeStyle Freedom Lite Glucometer (Abbot, Wiesbaden, Germany). Thereafter, mice received a glucose bolus (2g glucose/kg body weight) (B Braun, Melsungen, Germany) orally then blood glucose levels were measured at 15, 30, 60, 90 and 120 min time points using a FreeStyle Freedom Lite Glucometer.

2.2.1.4 Insulin tolerance test

Mice were separated and single housed in new, clean cages without food but with *ad libitum* access to water for 4 hours. Thus, mice were fasted for 4 hours during the light phase. After that, mice tails were pierced with a needle and blood glucose levels were measured (fasting glycemia) using a FreeStyle Freedom Lite Glucometer. Thereafter, mice received different insulin (Novo Nordisk, Bagsværd, Denmark) doses (Table 8) depending on diet and age of mice via intraperitoneal injection with a syringe then blood glucose levels were measured at 15,30, 60, 90, 120 min post injection using a FreeStyle Freedom Lite Glucometer.

Table 8: Insulin doses

Genotype	Diet	Gender	Insulin does (IU/kg)
$SRR^{Adipo\text{-}KO}$	Chow	male	1.25
$SRR^{Adipo\text{-}KO}$	High fat diet	male	1.5
$Grin1^{Adipo\text{-}KO}$	Chow	male	0.75
Terc KO	Chow	male	1.5
Terc KO	Chow	female	0.75

2.2.1.5 Body composition analysis

Mice body composition (fat mass and lean mass) was measured via nuclear magnetic resonance whole body composition analyzer (EchoMRI, Houston, Texas, USA) during the light phase without fasting.

2.2.1.6 Energy metabolism studies

Mice were single housed in metabolic cages with *ad libitum* access to food and water. Respiratory gases (CO2 and O2) were measured via indirect calorimetry (TSE systems, Berlin, Germany) to calculate energy expenditure (EE) and respiratory exchange ratio (RER). Food intake, water intake as well as locomotor activity were also analyzed.

2.2.1.7 Glycosylated hemoglobin (HbA1c) measurement

HbA1c was measured from random fed mice without fasting during the light phase. The measurement was done by piercing the mice tail to collect a drop of blood. Blood was analyzed using a DCA vantage analyzer (Siemens, Munich, Germany) and the percentage of HbA1c was given.

2.2.1.8 Sacrifice and tissue collection

Mice were euthanized through intraperitoneal injection of Ketamin (100mg/kg) (Pharmanovo, Garbsen, Germany) and Xylazine (7mg/kg) (Prodivet pharmaceuticals, Raeren, Belgium). Blood was collected through heart puncture and placed in Microvette 500 Serum Gel tubes (Sarstedt, Nümbrecht, Germany) on ice. The blood was then centrifuged at 12000g for 10 min at 4°C and the serum was collected and stored at -80°C until further use. After blood collection, the mice were killed by cervical dislocation. Tissues were excised and either 1) snap frozen on dry ice and later placed at -80°C for protein and mRNA analysis or 2) placed in 4% paraformaldehyde (PFA) in PBS (Gibco, Waltham, Massachusetts, USA) for overnight incubation at 4°C to fix the tissues for histology. Tail pieces were taken to re-genotype the mice. For plasma insulin measurement, mice were fasted for 4 hours then the facial vein was pierced via a Goldenrod animal lancet (Medipoint, New York, USA) and blood was collected in Microvette CB 300 K2 EDTA tubes (Sarstedt) and then centrifuged at 12000g for 10 min at 4°C. Plasma was collected and stored at -80°C until later use.

2.2.1.9 Food intake measurement

Two mice of the same genotype were placed in a clean cage. A known amount (weight) of food was placed for the mice. After three days, the remaining food was collected and weighed. The bedding was examined to see any food pieces to ensure that all remaining food is weighed. Thereafter, the amount of food intake was calculated as Initial food weight minus remaining food weight. The value was then divided by three to calculate food intake per one day. Feces were also collected for bomb calorimetry (see below)

2.2.2 *Ex vivo* measurement

2.2.2.1 Genotyping

Ear clips were collected from mice upon weaning. Ear clips were stored at -20°C until use. To extract DNA for genotyping, 100µl of NaOH (50mM) was added to the ear clips followed by heating at 95°C for 30 min without shaking. The pH was then adjusted by addition of 10µl of Tris (1M) pH=8. 1µl of digested DNA was added to PCR master mix (Table 9) and amplified using the corresponding protocols for the different genes (Table 10-13). The amplified PCR product were loaded on 3% (w/v) agarose gel containing PeqGREEN

DNA/RNA binding dye (VWR, Radnor, Pennsylvania, USA) at 250V until complete separation of the bands. The bands were visualized using Chemidoc MP Imaging System (Sigma-Aldrich, St. Louis, Missouri, USA).

Table 9: PCR Master Mix

Reagent	Volume (µl)
Platinum Green Hot Start PCR Master Mix (2X)	5
Primers (10µM)	0.5
Nuclease-free water	4
Total	9.5

Table 10: *Srr* PCR protocol

PCR steps	Temperature (°C)	Time	Number of cycles
Denaturation	95	2 min	1
Melting	94	30 sec	35
Annealing	58	1 min	35
Extension	72	1 min	35
Extension	72	10 min	1
Cooling	8	Infinite	1

Table 11: *Adipoq-Cre* PCR protocol

PCR steps	Temperature (°C)	Time	Number of cycles
Denaturation	95	2 min	1
Melting	95	20 sec	10
Annealing	65 (-0.5°C/cycle)	15 sec	10
Extension	68	10 sec	10
Melting	94	15 sec	27
Annealing	60	15 sec	27
Extension	72	10 sec	27
Extension	72	5 min	1
Cooling	8	Infinite	1

Table 12: *Grin1* PCR protocol

PCR steps	Temperature (°C)	Time	Number of cycles
Denaturation	94	2 min	1
Melting	94	20 sec	10
Annealing	65 (-0.5°C/cycle)	15 sec	10
Extension	68	10 sec	10
Melting	94	15 sec	28
Annealing	60	15 sec	28
Extension	72	10 sec	28
Extension	72	5 min	1
Cooling	8	Infinite	1

Table 13: *Terc* PCR protocol

PCR steps	Temperature (°C)	Time	Number of cycles
Denaturation	94	2 min	1
Melting	94	20 sec	9
Annealing	65 (-0.5°C/cycle)	15 sec	9
Extension	68	10 sec	9
Melting	94	15 sec	27
Annealing	60	15 sec	27
Extension	72	10 sec	27
Extension	72	2 min	1
Cooling	8	Infinite	1

2.2.2.2 Feces bomb calorimetry

Feces were dried for three days at 65°C in a Hybridization incubator (ThermoFisher scientific, Waltham, Massachusetts, USA) along with samples of diet. 500 mg feces and diet were used for measurement of the fecal caloric content using C7000 calorimeter (Ika, Staufen, Germany). Feces (and diet) energy is presented as kilojoule per gram (kJ/g).

2.2.2.3 Free fatty acid extraction from feces

50 mg dried feces were weighed and placed in a tube followed by addition of 250 µl of 1% Triton X-100 in pure chloroform. A metal bead was added and feces were homogenized using Tissuelyser II (Qiagen, Hilden, Germany) for two runs. First run is for 5 min at 30 Hz and second run is for 10 min at 30 Hz. Thereafter, 1.7 ml of 1% Triton X-100 in pure chloroform was added and the tube was vortexed extensively. The tube was centrifuged for, at least, 10 min at 20000g at 4°C. 800µl solution was collected from the bottom of the tube (avoid the upper feces layer). This was followed by another round of centrifugation at 20000g for 10 min at 4°C then 400µl solution was collected from the bottom of the tube. One last centrifugation was done and 100µl solution was collected from the bottom of the tube (clear liquid). The solution was air dried in an oven for a few hours at 50-55°C then vacuum dried for 30 min in Savant DNA SpeedVac Concentrator (ThermoFisher scientific). The fatty acids were resuspended in the assay buffer from the Free Fatty Acid Quantification Colorimetric/Fluorometric kit (Biovision, California, USA).

2.2.2.4 Serum, liver and feces metabolites

100 mg of liver and feces samples were weighed. 1 ml of 5% NP-40 in water (Abcam, Cambridge, United Kingdom) and a metal bead were added to each sample. The samples were homogenized twice using Tissuelyser II for 3 min at 30Hz. The samples were heated at 95°C for 5 min then cooled to room temperature (RT). The samples were re-heated at 98°C for 6 min until the solution became cloudy. Thereafter, the samples were centrifuged at 20000g for 3 min at RT. 125µl of the sample solution (supernatant) was diluted with 875µl water and then used for analysis.

Serum, liver and feces triglycerides were measured using the fluorometric analysis of the Triglyceride Quantification Colorimetric/Fluorometric Kit (Biovision). Free fatty acids levels were determined using the Free Fatty acid Colorimetric/Fluorometric Kit (Biovision). Free glycerol levels were measured using Free Glycerol Colorimetric/Fluorometric Assay Kit (Biovision). Plasma insulin levels were measured using the Ultrasensitive insulin kit (Crystal Chem, Elk Grove Village, Illinois, USA)

2.2.2.5 Histology

For histological analysis, tissues were placed in 4% PFA in PBS overnight at 4°C. The tissues were then placed in 70% Ethanol. This was followed by dehydration steps in ascending concentrations of ethanol to remove the water. The tissues were moved to 80% Ethanol for 1h then 90% Ethanol for 1h then pure Ethanol for 1h followed by a second pure Ethanol incubation for 1h. The tissues were then cleared by Xylol incubation. This was done three times. The first and second incubation were for 10 min and the third incubation was for 15 min. After that, the tissues were infiltrated by paraffin which entailed two paraffin incubations for 1h followed by an overnight incubation with paraffin. All paraffin incubation steps were done at 65°C. Thereafter, the tissues were embedded into paraffin blocks using a paraffin embedding station (Leica, Wetzlar, Germany). The tissues were placed into a shaped mold, then molten paraffin was poured into the mold. The paraffin was rapidly cooled using cold plate (Leica). Thereafter the tissue, now embedded into a paraffin block, was removed from the shaped mold. The paraffin blocks were kept at RT for later use. Before usage (cutting the paraffin blocks), blocks were placed at 4°C for one day and then at -20°C the day before cutting. The blocks were cut into two micrometer sections using a semi-automated microtome (Leica). The tissue sections were placed on adhesion slides Superfrost PLUS (Carl Roth, Karlsruhe, Germany) and later stained

2.2.2.6 Hematoxylin and Eosin staining

Tissue sections were cleared twice with Xylol, each time for 2 min. After that, the sections were re-hydrated in descending concentration of Ethanol. This is done as follows, firstly the sections are incubated in pure Ethanol then 90% Ethanol then 70% Ethanol then deionized water. Each of these incubation steps was done for 2 min. Thereafter, the sections were incubated with Hematoxylin for 1.5 min followed by a dip in deionized water and then an incubation for 2 min under running tape water. The sections were then incubated in 98% Ethanol for 2 min then in pure Ethanol for 2 min. After that, the sections were incubated with Eosin for 3 min and then dipped three times in 98% Ethanol and incubated in pure Ethanol for 2 min. Then, the sections were cleared twice in Xylol. Each time for 5 min. After staining, few drops of Roti-Histokit II (Carl Roth) were added to the microscopic slide to permanently mount the coverslip. The sections were left to dry then imaged using ECLIPSE Ci microscope (Nikon, Minato city, Tokyo, Japan).

2.2.2.7 *Ex vivo* lipolysis

Mice were sacrificed by cervical dislocation. Inguinal subcutaneous white adipose tissue (scWAT) and perigonadal visceral white adipose tissue (pgWAT) were isolated from the mice and cut into small pieces using spring scissors and placed in PBS. Each piece was between 5 to 8 mg. Thereafter, small fat tissue pieces (fat pads) were placed in Dulbecco modified eagle medium (DMEM) (Life Technologies, Carlsbad, California, USA) + 2% fatty acid free bovine serum albumin (BSA) (Sigma-Aldrich) + 1% Penicillin/Streptomycin (P/S) (Life Technologies) and placed in cell culture incubator at 37°C for 30 min at 5% CO2. After that, the fat pads were transferred to DMEM without phenol red (ThermoFisher scientific) + 2% fatty acid free BSA + 1% P/S either with or without 1µM Isoproterenol (Sigma-Aldrich). After three hours, the fat pads were transferred to a Chloroform:Methanol (2:1) solution for 1h at 37°C to delipidate the fat pads and the culture medium was frozen at -80°C for later analysis of free glycerol levels. Then, the fat pads were transferred to 500µl of lysis buffer (0.3N NaOH + 0.1% sodium dodecyl sulfate (SDS) in water) at 40°C for an overnight incubation. The next day, the lysed/digested fat pads were frozen at -20°C for future protein concentration measurement.

2.2.2.8 Enterocytes isolation

This protocol is a modified version of a published protocol (Gracz, Puthoff, and Magness 2012). Small intestine was removed from dead mice. Small intestine was flushed with ice cold PBS to remove feces. Two centimeter pieces were cut from the duodenum, jejunum and ileum and placed in 4% PFA in PBS for histology (see above). Thereafter, the small intestine was opened longitudinally and was swirled around in ice cold PBS to remove remaining feces. Then, the small intestine was placed in solution 1 (30 mM ethylenediaminetetraacetic acid (EDTA), 1 mM dithiothreitol (DTT) in PBS) for 30 min at 4°C. After that, the small intestine was placed in solution 2 (30 mM EDTA in PBS) for 10 min at 37°C followed by shaking to dissociate the enterocytes from the basement membrane. The basement membrane was then discarded and the enterocytes were pelleted by centrifugation at 1000g for 5 min at 4°C. The supernatant was discarded and the pelleted enterocytes were frozen at -80°C for later use.

2.2.2.9 Stromal vascular fraction and mature adipocytes isolation

Mice were sacrificed by cervical dislocation. scWAT, pgWAT and interscapular brown adipose tissue (BAT) were extracted from dead mice and placed on a 10 cm petri dish. After that, the tissues were cut into small pieces using two razor blades. The tissue was then placed in digestion solution (10 ml) consisting of 1% BSA (Carl Roth) and 1 mg/ml Collagenase type IV (Life Technologies) in DMEM for 30 min at 37°C shaking at 1000rpm. Thereafter, 10 ml of PBS was added to stop the digestion at RT. The digested tissues were filtered through a 400µm filter to remove undigested tissue pieces and debris. The filtered solution was left for 10 min at RT to allow the mature adipocytes to float then it was centrifuged at 100g for 5 min at RT. The floating adipocytes were collected and frozen at -80°C for mRNA extraction while the remaining solution, containing the cells from the stromal vascular fraction (SVF), was centrifuged at 800g for 5 min at RT then the supernatant was discarded and the primary cells were immediately used for cell culturing (see below) or frozen at -80°C for later use.

2.2.2.10 Adipocyte size quantification

Hematoxylin and Eosin stained sections were used for adipocyte size quantification. Three images were taken from different areas per tissue per mouse. The quantification was done using the plugin Adiposoft in the free publically available software Fiji (imagej.net/software/fiji). The minimum and maximum adipocyte size depended on the magnification and the fat depot tested. The area of the adipocytes was measured in pixels and then converted to μm^2 using Fiji.

2.2.3 *In vitro* experiments

2.2.3.1 Isolation of primary cells

SVF cells were isolated as described above. The cells were re-suspended in DMEM + 10% fetal bovine serum (FBS) + 1% P/S (cell culture medium) then centrifuged at RT for 5 min at 500g. The supernatant was discarded and cells were re-suspended in 10 ml cell culture medium followed by another centrifugation round at 500g for 5 min at RT. The supernatant was discarded and cells were re-suspended in 2 ml of cell culture medium and plated on a 6-well plate (Sarstedt). The cell culture medium was exchanged the day after with a fresh culture medium.

2.2.3.2 Culturing and differentiation of pre-adipocytes

Pre-adipocytes were maintained in culture and the medium was replaced every other day until reaching 70% confluency. Upon reaching 70% confluency, the cells were washed with PBS then the PBS was

discarded. After that, 500µl trypsin (Life Technologies) was added to detach the cells. Thereafter, 1 ml of cell culture medium was added to the detached cells followed by centrifugation for 5 min at 500g at RT. The supernatant was discarded and the cells were re-suspended in 200µl cell culture medium and counted via addition of 10µl cell culture medium (containing re-suspended cells) to 10µl trypan blue (Sigma-Aldrich) then adding 10µl of the mixture to a Neubauer counting chamber (Hecht Assistant, Sondheim, Germany) and counting the cells manually. 10000 cells/well were added in a 12-well plate (Sarstedt). Upon reaching 95% confluency, Induction of pre-adipocytes differentiation was initiated (day 0) using induction mix (Table 14). At day two, the medium was exchanged with differentiation medium (Table 14). At day 8, the medium was discarded and the cells were frozen at -80°C for further analysis.

Table 14: Induction and differentiation medium for cultured cells

Compound	Induction medium (Final conc.)	Differentiation medium (Final conc.)
Insulin	100nM	100nM
Dexamethason	5µM	--
3-Isobutyl-1-methylxanthine (IBMX)	0.5mM	--
	In DMEM +10% FBS + 1% P/S	In DMEM +10% FBS + 1% P/S

2.2.4 Molecular biological techniques

2.2.4.1 RNA isolation from cells and tissues.

For *in vitro* differentiated cells, 150µl of 2% DTT in RLT buffer from RNeasy Mini Kit (Qiagen) was added per well. The cells were scraped using cell scraper (Sarstedt). 150µl of 70% Ethanol was added to the wells (total volume 300µl) and the whole volume was mixed by pipetting up and down. Thereafter, the whole volume was transferred to RNeasy Mini Kit columns. RNA extraction proceeded according to the manufacturer´s instructions (Protocol form RNeasy Mini Kit).

For RNA extraction from tissues, tissues were taken out of the -80°C freezer. Using liquid nitrogen, tissues were powdered using a pestle and mortar. One third of the powdered tissue was placed in a 2 ml tube then one metal bead was added per tube. 1 ml QIAzol (Qiagen) was added per tube. Thereafter, the tissue was lysed using Tissuelyser II twice. Each time for 2 min at 30Hz. After that, 200µl Chloroform was added per tube and the tube was shaken vigorously for 15sec. The tube was left standing at RT for 5 min followed by centrifugation at 12000g for 15 min at 4°C. The clear upper supernatant was collected in a new tube and same volume of 70% Ethanol (same volume as collected supernatant) was added to the supernatant. The solutions were mixed and transferred to RNeasy Mini Kit columns and RNA extraction proceeded according to the manufacturer´s instructions. RNA was re-suspended in Nuclease free water and RNA concentration was measured using Nanodrop (ThermoFisher scientific). Thereafter, RNA was stored at -80°C for future analysis.

2.2.4.2 cDNA synthesis and qPCR

Complementary DNA (cDNA) was reverse transcribed from isolated RNA. 1000ng/20µl RNA was reverse transcribed into cDNA using High-Capacity cDNA Reverse Transcription Kit (ThermoFisher scientific) and stored at -20°C for future analysis. Real-Time PCR (qPCR) was done using iTaq Universal SYBR Green Supermix (Biorad, Hercules, California, USA) in 384 well plates (Biorad) using CFX384 Touch Real-Time PCR

Detection System (Biorad) using the following protocol (Table 15). Samples were run in triplicates and data were analyzed using CFX Maestro Software (biorad). qPCR primer sequences are listed in table 4. Differential gene expression levels were calculated via the ΔCt method and are normalized to a house keeping gene.

Table 15: qPCR protocol

Steps	Temperature (°C)	Time (sec)	Number of cycles
Denaturation	95	30	1
Melting	95	5	40
Annealing, extension and fluorescence read	60	30	40
Melting	95	10	1
Annealing extension and fluorescence read	65 (+0.5°C/cycle)	5	60

2.2.4.3 Single cell RNA sequencing

Using the ChromiumTM Single-cell 3´Library and gel bead kit v2 from 10X genomics, single cell libraries were generated. The analysis including cell type assignment, heterogeneity analysis, differential expression analysis and gene set enrichment analysis were all done by Dr. Viktorian Miok from the institute of Diabetes and Obesity (Helmholtz Munich) as previously described (Suwandhi et al. 2021).

2.2.4.4 RNAseq analysis

Using Agilent 2100 Bioanalyzer automated electrophoresis system (Agilent, Santa Clara, California, USA), RNA integrity number (RIN) values were determined. Only RNA with RIN value above 9 was used for subsequent analysis. Dr. Elisabeth Graf from the institute of human genetics (Helmholtz Munich) kindly performed the RNAseq analysis. The analysis was done as previously described (Haack et al. 2013). Dr. Dominik Lutter from the institute of Diabetes and Obesity (Helmholtz Munich) evaluated the data using R package DESeq2 (Love, Huber, and Anders 2014). This data set is already presented in a recent publication (Karlina et al. 2021).

2.2.4.5 Protein isolation

Frozen tissue samples were taken from -80°C freezer. Tissues were powdered under liquid nitrogen using a pestle and a mortar. Two-thirds of the powdered tissue were taken in a 2 ml tube for protein extraction. Lysis buffer consisting of RIPA buffer (50mM Tris (pH 7.4), 150mM NaCl, 1mM EDTA and 1% Triton X100 (Sigma-Aldrich)), 1% protease inhibitor (Sigma-Aldrich), 1% phosphatase inhibitor cocktail II (Sigma-Aldrich) and 1% phosphatase inhibitor cocktail III (Sigma-Aldrich) was added to the powdered tissue along with a metal bead. Tissue was homogenized in the lysis buffer using Tissuelyser II twice. Each time for 2 min at 30Hz. 0.1% SDS was added to the lysis buffer and the tube was left standing on ice for 10 min. Thereafter, the tube was centrifuged at 14000g for 30 min at 4°C. The supernatant was collected and if the supernatant was not a clear liquid (due to the presence of lipid or debris), the centrifugation step was repeated and the clear supernatant was collected. After that, protein concentration was determined via Pierce BCA Protein Assay Kit (ThermoFisher scientific). Then, 4X sample buffer (containing 10% β-mercaptoethanol), nuclease free water and the protein lysate were mixed to get the desired protein concentration and 1X sample buffer (Final conc.: 2.5% β-mercaptoethanol). The mixture was boiled for 5 min at 95°C then frozen at -20°C for later analysis.

2.2.4.6 SDS-PAGE and western blot

Sodium dodecyl sulfate-poly acrylamide gel electrophoresis (SDS-PAGE) was performed to separate proteins according to their molecular weight. A 10% resolving gel was loaded followed by a 4% stacking gel according to table 16. Samples were loaded in the wells along with a FisherBioreagents EZ-Run Prestained *Rec* Protein Ladder (ThermoFisher scientific). The gel was run under 100V in running buffer (25mM Tris, 198mM Glycine and 0.1% SDS) until the samples reached the resolving gel. Thereafter, the voltage was changed to 120V until the samples reached the end of the resolving gel. After that, the samples were transferred from the gel to a 0.45µM polyvinylidendifluorid (PVDF) membrane (ThermoFisher scientific) in blotting buffer (25mM Tris, 198mM Glycine and 20% Methanol) for 70 min at 100V on ice. Thereafter the membrane was blocked by 5% milk in TBS-T (1.21g Tris, 8.5g NaCl and 1% TWEEN-20 (Santa Cruz, Dallas, Texas, USA) in one liter water) for 1h at RT to block unspecific binding sites. Primary antibodies were either prepared in 5% milk in TBS-T or 5% BSA in TBS-T and the membrane was incubated with the primary antibody over night at 4°C. The next day, the membrane was washed three times (each 5 min) with TBS-T and incubated with a secondary antibody conjugated with HRP for 1h at RT. Thereafter, the membrane bands were developed using Immobilon Western Chemiluminescent HRP Substrate (Merck, Darmstadt, Germany) and detected using Chemidoc MP Imaging System. After detection of the target protein, the membrane was stripped for 15 min at RT using Restore PLUS Western Blot Stripping-Puffer (ThermoFisher scientific) then re-blocked and re-incubated with an antibody against a house keeping (loading control) protein. The bands of the target protein were normalized to the bands of the house keeping protein using Fiji software.

Table 16: Resolving and stacking gels recipes

Solution	**Resolving gel**	**Stacking gel**
H_2O	4.1ml	3ml
Rotiphorese Gel 30	3.3ml	750µl
Tris-HCl 1.5M pH 8.8	2.6ml	--
Tris-HCl 0.5M pH 6.8	--	1.3ml
SDS 10%	100µl	50µl
APS 10%	50µl	25µl
TEMED	15µl	10µl
Total	10ml	5ml

2.2.4.7 Ultra High performance liquid chromatography/mass spectrometry

Ultra high performance liquid chromatography coupled with mass spectrometry (HPLC/MS) was done by Dr. Constanze Müller from the institute of analytical biochemistry (Helmholtz Munich) as already published in detail (Müller et al. 2014). In brief, the cells were disrupted using Tissuelyser II and protein was precipitated using 500µl Methanol. Derivatization of the samples was done using a freshly prepared o-phthalaldehyde and isobuteryl-L-cysteine solution. Enantiomeric separation was done using ACQUITY UPLC system (Waters, Milford, USA) coupled to a fluorescence detector. The ACQUITY UPLC system was coupled to a mass spectrometer to permit mass spectrometric detection. All D-serine values are normalized to Methionine.

2.2.5 Statistical analysis

Data are presented as mean ± standard error of the mean (SEM) unless indicated otherwise. Statistical significance was calculated using unpaired student´s t-test. For multiple comparisons, statistical significance was determined using one- or two-way analysis of variance (ANOVA) followed by turkey´s or Sidak´s multiple comparison´s test. For one-way analysis of co-variance (ANCOVA), statistical significance was calculated using SPSS statistics. P-value below 0.05 was considered significant. *P<0.05, **P<0.01, ***P<0.001, ****P<0.0001.

3 Results

3.1 Terc deletion reduces body weight in mice

One risk factor for the development of the type 2 diabetes and the metabolic syndrome is aging (Chang and Halter 2003) and it is well known that glucose intolerance increases with aging (DeFronzo 1981). Several impairments on the tissue and whole body level associate with the increased propensity to develop type 2 diabetes and the metabolic syndrome. One of these impairments is telomere shortening (Khalangot et al. 2019; Révész et al. 2015; Wang et al. 2016). Glucose intolerant individuals show shorter telomeres than controls and this shortening of telomeres is exacerbated in type 2 diabetic individuals (Adaikalakoteswari et al. 2007). Moreover, obese individuals have shorter telomeres than lean counterparts and aging is associated with increased fat mass and shorter telomeres (LaRocca, Seals, and Pierce 2010; Valdes et al. 2005). Therefore, to study the effect of telomere shortening on body composition and whole body energy metabolism, we studied second generation Terc KO mice. 13 months old Terc KO mice showed a marked reduction in body weight in both sexes (Figure 1a&d). This reduction was seen in both lean and fat mass (Figure 1b&e) and also evident in different tissues weight (Figure 1c&f). Histological examination of pgWAT via H&E staining revealed clearly different morphology between the genotypes (Figure 1g). This was followed by adipocyte size quantification which demonstrated marked reduction in adipocyte size in Terc KO mice (Figure 1h). Moreover, Terc KO mice exhibited a reduction in liver triglyceride content (Figure 1i). These observations are in line with the reduction in fat mass and body weight. Thus, telomere shortening reduces body weight, body composition and tissues weight in mice.

The clear reduction in body weight of Terc KO mice could be due to a reduction in food intake. To answer this question, food intake was measured. Interestingly, both male and female Terc KO mice showed no reduction in food intake in comparison to controls (Figure 2a). Moreover, Terc KO mice showed no difference in water intake in comparison to controls (Figure 2b). One other explanation for the reduction in body weight could be an increase in energy expenditure. However, Terc KO mice displayed no difference in energy expenditure in comparison to controls when energy expenditure is normalized to body weight (Figure 2c). At the same time no significant difference in the cumulative locomotor activity was observed between the genotypes in both sexes (Figure 2d). Therefore, the reduction in body weight in Terc KO mice could not be explained by alterations in food intake, energy expenditure or locomotor activity.

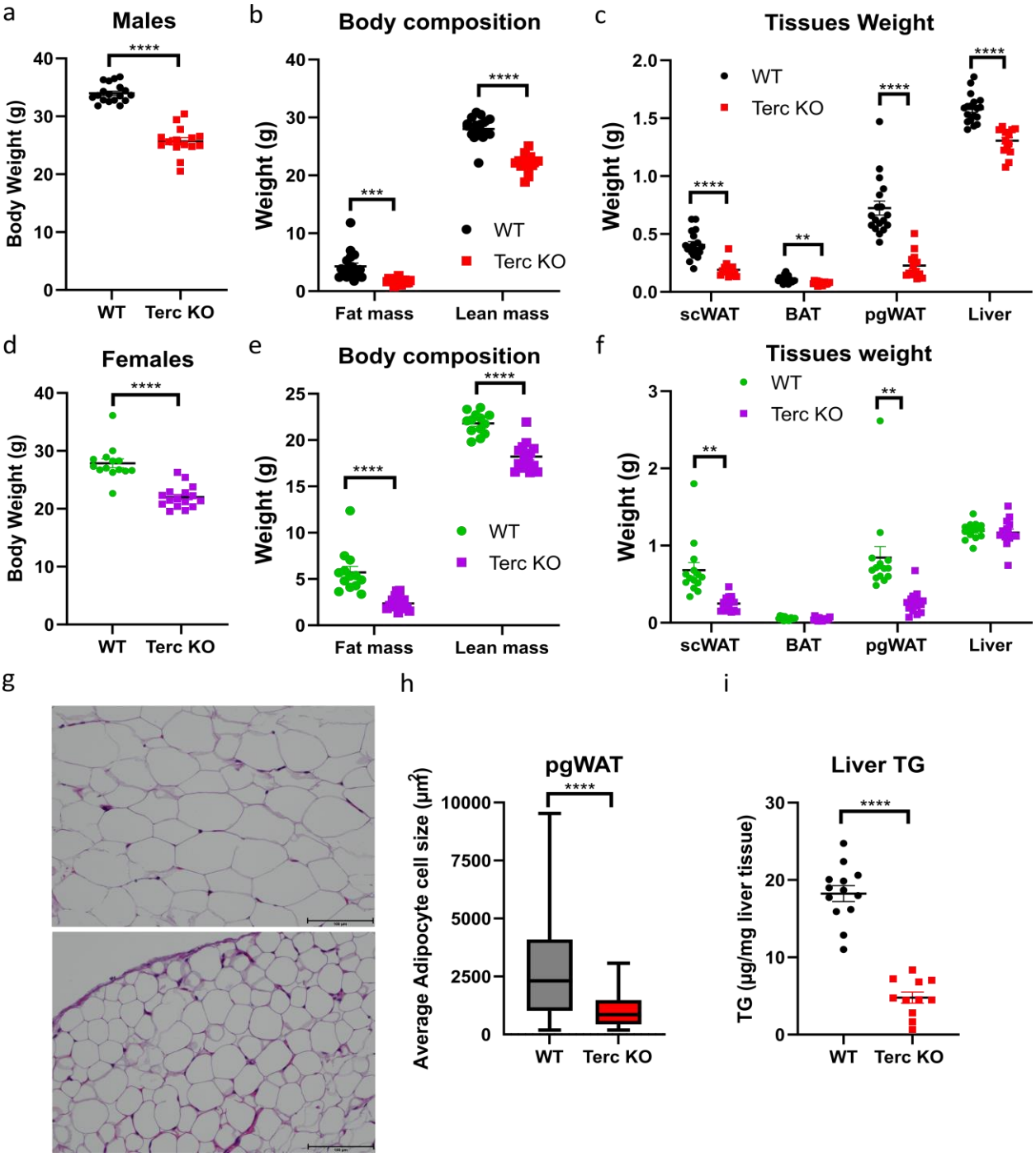

Figure 1: Terc KO mice show reduced body weight, body composition and tissues weight.
a) Body weight, b) body composition and c) tissues weights in male Terc KO mice (n=15) and controls (n=18). d) Body weight, e) body composition and f) tissues weight in female Terc KO mice (n=16) and controls (n=13-14). g) Representative H&E stained histological images from male Terc KO mice and controls. h) Average pgWAT adipocyte size from male Terc KO mice (n=4, cells 5000<) controls (n=3, cells 2500<). **P<0.01, ***P<0.001, ****P<0.0001. Data are shown as mean ± SEM. Statistics were calculated using unpaired t-test or Two-way ANOVA followed by Sidak´s multiple comparison test. Scale=100µm.

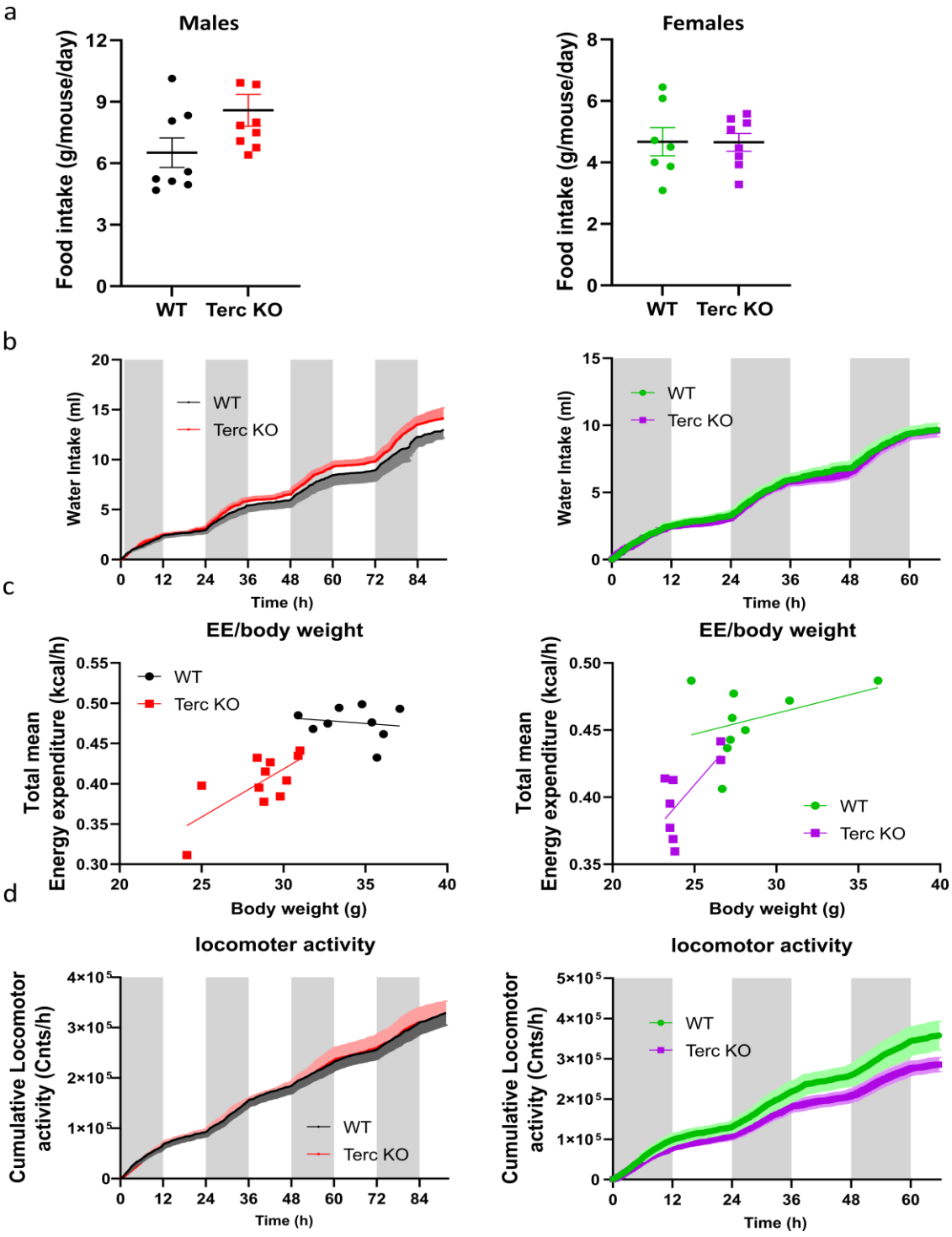

Figure 2: Telomere shortening does not alter energy expenditure, food intake, water intake or locomotor activity in mice.

a) Food intake, b) water intake, c) total mean energy expenditure plotted against body weight and d) cumulative locomotor activity in male Terc KO mice (n=11-12) and controls (n=9) (left side) and female Terc KO mice (n=8) and controls (n=8) (right side). Data are shown as mean ± SEM. Statistics were calculated using unpaired t-test or Two-way ANOVA followed by Sidak´s multiple comparison test.

Another explanation for the reduction in body weight in Terc KO is Villi atrophy. Vilii atrophy was observed in G4 Terc KO mice and a slight villi atrophy was observed in G3 Terc KO mice (Samper, Flores, and Blasco 2001). Atrophied villi could result in malabsorption (Eijsbouts et al. 1995; Ziegler et al. 2003) and, hence, reduction in body weight. However, Terc KO mice show no difference in villi morphology in comparison to controls as evident by H&E staining (Figure 3a) and show similar duodenum and jejunum villi length (Figure 3b) in comparison to controls. Moreover, male Terc KO mice exhibit no difference in fecal caloric (Figure 4a) content while female Terc KO show higher fecal caloric content (Figure 4e) in comparison to controls. Hence, female Terc KO mice show a sign of malabsorption as evident by lower body weight and higher fecal caloric content in comparison to controls.

Dissection of feces composition revealed lower glycerol level in feces of male Terc KO mice (Figure 4b) and a trend to higher triglyceride content (although statistically insignificant) than controls (Figure 4c). On the other hand female Terc KO mice showed no differences in either fecal glycerol content (Figure 4f) or triglyceride content (Figure 4g) in comparison to controls. Male Terc KO mice also showed a trend towards lower fecal free fatty acids level in comparison to controls (Figure 4d) while female Terc KO mice showed no difference (or even a trend) in fecal free fatty acids level (Figure 4h). Male Terc KO mice seem to show impairment in intestinal lipolysis as evident by higher fecal triglyceride content and lower glycerol and fatty acids content.

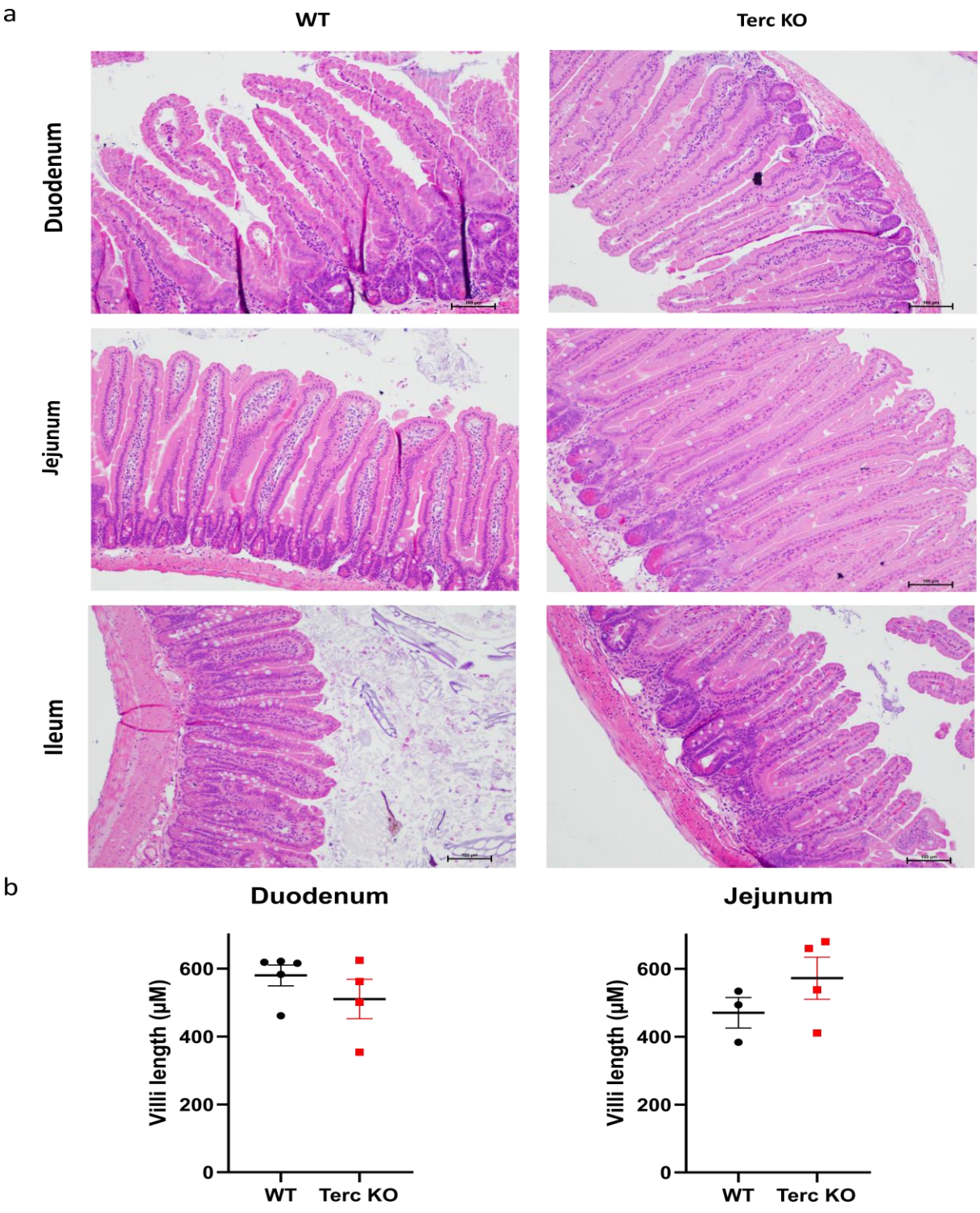

Figure 3: Terc KO mice show no villi atrophy and similar villi length to controls.
a) Representative H&E stained histological images from duodenum, jejunum and ileum of male Terc KO mice and controls. b) Villi length quantification of duodenum and jejunum villi length from male Terc KO mice (n=4) and controls (n=3-5). Data are shown as mean ± SEM. Statistics were calculated using unpaired t-test. Scale=100µm.

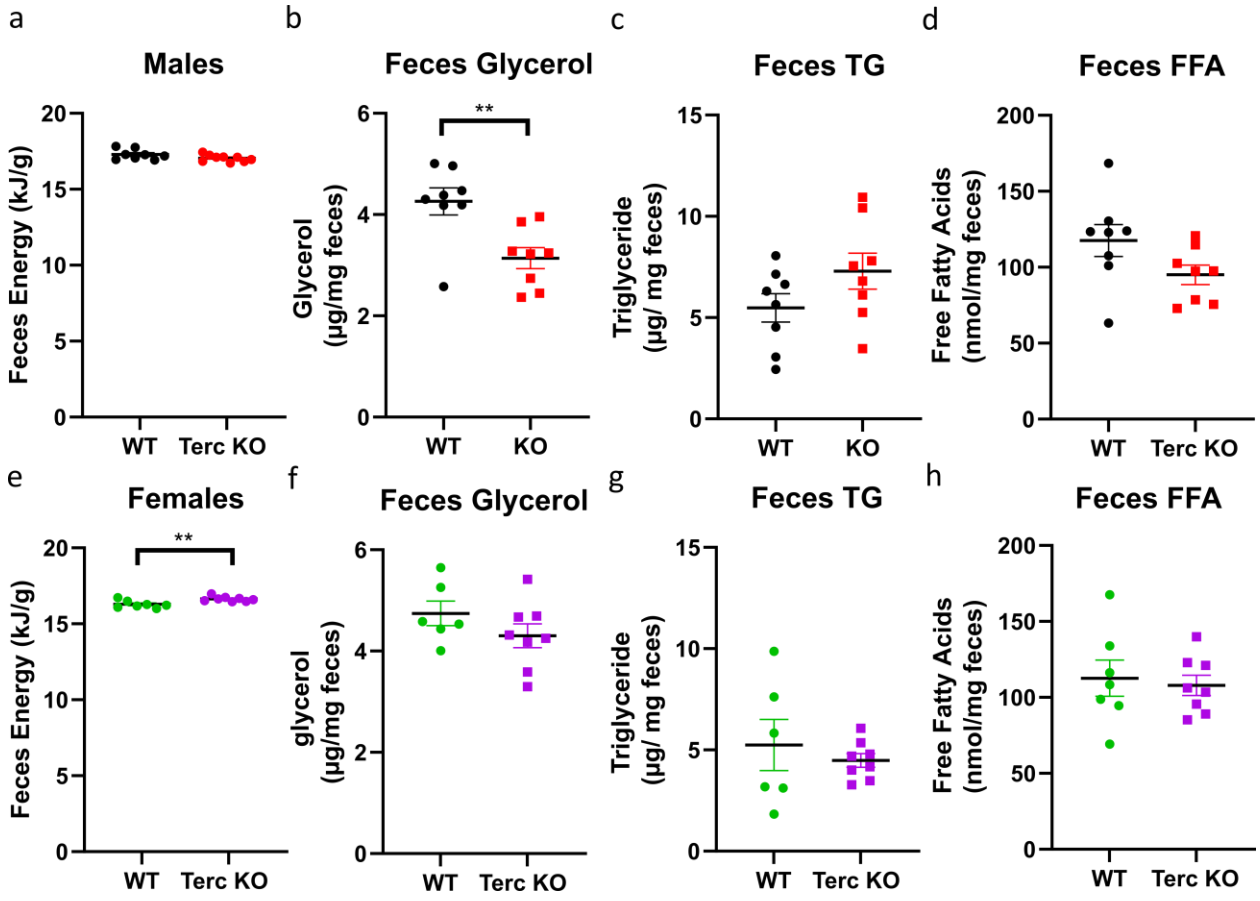

Figure 4: Feces energy and composition in male and female Terc KO mice and controls.
a) feces energy, b) feces glycerol, c) feces triglyceride (TG) and d) feces free fatty acids (FFA) in male Terc KO mice (n=8) and controls (n=8). e) Feces energy, f) feces glycerol, g) feces triglyceride and h) feces free fatty acids (FFA) in female Terc KO mice (n=8) and controls (n=6-7). Data are shown as mean ± SEM. Statistics were calculated using unpaired t-test. **P<0.01

The small intestine is the major site for nutrient absorption and intestinal enterocytes play a crucial role in this process (Montoro-Huguet, Belloc, and Domínguez-Cajal 2021). Therefore, we examined, via Real-Time PCR (qPCR), gene expression of fatty acid uptake genes in small intestine enterocytes of both male and female Terc KO mice and controls. Interestingly, all tested fatty uptake genes, namely *Slc27a2*, *Slc27a4*, *Cd36*, *Got2*, showed lower expression in both male (Figure 5a) and female Terc KO mice (Figure 5b) and controls. Remarkably, male Terc KO mice showed higher expression of the inflammatory marker *Il1b* (Figure 5a), while female mice showed higher expression of the inflammatory markers *Il1b* and *Tnfa* (Figure 5b). Thus, we here show that Terc KO mice show lower expression of fatty acid uptake genes and higher expression of inflammatory genes in small intestine enterocytes in comparison to controls. This in turn could explain the reduction in body weight in both genders as a deficit in the ability of the Terc KO mice to uptake fatty acids.

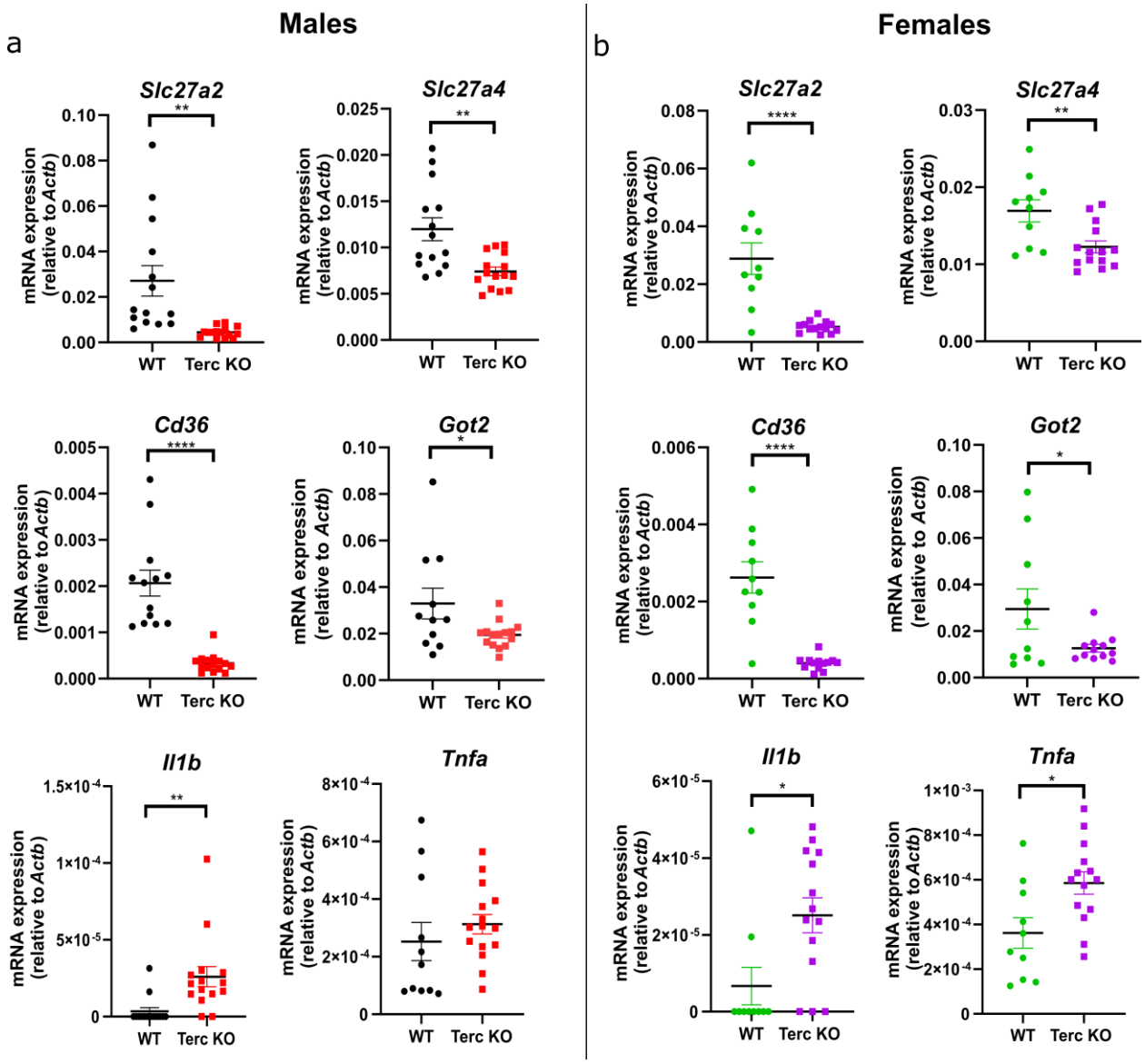

Figure 5: Terc Ko mice show reduced expression of fatty acid uptake gene and higher expression of inflammatory genes in small intestine enterocytes.
qPCR analysis of genes involved in fatty acid uptake and inflammation in small intestine enterocytes from a) male Terc KO (n=14-15) mice and controls (n=12-16) and b) female Terc KO (n=12-14) mice and controls (n=10). Data are shown as mean ± SEM. Statistics were calculated using unpaired t-test. *P<0.05, **P<0.01, ****P<0.0001

3.2 Terc KO mice show sexual dimorphism.

A remarkable finding in this study was the differences between sexes. The first observation was that 10 weeks old male Terc KO mice show a reduction in body weight and lean mass in comparison to controls (Figure 6a) while female Terc KO mice do not (Figure 6b). Another interesting observation is that female Terc KO mice show higher dark phase RER than controls (Figure 7c) while male Terc KO mice do not (Figure 7a). There was also a marked reduction in serum triglyceride levels in male Terc KO mice (Figure 7b) and

this reduction was not seen in female Terc KO mice (Figure 7d) in comparison to controls. Regarding qPCR gene expression analysis in small intestine enterocytes, male Terc KO mice show higher expression of glucose uptake genes in comparison to controls (Figure 7e). While female Terc KO mice show reduced expression of glucose uptake genes (Figure 7f). As the kidney is a major organ for glucose reabsorption (Mather and Pollock 2011), expression of several genes involved in kidney glucose uptake was examined. Female Terc KO mice show reduced expression of *Glut2*, *Slc5a1* (*Sglt1*) and *Slc5a2* (*Sglt2*) while showing higher expression of *Glut1* in comparison to controls (Figure 7h). On the other hand, kidney of male Terc KO mice show lower expression of *Slc5a2* (*Sglt2*) only while showing higher expression of both *Glut1* and *Slc5a1* (*Sglt1*) (Figure 7g). These data demonstrate sexual dimorphism in Terc KO mice upon telomere shortening.

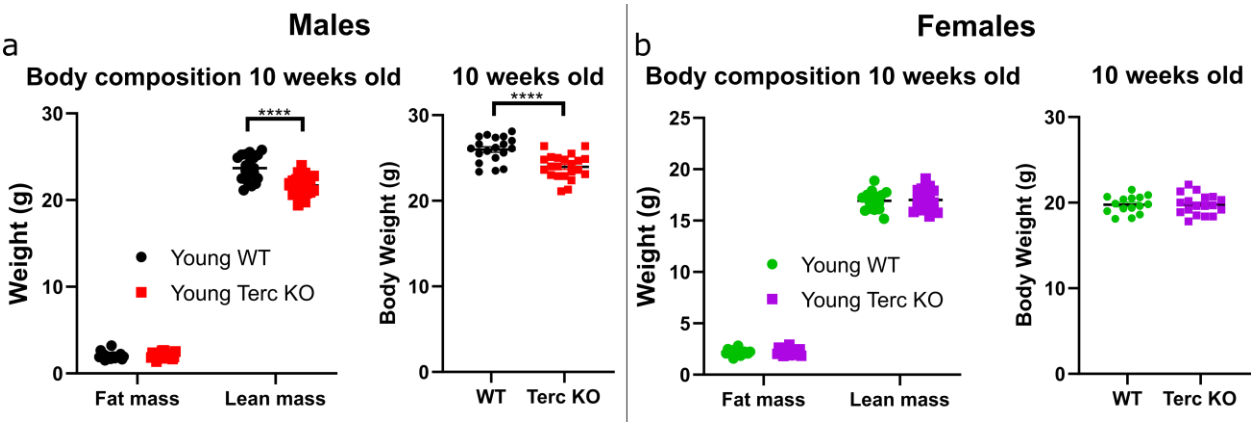

Figure 6: 10 weeks old male Terc KO mice show reduced body weight and lean mass.
a) Body composition and body weight in 10 weeks old male Terc KO mice (n=22) and controls (n=19). b) Body composition and body weight in 10 weeks old female Terc KO mice (n=18) and controls (n=15). Data are shown as mean ± SEM. Statistics were calculated using unpaired t-test or Two-way ANOVA followed by Sidak´s multiple comparison test. ****P<0.0001

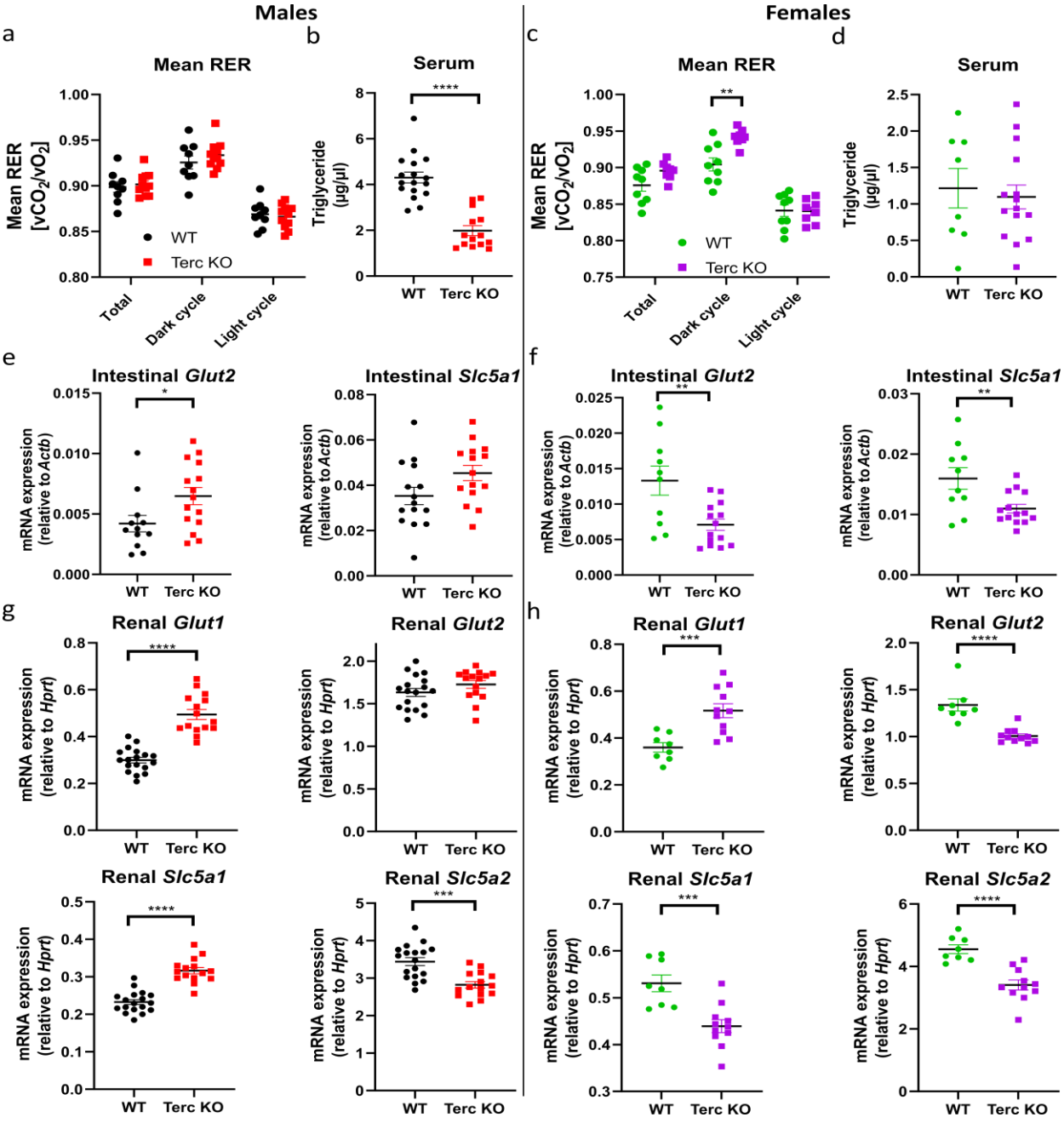

Figure 7: Differences between male and female Terc KO mice.
Mean respiratory exchange ratio (RER) in a) male Terc KO mice (n=11) and controls (n=9) and c) in female Terc KO mice (n=8) and controls (n=9). Serum triglyceride levels in b) male Terc KO mice (n=14) and controls (n=17) and d) female Terc KO mice (n=15) and controls (n=8). qPCR gene expression analysis of glucose uptake genes in small intestine enterocytes of e) male Terc KO mice (n=15) and controls (n=12-15) and f) female Terc KO mice (n=14) and controls (n=10). qPCR gene expression analysis of glucose uptake genes in kidney of g) male Terc KO mice (n=15) and controls (n=18) and h) female Terc KO mice (n=11) and controls (n=8). Data are shown as mean ± SEM. Statistics were calculated using unpaired t-test. *P<0.05, **P<0.01, ***P<0.001, ****P<0.0001.

3.3 Serine racemase expression in adipose tissue

To examine the expression of the serine racemase gene in adipose tissues and whether it is expressed in stromal vascular fraction or mature adipocytes, scWAT, pgWAT and BAT were isolated from Wildtype mice. Thereafter, the tissues were separated into mature adipocytes and stromal vascular fraction. Mature adipocytes isolation was confirmed by *Adipoq* gene expression and mature brown adipocyte isolation was confirmed by *Ucp1* gene expression (Figure 8a). Here we show for the first time that *Srr* is expressed in both stromal vascular fraction and mature adipocytes in all fat depots tested (Figure 8a). After that, we generated mice with specific deletion of serine racemase in mature adipocytes. This was done by mating $SRR^{fl/fl}$ mice (Basu et al. 2009; Benneyworth et al. 2012), where the first coding exon of serine racemase in flanked by two *LoxP* sites, with Adiponectin-Cre^{+} mice, where Cre-recombinase expression is under the control of the adiponectin promoter (Eguchi et al. 2011). Thus, the Cre-recombinase will only be expressed in cells which express adiponectin (adipocytes) and will excise *LoxP* flanked sites. Therefore, the resulting $SRR^{fl/fl}$ Adiponectin-Cre^{+} ($SRR^{Adipo\text{-}KO}$) mice have specific deletion of serine racemase only in adipocytes which express adiponectin. As *Srr* is expressed in the stromal vascular fraction, its deletion in adipose tissues of $SRR^{Adipo\text{-}KO}$ did not result in complete ablation of protein level but simply a reduction (Figure 8b) as the gene is only deleted in mature adipocytes.

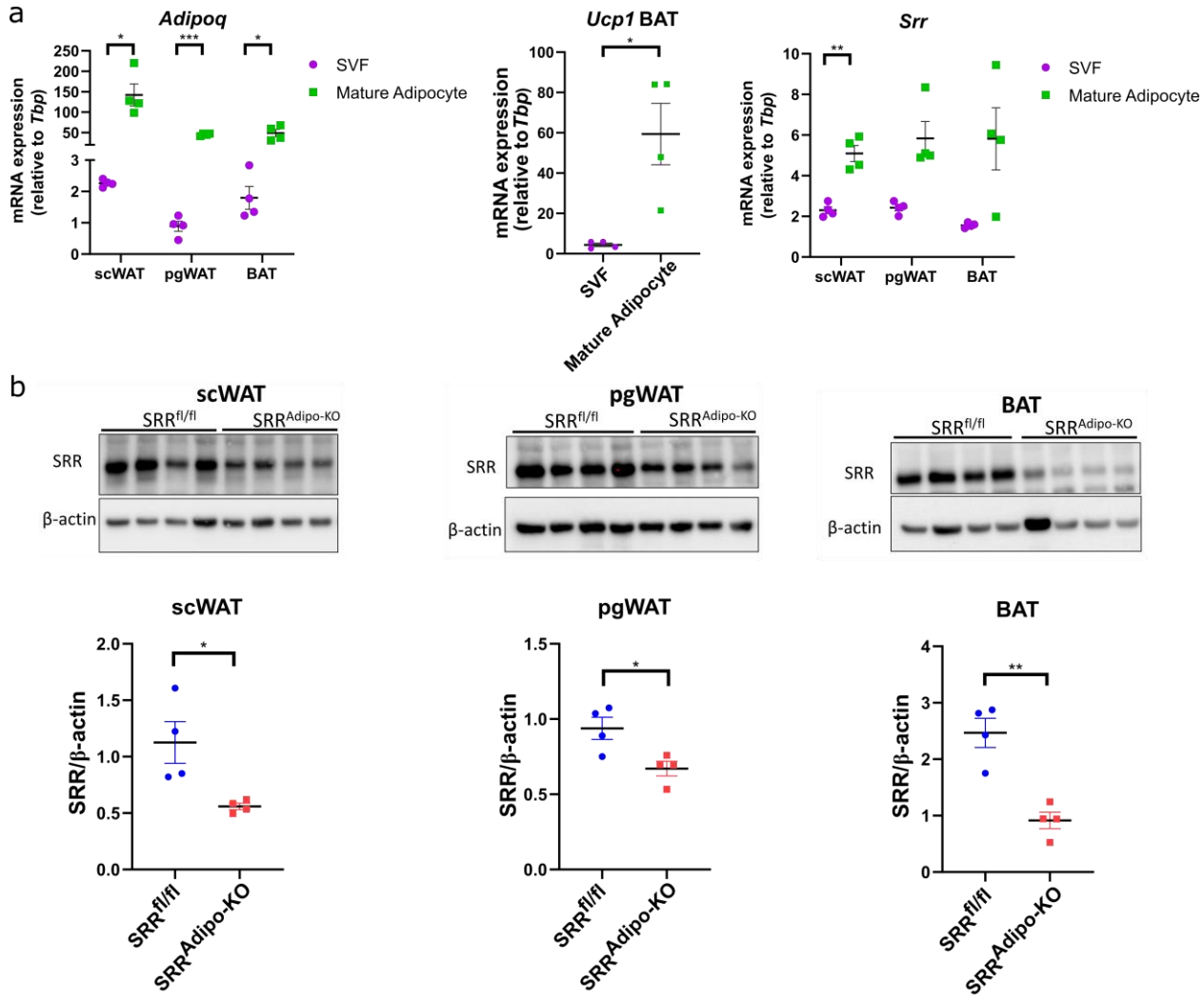

Figure 8: Serine racemase is expressed in both adipocytes and stromal vascular fraction of adipose tissues and its expression is reduced upon its deletion in adipose tissues of SRR$^{Adipo\text{-}KO}$ mice

a) qPCR gene expression analysis of *Adipoq*, *Ucp1* and *Srr* in stromal vascular fraction (SVF) (n=4) and mature adipocytes (n=4) of wild type mice b) SRR and β-actin protein expression in scWAT, pgWAT and BAT of SRR$^{Adipo\text{-}KO}$ mice (n=4) and controls (n=4). Data are shown as mean ± SEM. Statistics were calculated using unpaired t-test or Two-way ANOVA followed by Sidak´s multiple comparison test. *P<0.05, **P<0.01, ***P<0.001

3.4 Adipose tissue specific deletion of serine racemase leads to hypertrophy and alters gene expression in fat depots without impairing glucose homeostasis

Body weight development, lean and fat mass were not altered in SRR$^{Adipo\text{-}KO}$ mice fed chow diet (Figure 9a). To examine if deletion of serine racemase in mature adipocytes alter their morphology, Hematoxylin and Eosin (H&E) staining was performed. Deletion of serine racemase in mature adipocytes altered

adipose tissue morphology (Figure 9b). This was due to an increase in adipocyte size in scWAT and increase in lipid droplet size in BAT (Figure 9c).

qPCR gene expression analysis was done to study genes involved in different pathways involved in adipose tissue maintenance and function. This was done to understand the reason behind the observed hypertrophy in scWAT and BAT. Genes involved in adipogenesis, lipogenesis, β-adrenergic signaling, thermogenesis, L-serine biogenesis, creatine pathway and D-serine related genes were examined. In scWAT, expression of several beiging markers was upregulated in $SRR^{Adipo\text{-}KO}$ mice, namely *Ppargc1a*, *P2rx5* and *Pat2*. However, this upregulation of beiging markers in scWAT of $SRR^{Adipo\text{-}KO}$ mice did not result in an increase in *Ucp1* gene expression (Figure 10a) or protein levels (Figure 10b). Interestingly, phosphoglycerate dehydrogenase (*Phgdh*) expression was upregulated on the mRNA level (Figure 10a) indicating an effect of serine racemase deletion on serine synthesis pathway (Reid et al. 2018). However, this upregulation was not seen on the PHGDH protein level in $SRR^{Adipo\text{-}KO}$ mice (Figure 10b). In pgWAT of $SRR^{Adipo\text{-}KO}$ mice, a significant downregulation in the adipogenesis marker *Cebpa* was observed (Figure 10a). *Cebpa* is a transcription factor whose expression is necessary and sufficient for the differentiation of 3T3-L1 pre-adipocytes into mature adipocytes (Darlington, Ross, and MacDougald 1998). Moreover, other adipogenesis markers showed a trend towards downregulation namely *Pparg* and *Cebpb*. Although this was not statistically significant. The lipogenesis gene fatty acid synthase (*Fasn*) also showed a trend towards downregulation (with no significant difference) (Figure 10a). In BAT of $SRR^{Adipo\text{-}KO}$ mice, there was a significant downregulation of the adipogenesis marker *Pparg* (Figure 10a). *Pparg* is essential for adipocyte differentiation *in vitro* and *in vivo* (Siersbæk, Nielsen, and Mandrup 2010). Both the adipogenesis marker *Cebpa* and the lipogenesis markers *Fasn* showed a trend towards reduced gene expression (with no significant difference). Interestingly, an upregulation of glycine amidinotransferase (*Gatm*) was observed (Figure 10a). *Gatm* is the first and rate limiting enzyme in creatine biosynthesis and its deletion in adipose tissues impairs diet-induced thermogenesis (Kazak et al. 2017). This observation points to an association between serine racemase and *Gatm*/thermogenesis in thermogenic adipocytes. All these data demonstrate the effects of serine racemase deletion in the adipose tissue on several genes and pathways in adipocytes, highlighting a role for serine racemase in the adipose tissue.

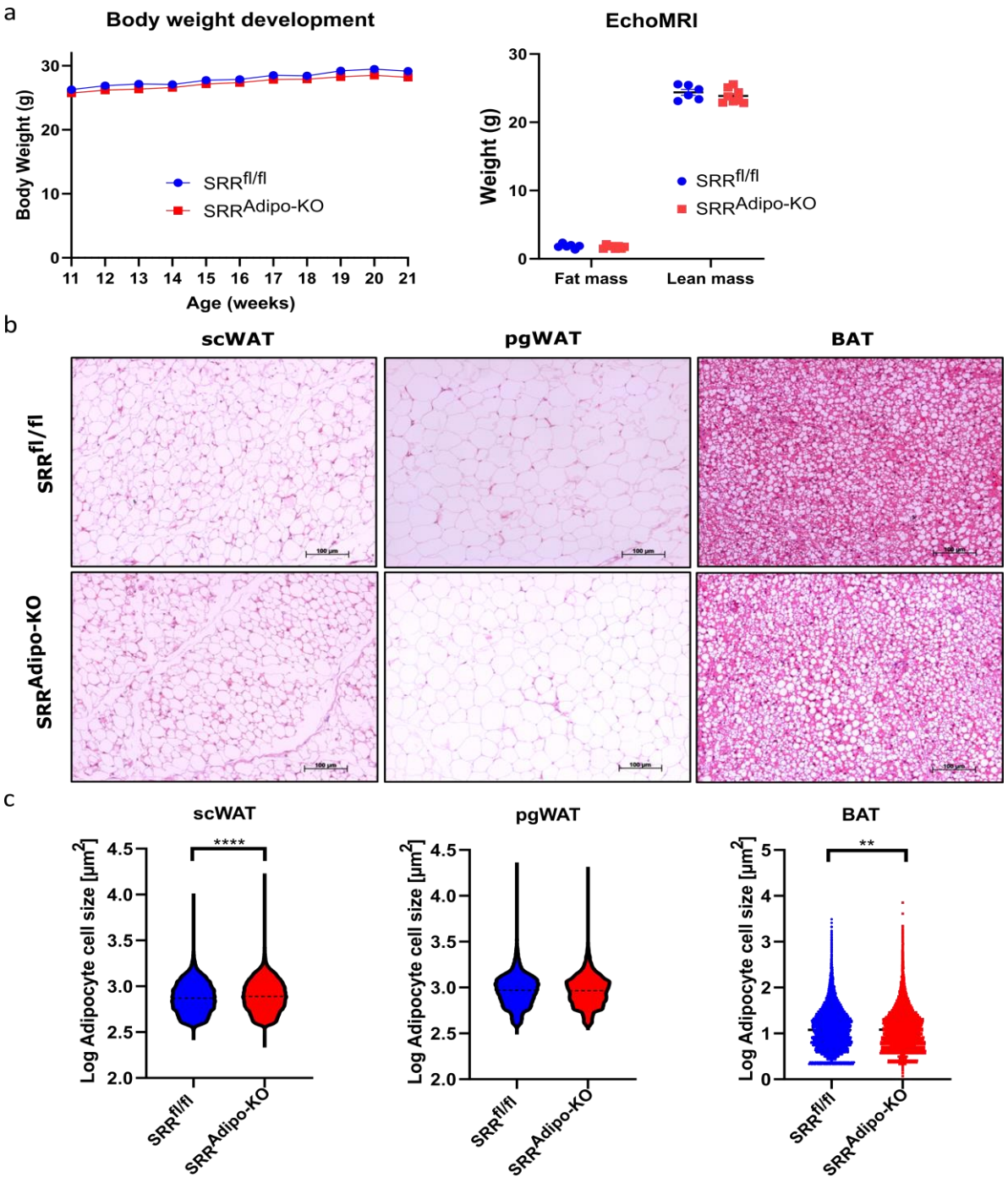

Figure 9: Adipose tissue specific deletion of serine racemase leads to hypertrophy in scWAT and BAT under chow diet

a) Body weight development and body composition in $SRR^{Adipo\text{-}KO}$ mice (n=8) and controls (n=6) fed chow diet b) Representative hematoxylin and Eosin (H&E) stained sections from scWAT, pgWAT and BAT of $SRR^{Adipo\text{-}KO}$ mice and controls fed chow diet. c) Quantification of adipocyte size in scWAT and pgWAT and lipid droplet size in BAT of H&E stained sections from $SRR^{Adipo\text{-}KO}$ mice and controls (scWAT, $SRR^{Adipo\text{-}KO}$ n=5, controls n=4), (pgWAT, $SRR^{Adipo\text{-}KO}$ n=6, controls n=5), (BAT, $SRR^{Adipo\text{-}KO}$ n=6, controls n=7). Data are show as violin blots. Statistics were calculated using unpaired t-test. **P<0.01, ****P<0.0001

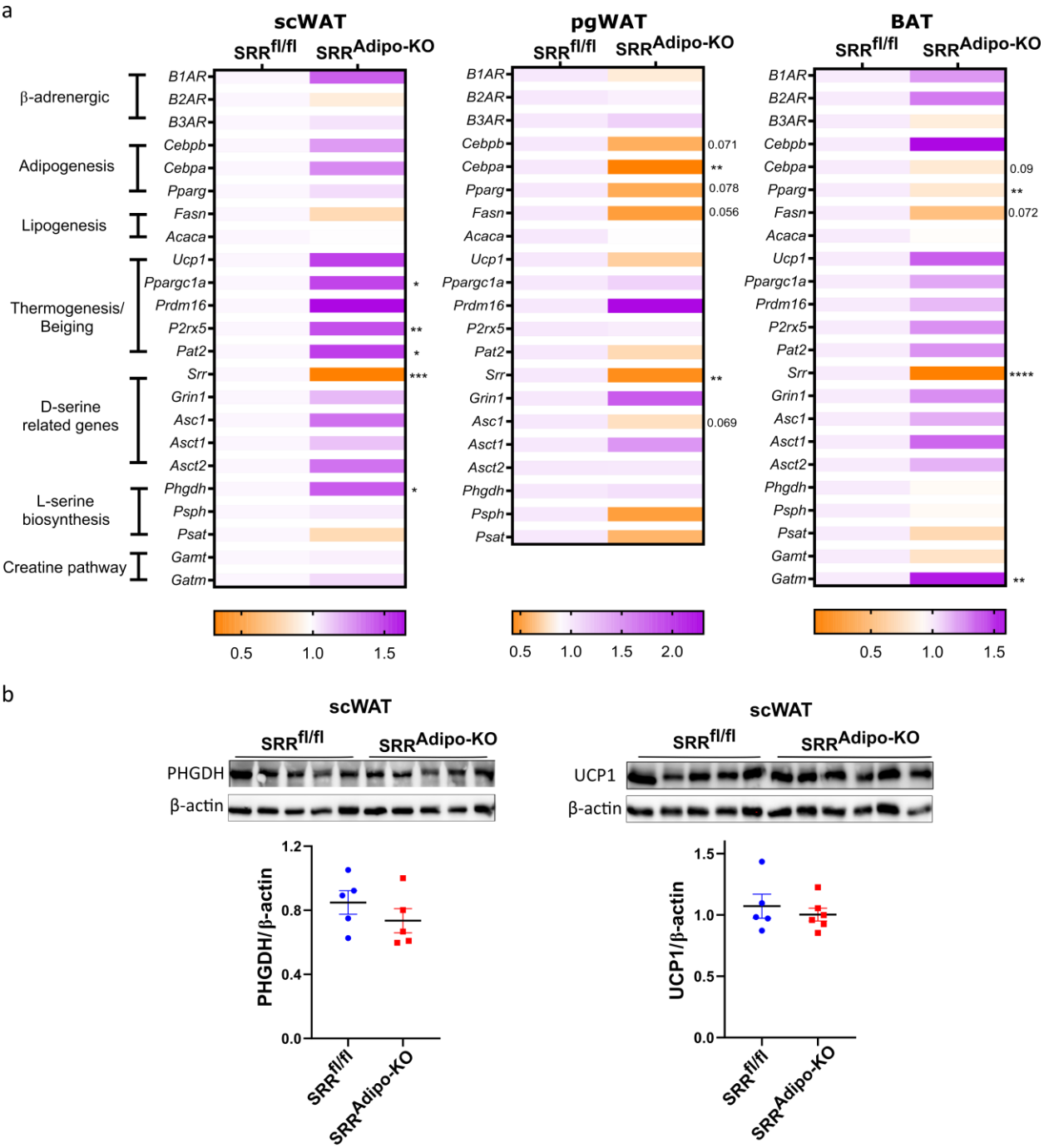

Figure 10: Adipose tissue specific deletion of serine racemase alters fat depots gene expression under chow diet.

a) qPCR gene expression analysis of scWAT, pgWAT and BAT from $SRR^{Adipo\text{-}KO}$ mice (n=8) and controls (n=7). Data are log transformed then normalized to controls. Median is shown. t-test was performed to compare each gene between the genotypes. b) Protein expression analysis via western plot of PHGDH, UCP1 and a control protein (β-actin). Data are shown as mean ±SEM. Statistics were calculated using unpaired t-test. *P<0.05, **P<0.01, ***P<0.001, ****P<0.0001.

To test the cell autonomous effects of serine racemase deletion on adipocytes and to examine if the differences in gene expression seen *in vivo* can be recapitulated *in vitro*, primary subcutaneous pre-adipocytes were isolated from $SRR^{Adipo\text{-}KO}$ mice and controls and differentiated *in vitro*. Primary subcutaneous adipocytes were examined to assess whether the beiging effect seen *in vivo* under room temperature is reproducible *in vitro*. Surprisingly, *in vitro* differentiated subcutaneous adipocytes from $SRR^{Adipo\text{-}KO}$ mice showed higher gene expression of several adipogenesis markers in comparison to controls (Figure 11a). This was accompanied by a trend to increased gene expression of several beiging markers including *Ucp-1* and a statistically significant increase in *Pat2* (Figure 11b). Therefore, similar to the *in vivo* data, primary subcutaneous adipocytes from $SRR^{Adipo\text{-}KO}$ show higher beiging markers gene expression *in vitro* in comparison to controls.

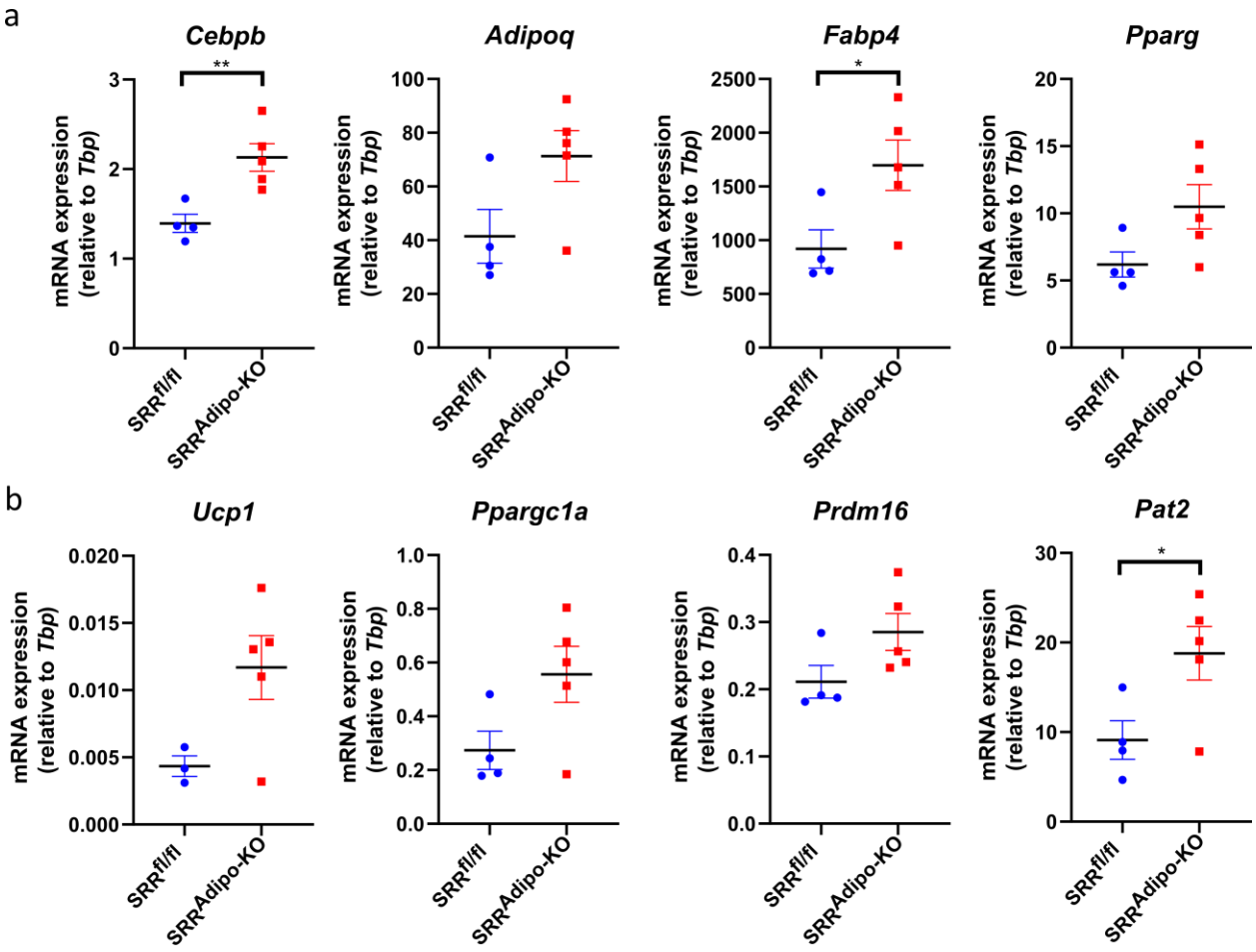

Figure 11: *In vitro* differentiated primary subcutaneous adipocytes from $SRR^{Adipo\text{-}KO}$ mice show higher adipogeneis and beiging markers gene expression in comparison to controls.
a) qPCR gene expression analysis of adipogenesis markers and b) beiging markers relative to *Tbp* in mature *in vitro* differentiated primary adipocytes from $SRR^{Adipo\text{-}KO}$ mice (n=5) and controls (n=3-4). Data are shown as mean ± SEM. Statistics were calculated using unpaired t-test. *P<0.05, **P<0.01

One could postulate that the hypertrophy observed in adipose depots under chow diet could be due to impaired lipolysis. To address this, several scWAT and pgWAT tissue pieces were excised and placed in

culture and stimulated with isoproterenol. Free glycerol levels were measured in the medium as a surrogate for lipolysis. Additional samples were left unstimulated to measure basal lipolysis. There was no difference in either basal or isoproterenol stimulated lipolysis in scWAT or pgWAT between $SRR^{Adipo\text{-}KO}$ mice and controls (Figure 12). These data show that lipolysis is not impeded upon serine racemase deletion in white adipose tissues.

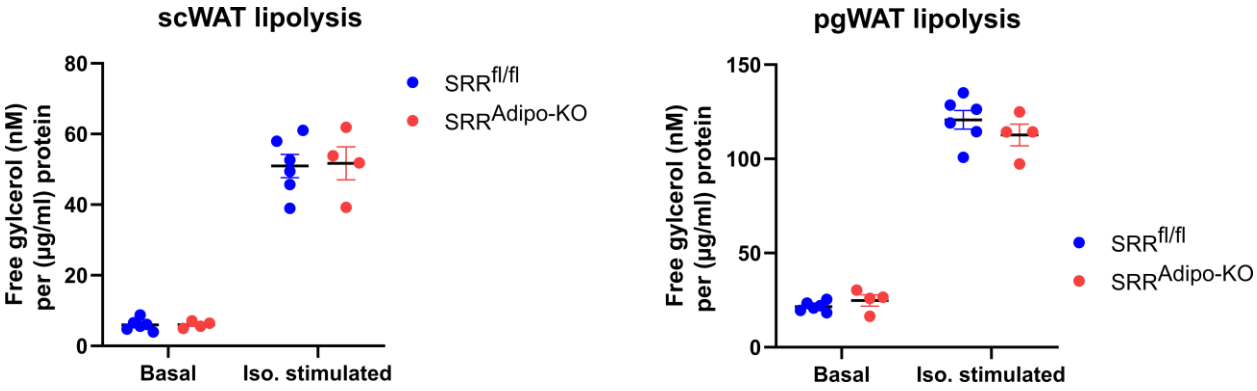

Figure 12: Adipose tissue specific deletion of serine racemase does not impair lipolysis in white fat.
Ex vivo lipolysis assay was performed using scWAT and pgWAT tissues pieces from $SRR^{Adipo\text{-}KO}$ (n=4) and controls (n=6). The tissue pieces were stimulated with Isoproterenol or not stimulated (basal lipolysis). Free glycerol levels were measured as end point and values were normalized to protein concentration. Data are shown as mean ± SEM. Statistics were calculated using Two-way ANOVA followed by Sidak´s multiple comparison test.

Given the observed hypertrophy phenotype, one could expect an impairment in glucose homeostasis. Moreover, elevated gene expression of the inflammatory marker *Tnfa* was observed in BAT of $SRR^{Adipo\text{-}KO}$ mice (Figure 13a). On the other hand, decreased gene expression of *Tnfa* was observed in pgWAT of $SRR^{Adipo\text{-}KO}$ mice (Figure 13a). However, there was no difference in glucose tolerance or insulin sensitivity as evident by glucose tolerance test (GTT) (Figure 13b) and insulin tolerance test (ITT) (Figure 13c) respectively. Moreover, there was no difference in fasting glycaemia (Figure 13d) or serum insulin levels (Figure 13e) between $SRR^{Adipo\text{-}KO}$ mice and controls. Furthermore, No difference in serum free fatty acid levels were seen between the genotypes (Figure 13f). Although the Srr whole body knockout mice showed an improvement in insulin sensitivity (Lockridge et al. 2016). Here we show no improvement or impairment in glucose tolerance or insulin sensitivity under chow diet in $SRR^{Adipo\text{-}KO}$ mice.

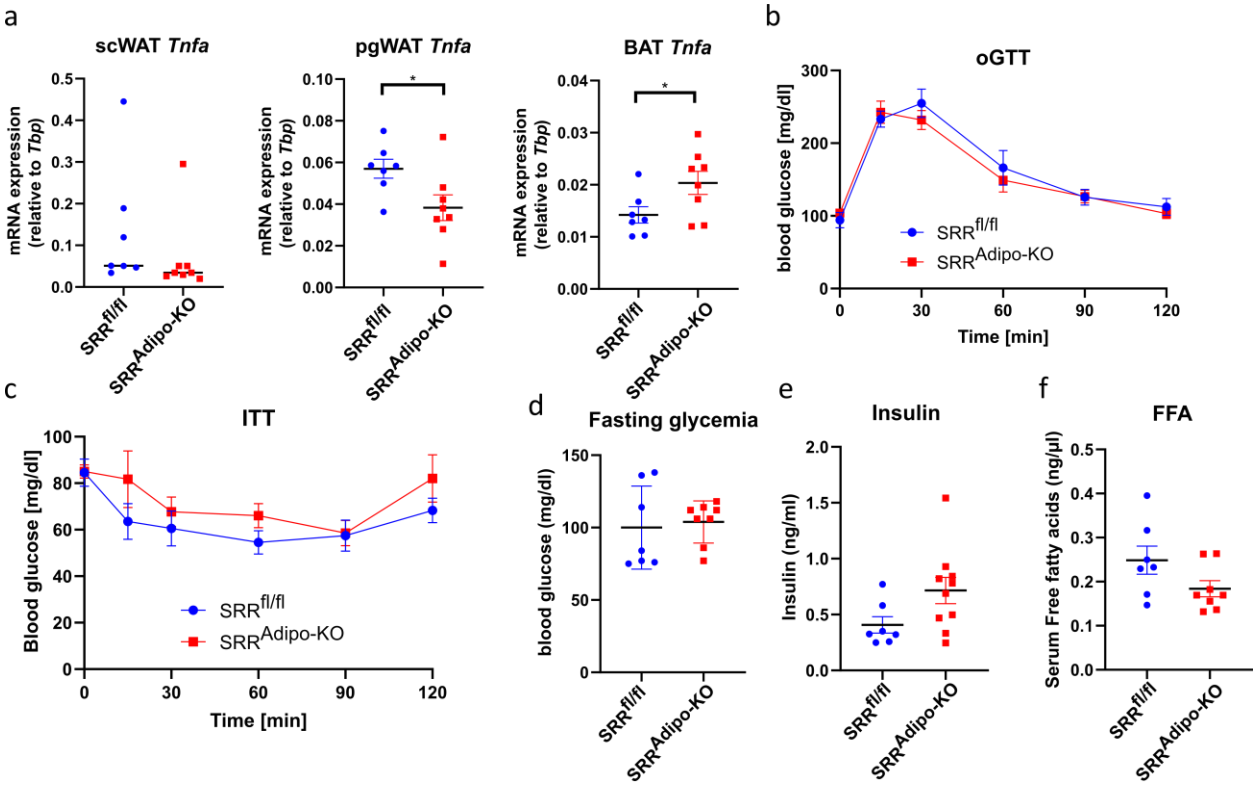

Figure 13: Adipose tissue specific deletion of serine racemase does not impair glucose homeostasis under chow diet.

a) qPCR gene expression analysis of *Tnfa* in scWAT, pgWAT and BAT of $SRR^{Adipo\text{-}KO}$ mice (n=8) and controls (n=7). b) Oral glucose tolerance test (oGTT) in $SRR^{Adipo\text{-}KO}$ (n=8) and controls (n=6) and c) insulin tolerance test (ITT) in $SRR^{Adipo\text{-}KO}$ mice (n=7) and controls (n=7). d) Fasting Glycemia and e) serum free fatty acid (FFA) levels in $SRR^{Adipo\text{-}KO}$ (n=8) and controls (n=7). f) Insulin level in $SRR^{Adipo\text{-}KO}$ mice (n=10) and controls (n=7). Data are presented as mean ± SEM. Statistics were calculated using unpaired t-test in or using Two-way ANOVA followed by Sidak´s multiple comparison test. *P<0.05

3.5 Adipose tissue specific deletion of serine racemase reduces whole body energy expenditure without impairing BAT function

In BAT of $SRR^{Adipo\text{-}KO}$ mice, there was an increase in lipid droplets size and a decrease in adipogenesis gene expression. These data point towards a malfunction in BAT function. To test this hypothesis, mice were implanted with temperature sensors in the peritoneal cavity and placed in metabolic cages to measure body temperature under acute (4°C) cold exposure. A condition known to induce BAT activity (Saito et al. 2020). Mice were placed for 5 hours at 4°C and body temperature was monitored. $SRR^{Adipo\text{-}KO}$ mice showed no impairment in their ability to defend their body temperature at 4°C and showed no significant difference in body temperature in comparison to controls (Figure 14a). These data show that BAT function is intact even after the loss of serine racemase.

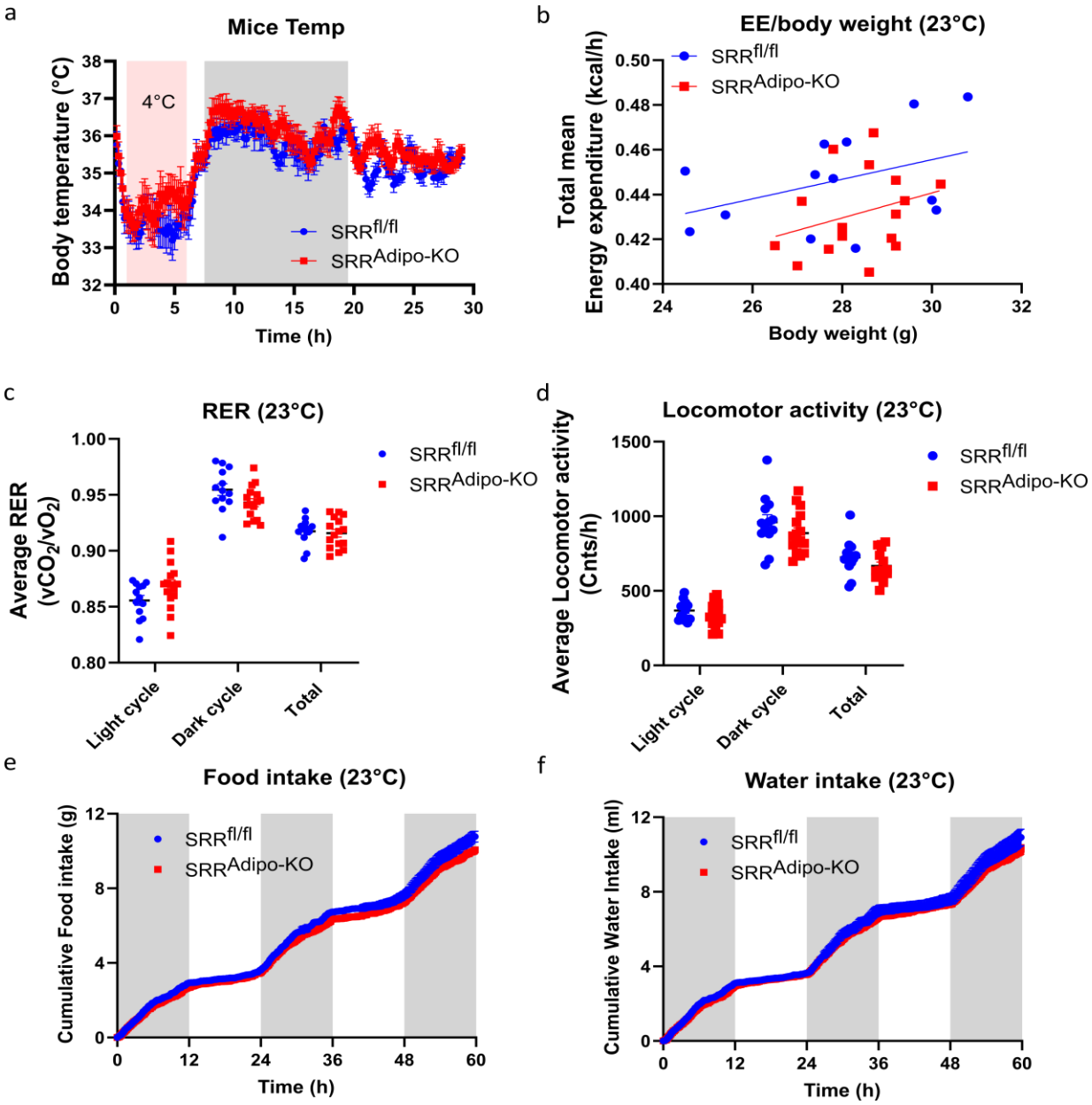

Figure 14: Adipose tissue specific deletion of serine racemase reduces whole body energy expenditure. a) Body temperature of SRR$^{Adipo-KO}$ mice (n=8) and controls (n=7) during acute cold exposure (4°C). b) Total mean energy expenditure normalized to body weight. c) Average respiratory exchange ratio and d) average locomotor activity during light, dark and total period. e) Food intake and f) water intake of SRR$^{Adipo-KO}$ mice (n=16) and controls (n=13). Data are shown as mean ± SEM. Statistics were calculated using Two-way ANOVA followed by Sidak´s multiple comparison test except for b) where data are shown as mean and statistics were calculated using One-way ANCOVA using SPSS statistics.

The questions remained whether the observed hypertrophy in scWAT and BAT of SRR$^{Adipo-KO}$ mice and the differences in gene expression in all fat depots between the genotypes would affect any physiological parameters. As the mice were in metabolic cages, energy expenditure and respiratory exchange ratio were measured via indirect calorimetry. Energy expenditure was plotted against body weight and,

interestingly, $SRR^{Adipo\text{-}KO}$ mice showed a significant reduction in whole body energy expenditure as assessed by one-way ANCOVA analysis (Figure 14b). However, serine racemase deletion in adipose tissues did not alter respiratory exchange ratio, locomotor activity, food intake or water intake (Figure 14c-14f). These data show that serine racemase deletion in fat depots decreased whole body energy expenditure in mice fed chow diet under room temperature without altering food intake, substrate utilization or locomotor activity.

3.6 Adipose tissue specific deletion of serine racemase does not reduce energy expenditure or alter gene expression in fat depots under chronic cold exposure (4°C).

$SRR^{Adipo\text{-}KO}$ mice showed higher expression of several beiging markers in scWAT in comparison to controls. Therefore, mice where chronically exposed to cold (4°C) for one week. A condition which is known to induce beiging (Herz and Kiefer 2019). The hypothesis was that chronic cold exposure would exacerbate the beiging effect seen under room temperature.

Surprisingly, chronic cold exposure abolished the changes seen in beiging markers in scWAT (Figure 15a) between the genotypes under room temperature. Moreover, the changes seen in adipogenesis markers in pgWAT and BAT in $SRR^{Adipo\text{-}KO}$ mice under room temperature were not seen under chronic cold exposure (Figure 15b&15c). This was complemented by histological analysis of fat depots, which did not reveal any observable differences between the genotypes (Figure 15e). Furthermore, in BAT, there was no difference in UCP1 protein levels between the genotypes (Figure 15d). Therefore, chronic cold exposure abolishes all changes seen in fat depots of $SRR^{Adipo\text{-}KO}$ under room temperature.

Mice were later placed in metabolic cages to measure energy expenditure via indirect calorimetry. Chronic cold exposure in $SRR^{Adipo\text{-}KO}$ mice did not affect respiratory exchange ratio, locomotor activity or water intake in comparison to controls (Figure 16b-16d). Surprisingly, the reduction in whole body energy expenditure in $SRR^{Adipo\text{-}KO}$ mice seen under room temperature was not recapitulated under chronic cold exposure (Figure 16a). Moreover, after one week of chronic cold exposure (4°C), $SRR^{Adipo\text{-}KO}$ mice did not show any difference in either lean or fat mass in comparison to controls (Figure 16e). Additionally, no differences in tissues weights were observed between the genotypes (Figure 16f). At the end, no differences were seen between $SRR^{Adipo\text{-}KO}$ mice and controls under chronic cold exposure (4°C).

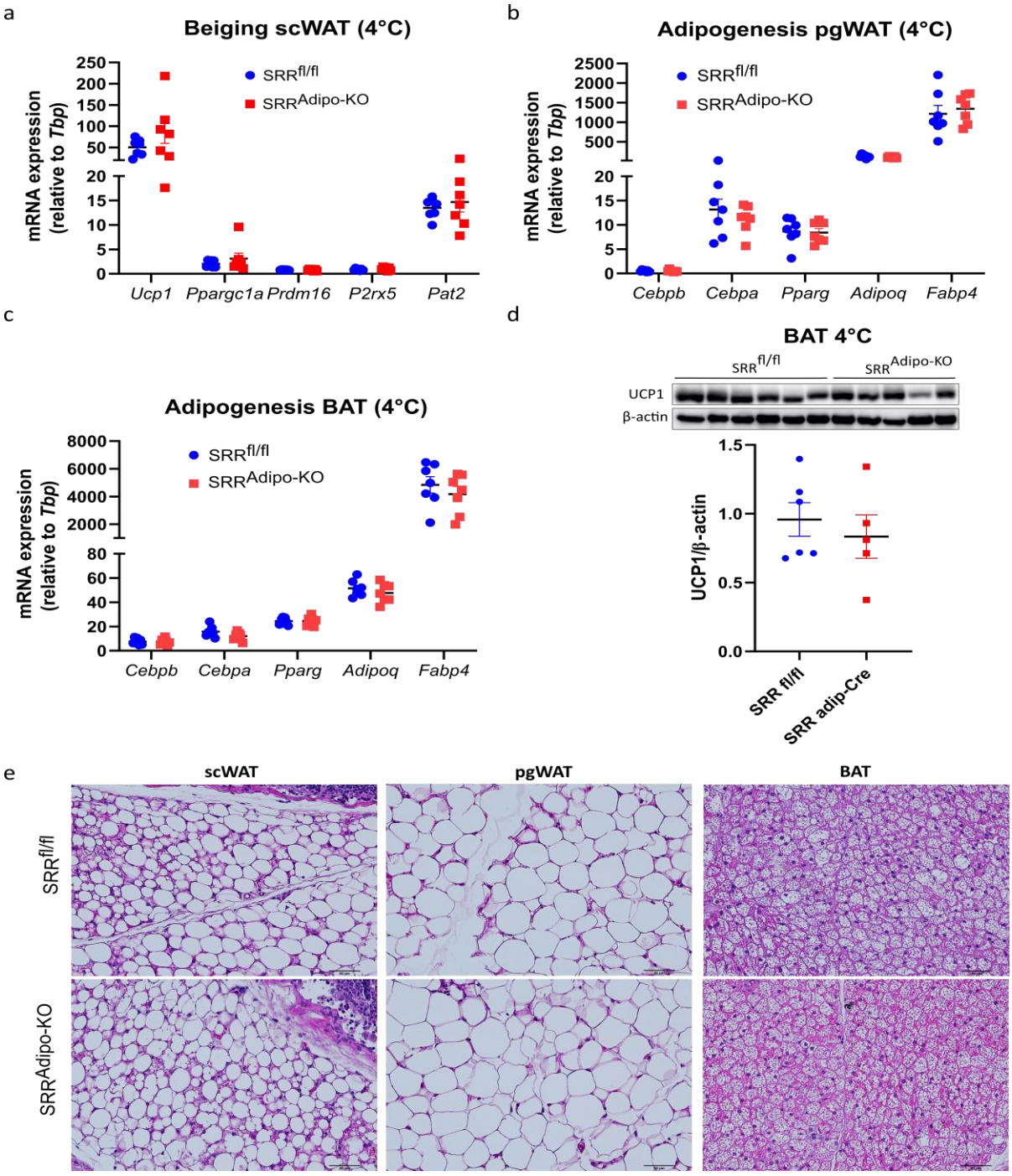

Figure 15: Adipose tissue specific deletion of serine racemase does not alter fat depots gene expression or histology under chronic cold exposure (4°C).

qPCR gene expression analysis of a) beiging markers in scWAT, b) adipogenesis markers in pgWAT and c) adipogenesis markers in BAT of $SRR^{Adipo\text{-}KO}$ mice (n=7) and controls (n=7). d) Protein expression analysis of UCP1 and control (β-actin) in BAT of $SRR^{Adipo\text{-}KO}$ (n=5) and controls (n=6). H&E staining of scWAT, pgWAT and BAT of $SRR^{Adipo\text{-}KO}$ mice and controls. Data are shown as mean ± SEM. Statistics were calculated using unpaired t-test or Two-way ANOVA followed by Sidak´s multiple comparison test. Scale=50µm.

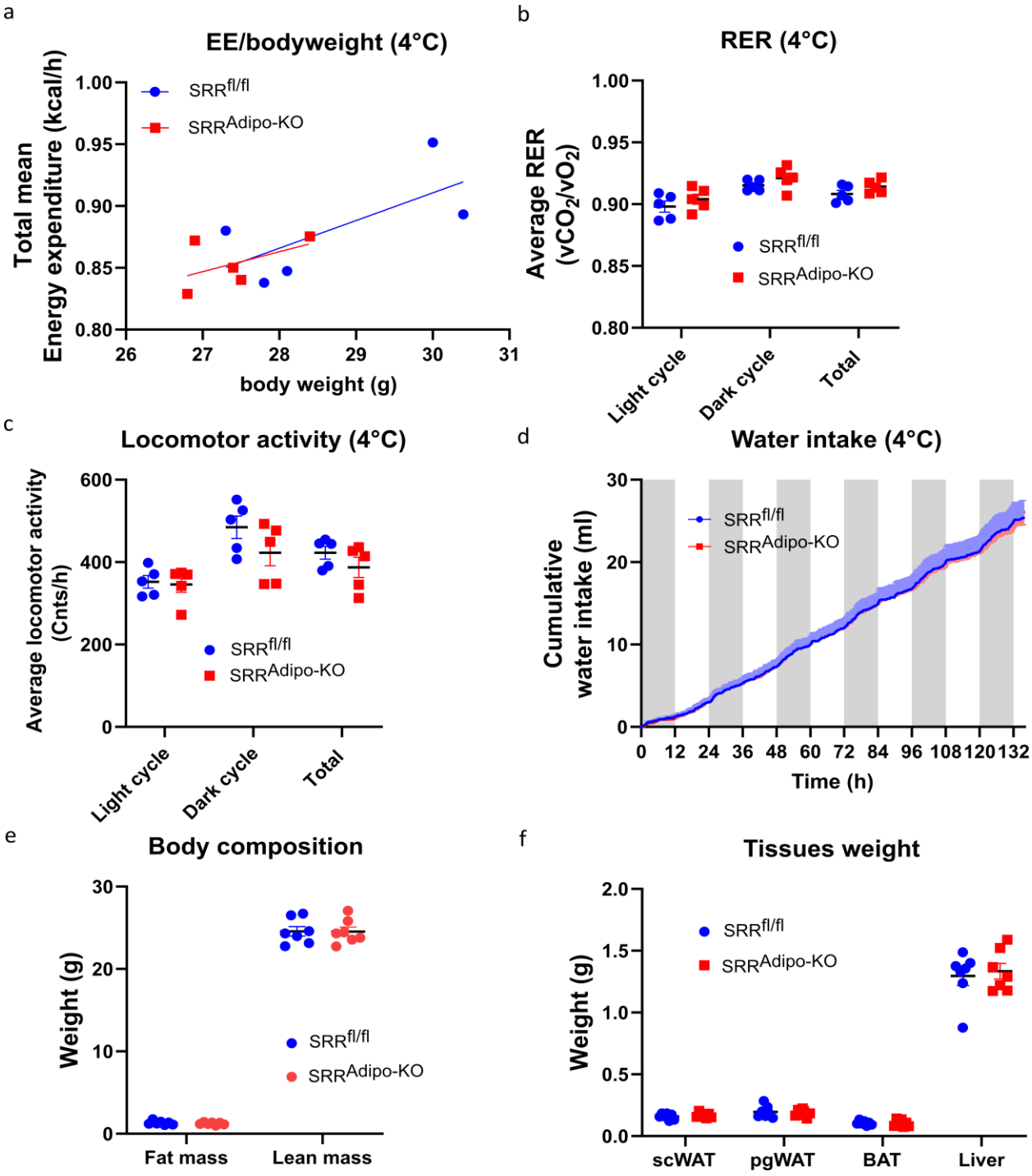

Figure 16: Adipose tissue specific deletion of serine racemase does not alter energy expenditure or body composition under chronic cold exposure (4°C).

a) Total mean energy expenditure plotted against body weight, b) average respiratory exchange ratio (RER), c) average locomotor activity and d) cumulative water intake in $SRR^{Adipo\text{-}KO}$ mice (n=5) and controls (n=5). e) Body composition and f) tissues weight in $SRR^{Adipo\text{-}KO}$ mice (n=7) and controls (n=7). Data are shown as mean ± SEM. Statistics were calculated using Two-way ANOVA followed by Sidak´s multiple comparison test.

3.7 Adipose tissue specific deletion of serine racemase does not alter energy expenditure or respiratory exchange ratio at thermoneutrality (30°C)

Cold exposure is known to stimulate the adrenergic system (Young et al. 1982), thereby, inducing BAT activity and adipose tissue lipolysis (Collins and Surwit 2001). We reasoned that activating the adrenergic system could mask the effects of serine racemase deletion in fat depots as we could only see statistically significant differences between the genotypes under room temperature and not under chronic cold exposure. Therefore, mice were placed under thermoneutrality (30°C), a condition with little sympathetic activity (Nedergaard and Cannon 2014). After that, mice were placed in metabolic cages and energy expenditure was measured via indirect calorimetry. Surprisingly, $SRR^{Adipo\text{-}KO}$ mice did not show any differences in energy expenditure in comparison to controls (Figure 17a). Furthermore, there was no differences in respiratory exchange ratio, locomotor activity, water intake and food intake between the genotypes (Figure 17b-17e). Thus, the reduction in energy expenditure seen under room temperature was not recapitulated under thermoneutrality (30°C) or chronic cold exposure (4°C).

Furthermore, $SRR^{Adipo\text{-}KO}$ mice did not show any differences in body weight development, body composition or tissues weights in comparison to controls (Figure 18a-18c). Moreover, no difference in serum free fatty acid levels was seen between the genotypes (Figure 18d). Additionally there was no impairment in glucose tolerance (Figure 18f) or insulin sensitivity (Figure 18g) in $SRR^{Adipo\text{-}KO}$ mice as assessed by glucose tolerance test and insulin tolerance test respectively and glycosylated hemoglobin (HbA1c) levels were similar between the genotypes (Figure 18e). Thus, we can conclude that serine racemase deletion in fat depots does not impair glucose homeostasis parameters or affect body weight or body composition under themoneutrality (30°C).

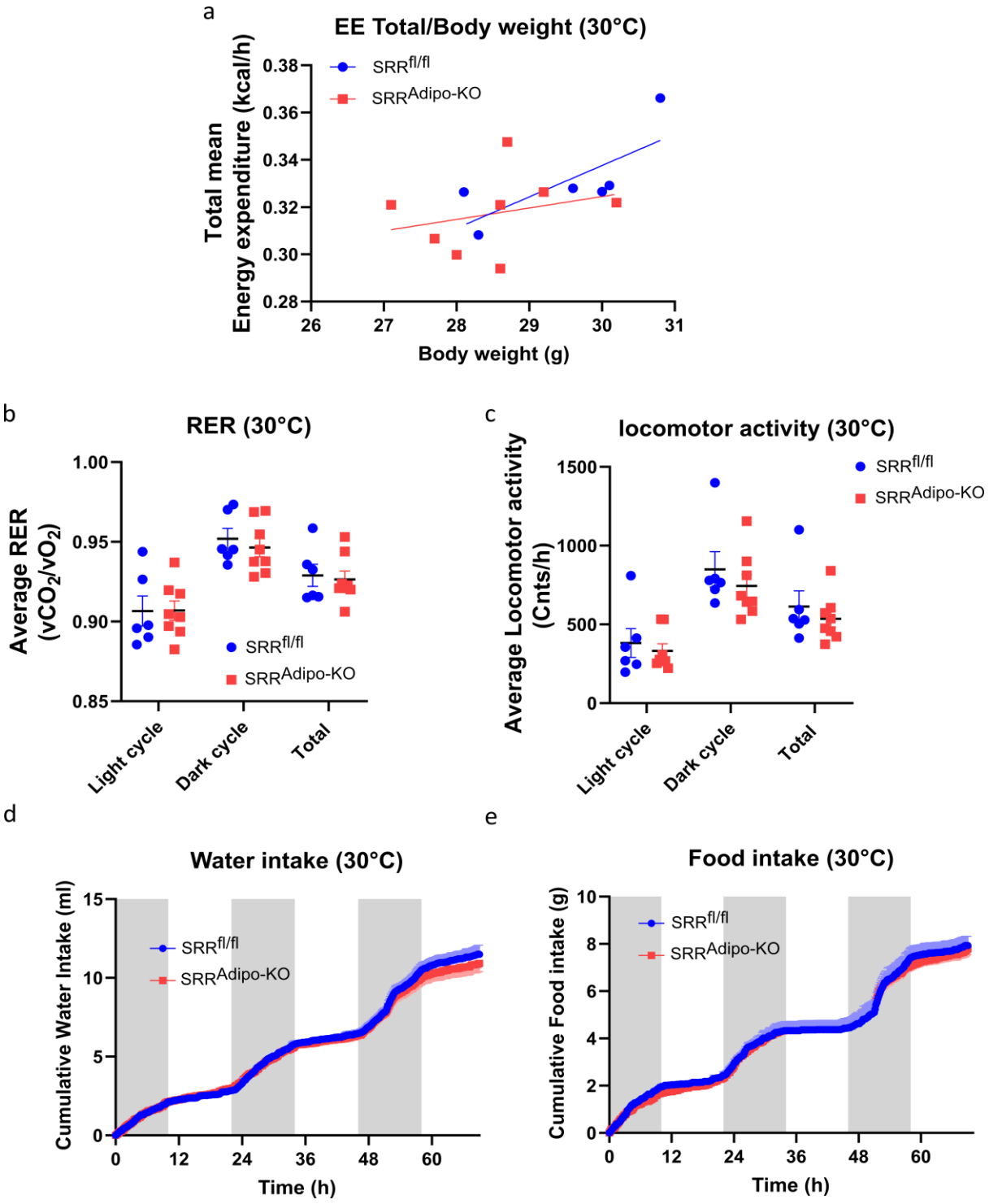

Figure 17: Serine racemase deletion in adipose tissues does not alter energy expenditure, respiratory exchange ratio or food intake under thermoneutrality (30°C).

a) Energy expenditure (EE) plotted against body weight, b) respiratory exchange ratio (RER), c) cumulative locomotor activity, d) water intake and e) food intake in $SRR^{Adipo\text{-}KO}$ mice (n=8) and controls (n=6). Data are shown as mean ± SEM. Statistics were calculated using Two-way ANOVA followed by Sidak´s multiple comparison test.

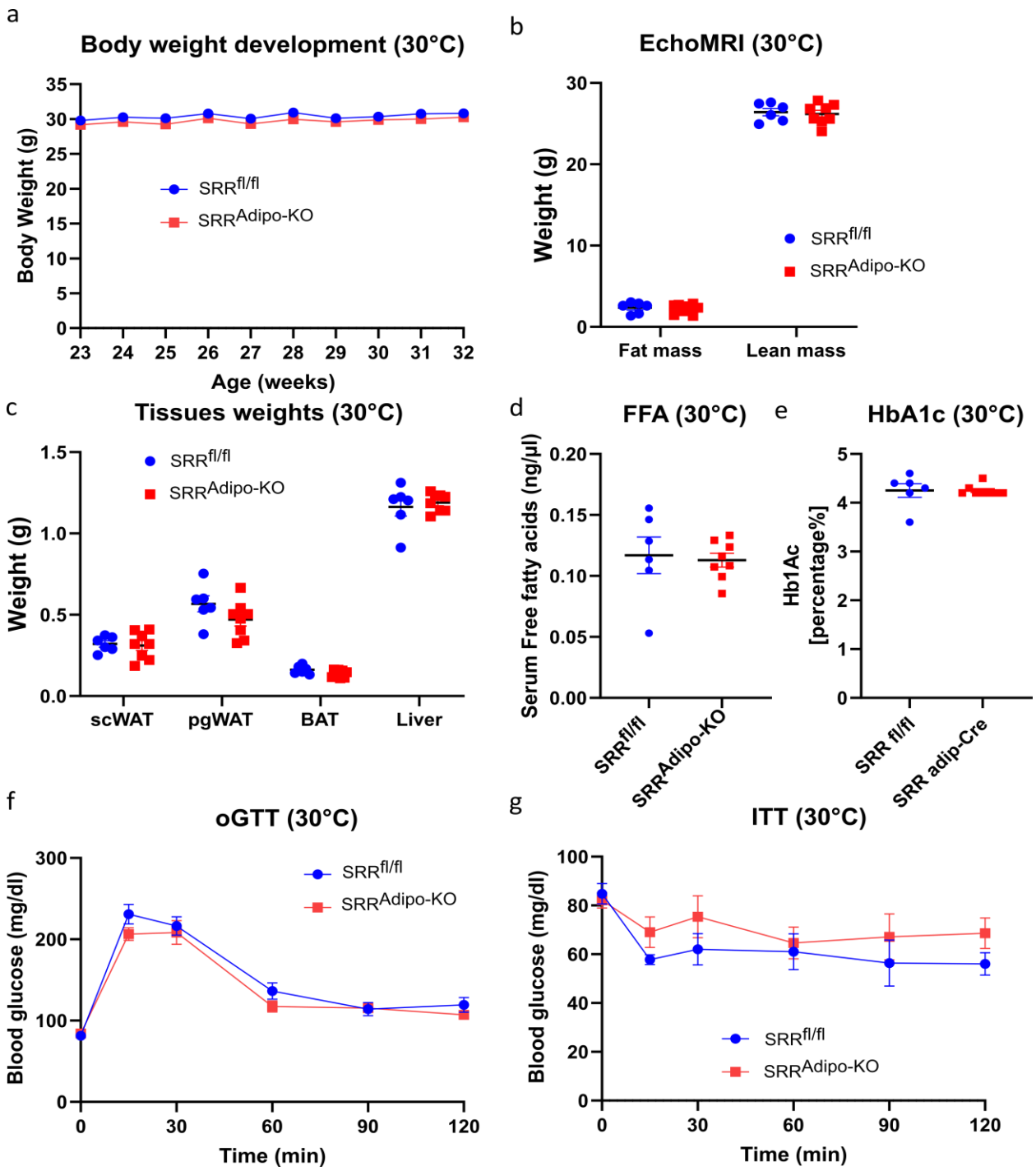

Figure 18: Adipose tissue specific deletion of serine racemase does not alter body weight, body composition or glucose homeostasis under thermoneutrality (30°C).

a) Body weight development, b) body composition, c) tissues weights, d) serum free fatty acid levels, e) HbA1c percentage under thermoneutrality in $SRR^{Adipo\text{-}KO}$ mice (n=8) mice and controls (n=6). f) Oral glucose tolerance test (oGSIS) and g) insulin tolerance test (ITT) in $SRR^{Adipo\text{-}KO}$ (n=8) mice and controls (n=5) under themoneutrality (30°C). Data are shown as mean ± SEM. Statistics were calculated using unpaired t-test or Two-way ANOVA followed by Sidak´s multiple comparison test.

3.8 High fat diet feeding exacerbates adipose hypertrophy and ameliorates high fat diet induced glucose intolerance in SRR$^{Adipo\text{-}KO}$ mice.

One major observation that was seen in SRR$^{Adipo\text{-}KO}$ mice fed chow diet under room temperature is that scWAT and BAT showed hypertrophy in adipocyte size and lipid droplet size respectively. High fat diet (HFD) feeding of mice is known to boost adipose tissue hypertrophy (Poret et al. 2018). So, one would assume that HFD feeding would exacerbate the hypertrophy phenotype seen under chow diet in SRR$^{Adipo\text{-}KO}$. Therefore, we fed SRR$^{Adipo\text{-}KO}$ mice and controls HFD. However, firstly, we wanted to study the effect of HFD on serine racemase expression in fat depots. Therefore, we examined fat depots of wild type mice fed chow diet and HFD. We saw a clear trend towards higher expression in white fat depots (although it did not reach statistical significance) (Figure 19a). On the other hand, HFD significantly down regulated serine racemase protein expression in BAT (Figure 19a).

Adipose tissues of SRR$^{Adipo\text{-}KO}$ mice fed HFD and controls were examined via H&E staining (Figure 19b) and adipocytes size and lipid droplets size were measured in white fat and brown fat respectively (Figure 19c). SRR$^{Adipo\text{-}KO}$ mice showed hypertrophy in all fat depots tested (Figure 19c). Even pgWAT of SRR$^{Adipo\text{-}KO}$ mice, which did not show hypertrophy under chow diet (Figure 9b), exhibited hypertrophy under HFD (Figure 19c). Thus, HFD exacerbates fat depots hypertrophy in SRR$^{Adipo\text{-}KO}$ mice.

SRR$^{Adipo\text{-}KO}$ mice placed under HFD showed no difference in body weight gain in comparison to controls (Figure 20a). Moreover, fat mass and lean mass were similar between the genotypes (Figure 20b). Furthermore, after sacrificing the mice, tissues weights were measured and SRR$^{Adipo\text{-}KO}$ mice exhibited no differences in any of the tissues weights in comparison to controls (Figure 20c). Under chow diet, several genes were differentially expressed in fat depots of SRR$^{Adipo\text{-}KO}$ mice in comparison to controls. Thus, we aimed to see if HFD challenge would augment or alter these changes. Therefore, using qPCR, several genes involved in the development, function and maintenance of fat depots were examined in SRR$^{Adipo\text{-}KO}$ mice and controls fed HFD. Interestingly, no significant differences in gene expression were seen between the genotypes in any of the genes or depots tested except for *Asc1* which was downregulated in pgWAT of SRR$^{Adipo\text{-}KO}$ mice (Figure 20d). Therefore, these data show that, although, there is an observed hypertrophy in all fat depots, serine racemase deletion in fat depots does not alter body weight, body composition or gene expression in fat depots of SRR$^{Adipo\text{-}KO}$ mice fed HFD.

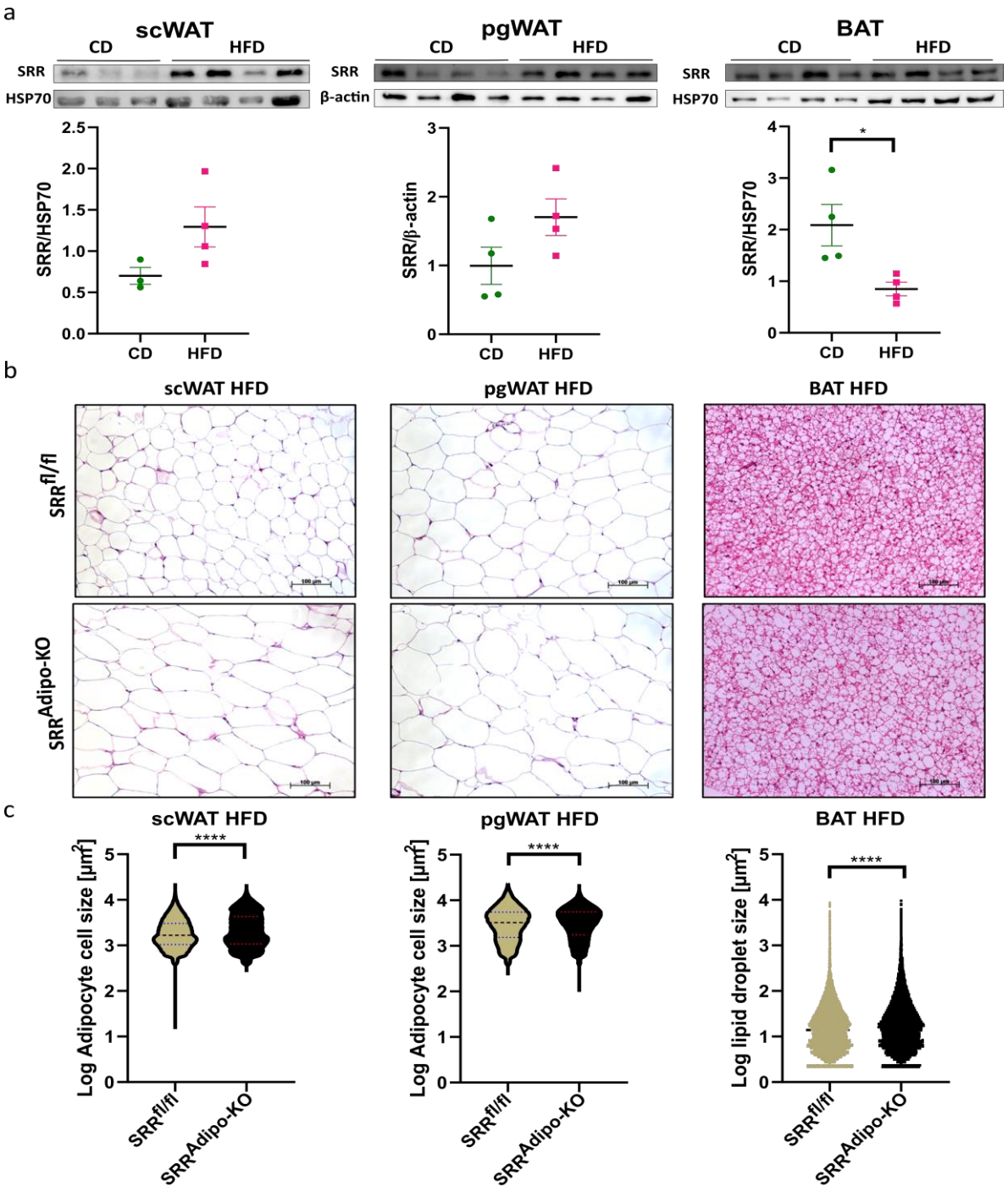

Figure 19: Serine racemase expression is modulated by HFD feeding and its deletion in adipose tissue leads to fat depots hypertrophy.

a) Protein expression analysis of serine racemase (SRR) relative to control (HSP70 or β-actin) in fat depots of Wildtype mice fed either chow or HFD. b) H&E staining of fat depots of $SRR^{Adipo\text{-}KO}$ mice and controls fed HFD. c) Adipocyte size quantification and lipid droplet size quantification in white and brown fat respectively. (scWAT, $SRR^{Adipo\text{-}KO}$ n=4, controls n=5), (pgWAT, $SRR^{Adipo\text{-}KO}$ n=3, controls n=5), (BAT, $SRR^{Adipo\text{-}KO}$ n=3, controls n=5). Data are shown as mean ± SEM. Statistics were calculated using unpaired t-test. *P<0.05, ****P<0.0001

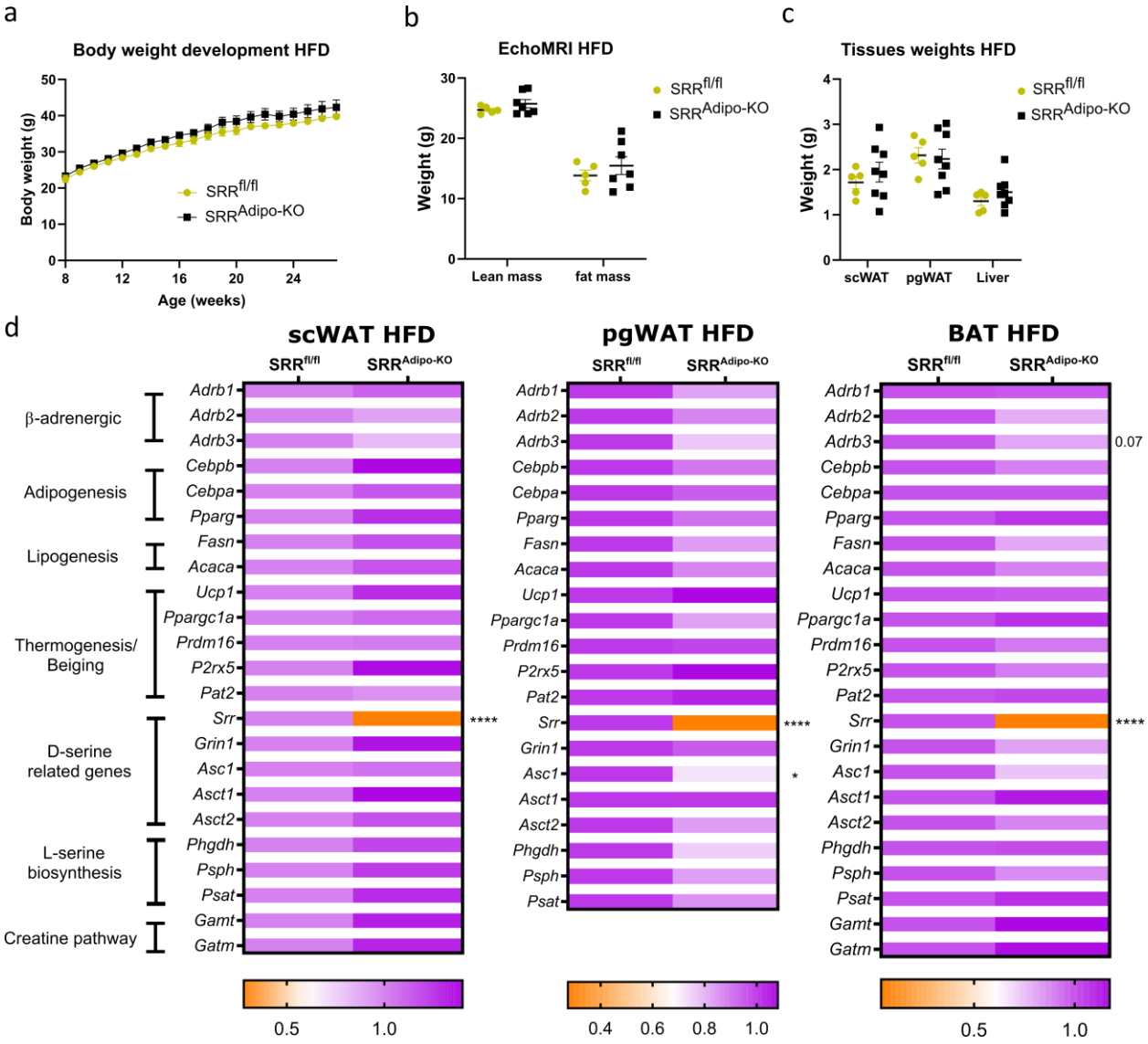

Figure 20: Adipose tissue specific deletion of serine racemase does not alter body weight development, body composition, tissues weights or fat depots gene expression under HFD.

a) Body weight development, b) body composition and c) tissues weights in $SRR^{Adipo\text{-}KO}$ (n=8) mice and controls (n=5) after 19 weeks on HFD. d) qPCR gene expression analysis in scWAT, pgWAT and BAT of $SRR^{Adipo\text{-}KO}$ mice (n=8) and controls (n=5). a-c) Data are shown as mean ± SEM. Statistics were calculated using Two-way ANOVA followed by Sidak´s multiple comparison test. d) Data are normalized to controls and presented as median. Unpaired t-test was done to calculate significance for each gene. *P<0.05, ****P<0.0001

One could postulate that the fat depots hypertrophy in $SRR^{Adipo\text{-}KO}$ mice fed HFD is a sign of adipose tissue insulin resistance and systemic glucose intolerance. Therefore, mice were challenged with oral glucose tolerance test and insulin tolerance test to assess systemic glucose tolerance and insulin sensitivity. Interestingly, $SRR^{Adipo\text{-}KO}$ mice showed improved glucose tolerance after 8 weeks on HFD as evident by the area under curve (Figure 21a). Surprisingly, this improvement in glucose tolerance was gone after 16 weeks on HFD (Figure 21c). Furthermore, there was no difference in HbA1c levels between the genotypes

after 19 weeks on HFD (Figure 21d). Additionally, $SRR^{Adipo\text{-}KO}$ mice did not show any difference in insulin sensitivity in comparison to controls after 18 weeks on HFD (Figure 21e). Moreover, there was no difference in plasma insulin (Figure 21f) and serum free fatty acid levels (Figure 21b) between the genotypes. Thus, serine racemase deletion in fat depots ameliorates HFD induced glucose intolerance only after 8 weeks of HFD and this protection against HFD induced glucose intolerance is gone after prolonged exposure to HFD.

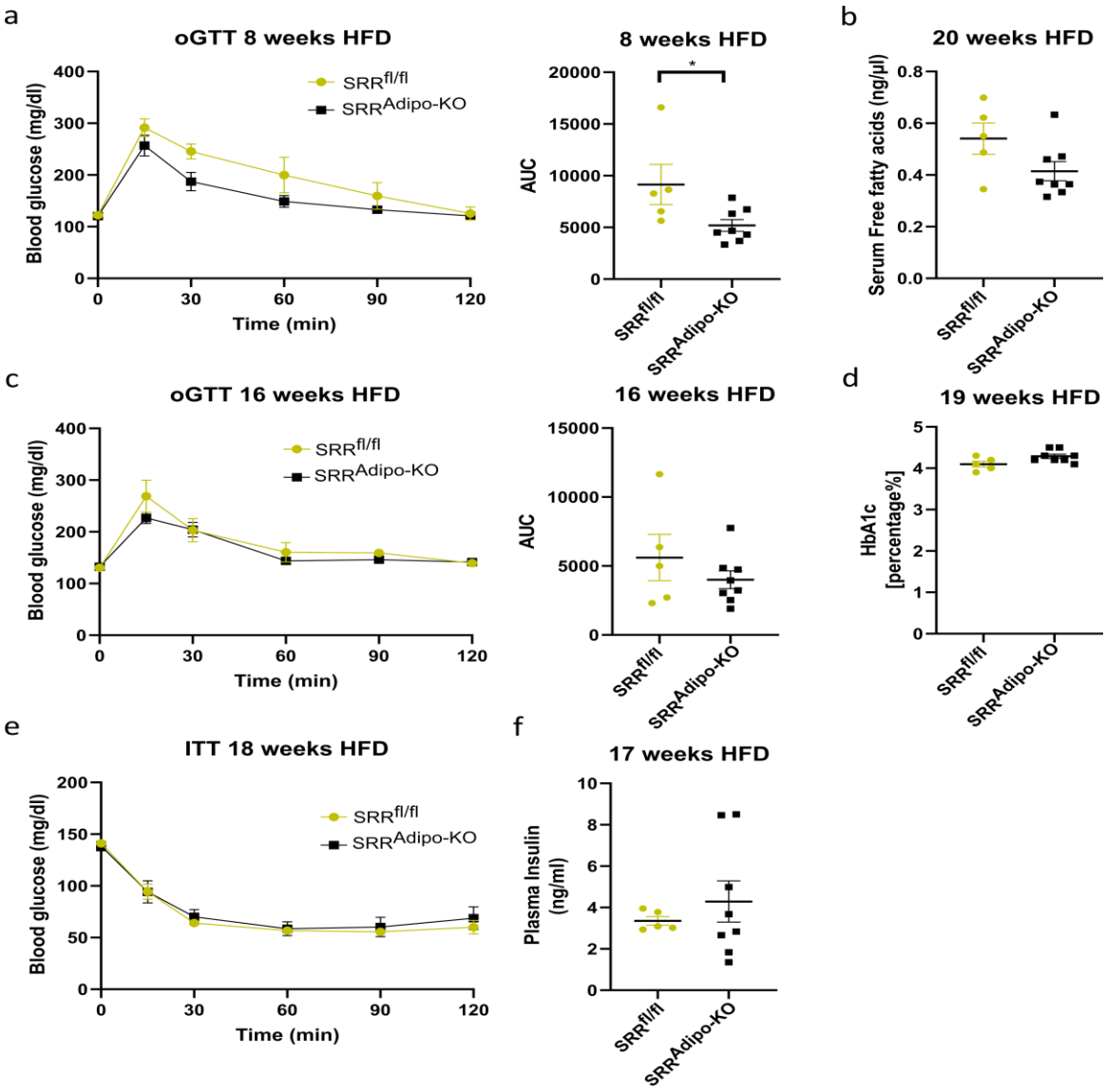

Figure 21: Adipose tissue specific deletion of serine racemase ameliorates diet induced glucose intolerance only after 8 weeks of HFD feeding.

a) Oral glucose tolerance test (oGTT) after 8 weeks of HFD and area under the curve. b) Serum free fatty acid levels after 20 weeks of HFD. c) oGTT after 16 weeks of HFD and area under the curve. d) Percentage of glycosylated hemoglobin (HbA1c) after 19 weeks of HFD. e) Insulin tolerance test (ITT) after 18 weeks on HFD. f) Plasma insulin levels after 17 weeks on HFD in $SRR^{Adipo\text{-}KO}$ (n=8) and controls (n=5). Data are shown as mean ± SEM. Statistics were calculated using unpaired t-test or Two-way ANOVA followed by Sidak´s multiple comparison test. *P<0.05

3.9 Adipose tissue specific deletion of serine racemase alters D-serine levels in isolated adipocytes from pgWAT and BAT

As serine racemase is deleted in mature adipocytes in the $SRR^{Adipo\text{-}KO}$ mice and serine racemase is the only enzyme known to produce D-serine *in vivo* (Miya et al. 2008; Wolosker, Blackshaw, and Snyder 1999), we reasoned that deletion of serine racemase in adipocytes will greatly reduce D-serine levels in adipocytes and this in turn will result in the observed phenotypes in $SRR^{Adipo\text{-}KO}$ mice. Therefore, mature adipocytes were isolated from scWAT, pgWAT and BAT from $SRR^{Adipo\text{-}KO}$ mice and controls. Thereafter, D-serine levels were quantified via ultra-high performance liquid chromatography followed by mass spectrometry and normalized to methionine levels. Surprisingly, serine racemase deletion in adipocytes did not alter D-serine levels in mature adipocytes isolated from scWAT (Figure 22). However, D-serine levels were, insignificantly, reduced in adipocytes isolated from pgWAT and BAT of $SRR^{Adipo\text{-}KO}$ mice in comparison to controls. Moreover, serine racemase deletion in adipocytes did not alter serum D-serine levels (Figure 22). Therefore, serine racemase deletion in adipocytes shows modest effect on D-serine levels in pgWAT and BAT and exhibits no effect on D-serine levels in scWAT and serum under our experimental conditions.

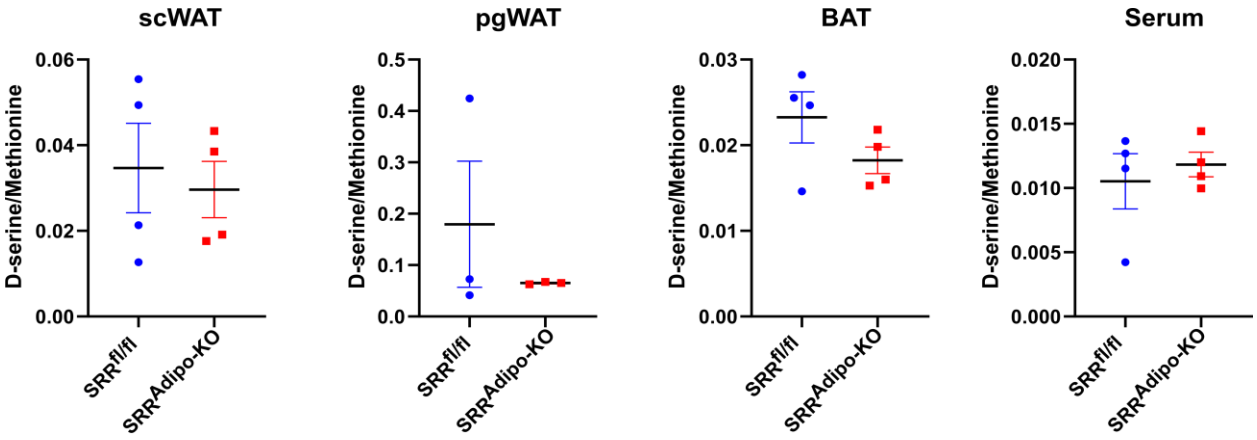

Figure 22: Adipose tissue specific deletion of serine racemase alters D-serine levels in mature adipocytes of pgWAT and BAT but not in mature adipocytes of scWAT or serum.
Ultra high performance liquid chromatography followed by mass spectrometry analysis of D-serine and Methionine from mature adipocytes isolated from scWAT, pgWAT and BAT and from serum of $SRR^{Adipo\text{-}KO}$ (n=3-4) and controls (n=3-4). Data are shown as mean ± SEM. Statistics were calculated using unpaired t-test.

3.10 *Grin1* expression *in vitro* and *in vivo*

D-serine acts as a co-agonist of the N-methyl-D-aspartate receptors (NMDAR). NMDAR play a vital role in synaptic plasticity, memory formation and learning. D-serine (or glycine) binds to GluN1 which is the obligatory subunit of the NMDAR and is encoded by *Grin1* (Hansen et al. 2018). I showed that serine racemase, which synthesizes D-serine, is present in both stromal vascular fraction and mature adipocytes of the adipose tissues. Therefore, we reasoned that the biological target of D-serine, namely GluN1, could be expressed in adipose tissue as well and is activated in an autocrine or paracrine way by D-serine. To test this, we examined single cell RNA sequencing data from stromal vascular fraction of scWAT, pgWAT and BAT from two and 8 weeks old mice. In this data set, all cells present in the adipose tissue, apart from

mature adipocytes, are examined. *Grin1* expression was almost undetectable regardless of the age of the mice or the type of fat depot examined (Figure 23a). However, one limitation of single cell RNA sequencing data is that it is noisy and have high biological variability (Chen, Ning, and Shi 2019). Therefore, to overcome this problem, existing bulk RNA data sequencing from pre- and mature brown adipocytes immortalized clones (Karlina et al. 2021) were analyzed. However, in line with the single cell RNA sequencing data, *Grin1* expression was almost undetectable in both pre- and mature brown adipocytes (indicated by a count number close to zero) (Figure 23b).

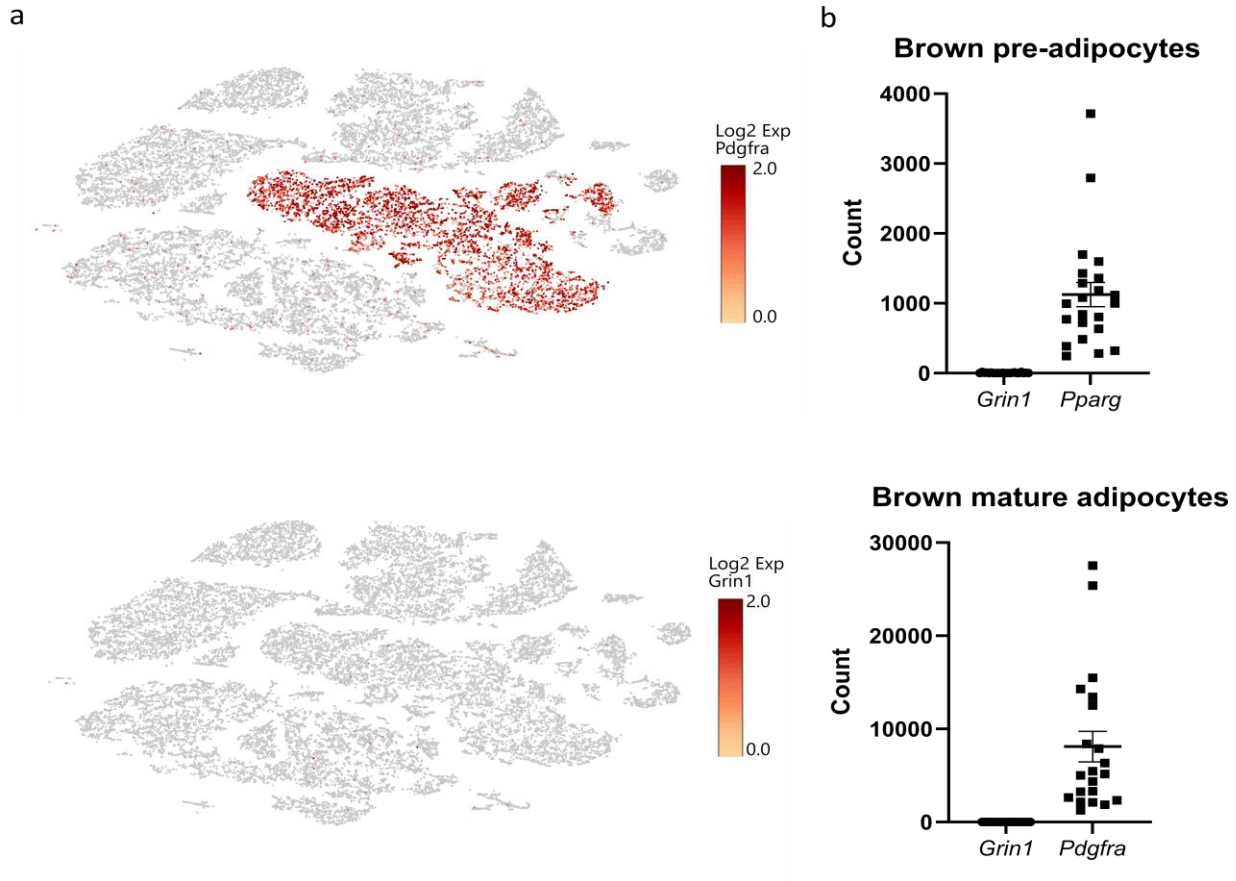

Figure 23: *Grin1* expression is not detected in stromal vascular fraction of fat depots and in mature immortalized brown adipocytes.
a) Single cell RNA sequencing data showing stromal vascular fraction of scWAT, pgWAT and BAT from two and 8 weeks old mice. *Pdgfra* (pre-adipocyte marker) upper panel, *Grin1* lower panel. b) Bulk RNA sequencing from pre- and mature immortalized brown adipocytes. Upper panel shows *Grin1* and *Pparg* count number in pre-adipocytes, lower panel shows *Grin1* and *Pdgfra* count number in mature adipocytes.

Thereafter, to examine *Grin1* expression *in vivo*, scWAT, pgWAT and BAT were isolated from mice. This was followed by separation into stromal vascular fraction and mature adipocytes. Interestingly, using qPCR, *Grin1* expression was detected only in the stromal vascular fraction and not in mature adipocytes of different fat depots in both male and female mice (Figure 24a&b). In female mice, stromal vascular fraction of BAT showed higher expression of *Grin1* than stromal vascular fraction of scWAT and pgWAT. (Figure 24b). However, in male mice, no difference in *Grin1* expression was seen between the stromal vascular fractions of different fat depots (Figure 24a). After that, primary subcutaneous pre-adipocytes

were isolated and differentiated *in vitro*. In primary cells, *Grin1* expression was detected in both pre- and mature adipocytes (Figure 24c). However, this could be due the presence of pre-adipocytes within the mature adipocytes culture. Lastly, GluN1 protein expression was examined in white and brown fat tissues. Remarkably, GluN1 is detected in scWAT, pgWAT and BAT of Wildtype mice (Figure 24d). These data show that *in vivo Grin1* is detected in the stromal vascular fraction and not in mature adipocytes of the adipose tissue and this in turn explains the observed GluN1 protein in white and brown whole tissue lysates.

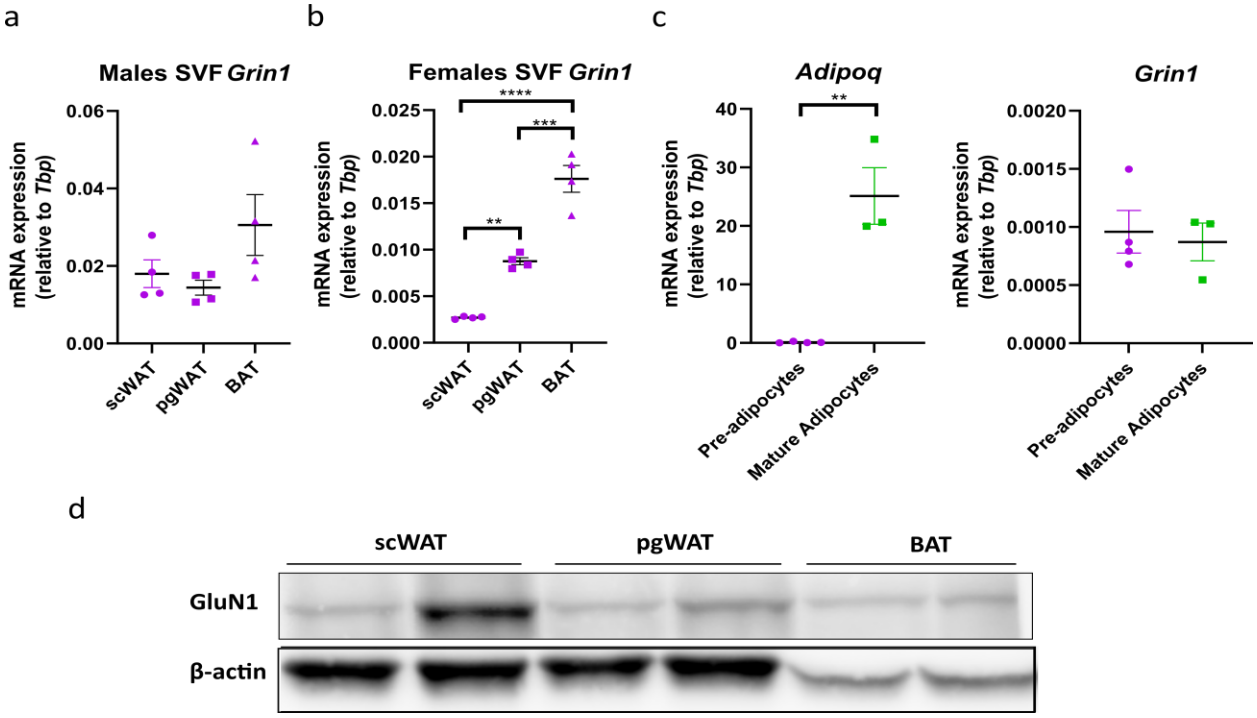

Figure 24: *Grin1* is detected in stromal vascular fraction of fat depots and GluN1 is detected in whole fat tissue lysates.

qPCR gene expression analysis of *Grin1* in stromal vascular fraction (SVF) of scWAT, pgWAT and BAT from a) male and b) female Wildtype mice. c) qPCR gene expression analysis of *Adipoq* and *Grin1* from primary pre-adipocytes and mature *in vitro* differentiated subcutaneous adipocytes. d) Protein expression analysis of GLUN1 and β-actin in scWAT, pgWAT and BAT from Wildtype mice. Data are shown as mean ± SEM. Statistics were calculated using unpaired t-test or One-way ANOVA followed by Turkey´s multiple comparison test. **P<0.01, ***P<0.001, ****P<0.0001

3.11 Reduced body weight in Grin1$^{Adipo\text{-}KO}$ mice

Grin1$^{fl/fl}$ mice were mated with Adiponectin-Cre^{+} mice to generate Grin1$^{fl/fl}$ Adiponectin-Cre^{+} mice (Grin1$^{Adipo\text{-}KO}$) and Grin1$^{fl/fl}$ Adiponectin-Cre^{-} mice (controls). *Grin1* is not detected in mature adipocytes. Surprisingly, in Grin1$^{Adipo\text{-}KO}$ mice where *Grin1* is only deleted in mature adipocytes, a phenotype is observed. Grin1$^{Adipo\text{-}KO}$ mice showed a reduction in lean mass and body weight in comparison to controls (Figure 25a-25c). However, Grin1$^{Adipo\text{-}KO}$ mice did not show any differences in glucose tolerance or insulin sensitivity as assessed by glucose tolerance and insulin tolerance tests respectively in comparison to controls (Figure 25d&e). Furthermore, there was no difference in HbA1c levels between the genotypes (Figure 25f) indicating no impairment in long term glucose homeostasis.

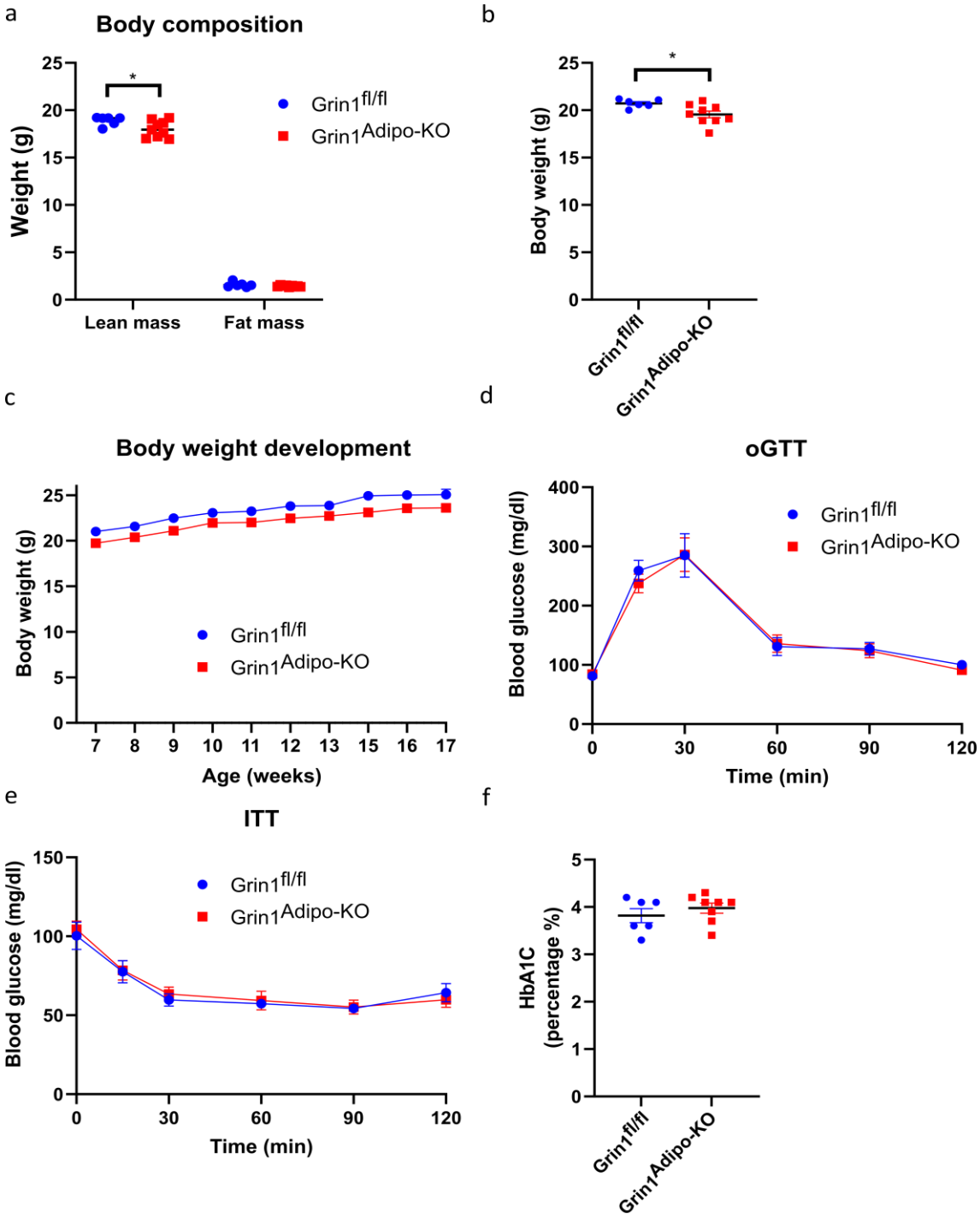

Figure 25: Adipose tissue specific deletion of *Grin1* reduces lean mass and body weight without altering glucose homeostasis.

a) EchoMRI analysis of fat and lean mass and b) body weight measurement of Grin1$^{Adipo\text{-}KO}$ mice (n=9) and controls (n=6). c) Body weight development of Grin1$^{Adipo\text{-}KO}$ mice (n=8) and controls (n=6). d) Oral glucose tolerance test (oGTT), e) insulin tolerance test (ITT) and glycosylated hemoglobin (HbA1c) analysis of Grin1$^{Adipo\text{-}KO}$ (n=8) mice and controls (n=6). Data are shown as mean ± SEM. Statistics were calculated using unpaired t-test or Two-way ANOVA followed by Sidak´s multiple comparison test. *P<0.05

4 Discussion

Obesity is a major health problem affecting millions of people worldwide. It is a growing pandemic affecting developing and developed countries and children and adults. Obesity itself is a disease associated with higher risk of morbidity and mortality. Moreover, it increases the risk of diseases like certain cancers, cardiovascular disorders and diabetes (Caballero 2019). Currently, therapies for obesity include nutritional, behavioral and physical changes. However, lifestyle intervention aiming at reducing caloric consumption show poor efficacy in the long term with most individuals regaining one-third to two-third of their lost weight in one year and >95% after 5 years following end of treatment (Foster 2006). Professional organizations like the obesity society and the endocrine society recommend drug therapy after 6 months if individuals are not responsive to lifestyle interventions (Apovian et al. 2015; Jensen et al. 2014). Several drugs are approved for short term and long term treatment of obesity. However, drugs are costly and show adverse effects in some individuals. Moreover, drugs only cause modest decrease in body weight (Müller et al. 2022; Tak and Lee 2021). On the other hand, surgical interventions show the highest efficacy but have serious side effects and are not feasible/available to everyone (Bult, van Dalen, and Muller 2008). Therefore, finding new therapies that can reduce or revert obesity can save millions of life and save billions of dollars (Cawley et al. 2021). One promising candidate is thermogenic fat (beige and brown adipocytes). Thermogenic adipocytes can generate heat instead of ATP. In this process, fatty acids and glucose are used to fuel non-shivering thermogenesis via the action of UCP1. Therefore, these energy substrates are used to produce heat and are not stored as triglycerides, thus, lowering blood glucose and fatty acid levels (Cheng et al. 2021). That´s why, mice without thermogenic adipocytes develop obesity (Lowell et al. 1993). In humans, brown and beige fat activity is inversely correlated with age, BMI, and levels of circulating lipids and glucose (Chondronikola et al. 2014; Lichtenbelt et al. 2009; Virtanen et al. 2009; Yoneshiro et al. 2011). However, even in lean individuals with large BAT depot, cold induced thermogenesis of BAT plays only a minor role in energy balance (Muzik et al. 2013; Raiko et al. 2016). Therefore, beiging of the big scWAT depot in humans is an appealing strategy to increase whole body energy expenditure and induce sustained decline in body weight. Beiging in humans can be induced by exercise (Otero-Díaz et al. 2018). However, the majority of individuals in the US do not do the recommended level of physical activity (Kruger, Kohl III, and Miles 2007). Beiging can also be seen under extreme conditions like in burn victims, cancer patients with severe weight loss or obese individuals after weight loss surgery (Rabiee 2020). Furthermore, 10 days of cold exposure were insufficient to induce WAT beiging, although they activated BAT (Chondronikola et al. 2016; van der Lans et al. 2013). Giving the lack of strategies to induce beiging in humans, study of molecular targets that modulate beiging and understanding proteins and pathways that regulate beiging is of crucial importance. A previous study from our lab showed that ASC1 is involved in beiging and that this beiging effect could be due to D-serine (Suwandhi et al. 2021). Other players that can modulate metabolic homeostasis are amino acids. Amino acids participate in many crucial functions in the human like protein synthesis, cell signaling or as energy source. One of these amino acids that is now garnering attention is Serine (Holm and Buschard 2019). In human, Serine levels are associated with improved glucose tolerance and insulin sensitivity. Moreover, low Serine levels are seen in both type 1 and type 2 diabetic individuals (Holm and Buschard 2019). However, one does not know if these effects are due to L-serine or due to its conversion to the enantiomer D-serine by serine racemase (Wolosker and Mori 2012). Interestingly, in mice D-serine supplementation blunts diet induced weight gain and leads to glucose intolerance (Suwandhi et al. 2018). Therefore, we aimed to investigate the role D-serine in adipose depots beiging by deleting the enzyme that synthesizes

it, serine racemase, specifically in the adipose tissue. We also aimed to examine the effect of the lack of serine racemase/D-serine in the adipose tissue on whole body energy and glucose homeostasis.

One major risk factor for the development of obesity and diabetes is aging (Jura and Kozak 2016). Glucose intolerance as well as fat mass increase with aging (DeFronzo 1981; Jiang et al. 2015). One mechanism contributing to aging is telomere shortening. Telomeres shorten with each cell cycle. That´s why aged individuals show shorter telomeres than young ones (LaRocca, Seals, and Pierce 2010). The study of telomere shortening in aged humans is complicated given the aging-accompanying co—morbidities that complicate the interpretation of the results. However, in mice one could study the effects of telomere shortening by inhibiting telomerase action. Telomerase is a ribonucleoprotein enzyme complex that elongates telomeres (Turner, Vasu, and Griffin 2019). In mice, inhibition of telomerase via deletion of *Terc* results in progressive shortening of telomeres with each generation (Blasco 2005). To understand the contribution of telomere shortening on body composition and energy homeostasis, we studied second generation (G2) male and female Terc KO mice.

4.1 Adipose tissue serine racemase modulates beiging and whole body energy expenditure

Here I show for the first time that serine racemase is detected in all adipose depots on gene and protein level. Moreover, not only is serine racemase expressed in mature adipocytes but also expressed in the stromal vascular fraction of fat depots. It is unknown which cells in the stromal vascular fraction express serine racemase and it would be an interesting topic for future experiments. Serine racemase expression is also modulated by HFD feeding. Interestingly, Serine racemase expression is reduced in BAT and shows, statistically insignificant, increase in WAT upon HFD feeding. Serine racemase deletion leads to hypertrophy in scWAT and BAT under chow diet and in all fat depots under HFD. Hypertrophy is associated with insulin resistance and glucose intolerance (Morigny et al. 2021). However, $SRR^{Adipo\text{-}KO}$ mice exhibit no impairment in glucose tolerance or insulin sensitivity under chow diet. Surprisingly, under HFD, $SRR^{Adipo\text{-}KO}$ mice show improvement in glucose tolerance after 8 weeks on HFD in comparison to controls. However, this improvement in glucose tolerance is gone after 16 weeks on HFD. These results indicate that serine racemase deletion in adipose tissue somehow delays the onset of diet-induced glucose intolerance even if deletion of serine racemase causes hypertrophy. The reason for this hypertrophy in fat depots could not be explained by impairment in lipolysis as there was no difference in FFA released from WAT pieces under basal or isoproterenol-stimulated conditions. Under chow diet, this hypertrophy could be explained by the decrease in energy expenditure in $SRR^{Adipo\text{-}KO}$ mice (thus, more energy storage) and in BAT with the decrease of adipogenesis markers in $SRR^{Adipo\text{-}KO}$ mice. Sadly, due to technical difficulties, $SRR^{Adipo\text{-}KO}$ mice energy expenditure was not measured in mice fed HFD. However, if one extrapolates the data, one could hypothesize that the hypertrophy seen in fat depots under HFD is due to decreased energy expenditure. Of note, several differences in gene expression in all fat depots were observed between the genotypes under chow diet. However, under high fat diet no differences in any of the genes expression were observed between the genotypes except for *Asc1* which was downregulated in pgWAT of $SRR^{Adipo\text{-}KO}$ mice. ASC1 is a marker of WAT (Ussar et al. 2014). ASC1 inhibition in human and murine adipocytes decreases Serine uptake and glutathione production and leads to an increase in reactive oxygen species production (Jersin et al. 2021). On the other hand, overexpression of ASC1 reduces reactive oxygen species production and increases mitochondrial respiration. Moreover, ASC1 is inversely correlated with visceral adiposity and insulin resistance. Interestingly inhibition of ASC1 is associated with higher expression of a lipid

storage marker (*SCD*) (Jersin et al. 2021). This is line with the observation that in pgWAT (visceral fat), lower *Asc1* expression is associated with hypertrophy (excess lipid storage) in $SRR^{Adipo\text{-}KO}$ mice. Under chow diet, the decreased adipogenesis gene expression in BAT coupled with the observed hypertrophy pointed towards a malfunction in BAT function. However, no difference in thermogenesis gene expression was seen between the genotypes. Furthermore, $SRR^{Adipo\text{-}KO}$ mice were able to find their body temperature under acute cold exposure (4°C). These results show that BAT function is intact in $SRR^{Adipo\text{-}KO}$ mice despite hypertrophy and decreased adipogenesis gene expression. Adipogenesis is the step where multipotent cells commit to the adipogenic lineage, absorb nutrients and differentiate into lipid-filled mature adipocytes (Ghaben and Scherer 2019). Several important transcription factors play a role in adipogenesis like PPARγ, which is the master transcription regulator for adipogenesis and is essential for formation of mature adipocytes (Rosen et al. 1999), and CEBPβ/α (Ghaben and Scherer 2019; Wu et al. 1999). Under nutrient access adipocyte can either expand via hypertrophy, increase in the adipocyte size, or hyperplasia which is the formation of new adipocytes from progenitor cells (adipogenesis) (Ghaben and Scherer 2019). Thus, decrease in adipogenesis will favor hypertrophy than hyperplasia and this is the case in BAT of $SRR^{Adipo\text{-}KO}$ mice. Interestingly, pgWAT of $SRR^{Adipo\text{-}KO}$ mice shows decreased adipogenesis gene expression without resulting in hypertrophy under chow diet. Hypertrophy increases the mechanical stress on the adipocytes as they expand in size and get in contact with surrounding cells and the extracellular matrix. Moreover, hypertrophic cells experience hypoxia as they expand in size reaching oxygen diffusion limits. These factors promote a pro-inflammatory environment in the hypertrophic fat depot (Ghaben and Scherer 2019). In $SRR^{Adipo\text{-}KO}$ mice fed chow diet, hypertrophic BAT show increased *Tnfa* expression. Meanwhile, scWAT of $SRR^{Adipo\text{-}KO}$ mice do not. However, this could be due to that scWAT of $SRR^{Adipo\text{-}KO}$ mice does not show reduction in adipogenesis gene expression. An interesting observation was that $SRR^{Adipo\text{-}KO}$ mice show higher beiging markers gene expression in scWAT than controls. This peaked our interest as *Asc1* knockdown in pre-adipocytes induced beiging upon differentiation. An effect that could be due to D-serine (Suwandhi et al. 2021). However, this increase in several beiging markers in scWAT of $SRR^{Adipo\text{-}KO}$ mice did not alter UCP1 protein or gene expression. However, only a low number of beige adipocytes appear in scWAT under room temperature. On the other hand, chronic cold exposure leads to augmented release of noradrenaline from sympathetic nerves and leads to enhanced BAT activation and thermogenesis. Moreover, chronic cold exposure recruits beige adipocyte in scWAT (Kissig, Shapira, and Seale 2016). That´s why, mice were placed under chronic cold exposure (4°C) for one week to induce beiging and exacerbate the differences seen in beiging of scWAT between the genotypes under room temperature. Interestingly, no difference in any of the beiging markers was seen under chronic cold exposure. UCP1 also showed similar levels between the genotypes. Furthermore, the reduction in energy expenditure in $SRR^{Adipo\text{-}KO}$ mice seen under room temperature was abolished under chronic cold exposure. Surprisingly, no differences were seen in any of the genes tested in any fat depots between the genotypes. Thus, chronic cold exposure normalized all gene levels in fat depots of $SRR^{Adipo\text{-}KO}$ mice to controls and eliminated the difference in energy expenditure between the genotypes. An explanation for this is that effect of serine racemase can only be seen under low β-adrenergic stimulation or that β-adrenergic stimulation completely masks and reverts the effects of serine racemase deletion. Therefore, we wanted to explore a situation where there is no or very little sympathetic activation. That´s why $SRR^{Adipo\text{-}KO}$ mice were placed under thermoneutrality (30°C) condition. Sadly, due to time restrictions, beiging markers were not examined in scWAT of these mice. However, under themoneutrality, no differences in glucose tolerance or insulin sensitivity were seen between the genotypes. Moreover, $SRR^{Adipo\text{-}KO}$ mice exhibited similar energy expenditure and respiratory exchange ratio to controls. At the end, no differences were

seen between the genotypes under thermoneutrality. Interestingly, *in vitro* differentiated primary subcutaneous adipocytes from $SRR^{Adipo\text{-}KO}$ mice show increased expression of adipogenesis markers and beiging markers. Thus, the beiging effect seen in scWAT *in vivo* under room temperature is recapitulated *in vitro* and could be due to cell autonomous effects due to serine racemase deletion.

How does deletion of serine racemase impact tissue and whole body physiology? Serine racemase produces D-serine from L-serine and the main function of D-serine is as a co-agonist of the NMDAR. It binds to GluN1 and together with glutamate, following membrane depolarization, activate NMDAR. This results in cations influx, mainly Ca^{+2}, which activate signaling cascades and, depending on the tissue, cause various outcomes (Hansen et al. 2018). Of note, serine racemase also produces pyruvate from both L-serine and D-serine. This function is thought to degrade D-serine in the brain in areas where there is no natural D-amino acid degrading enzyme (Wolosker and Mori 2012). However, serine racemase elicited pyruvate production promotes the growth of colorectal cancer cells (Ohshima et al. 2020), thus, showing that pyruvate produced by serine racemase could be useful as an energy source. This is of particular interest as serine racemase produces 4 pyruvate molecules for each molecule of D-serine (Wolosker and Mori 2012). Nonetheless, as we saw serine racemase expression in both stromal vascular fraction and adipocytes of all fat depots tested, we reasoned that D-serine could be produced from adipose depots and communicates with the nervous system to modulate its function. Therefore, we examined NMDAR presence in the adipose tissue. Interestingly, the obligatory subunit of the NMDAR, *Grin1*, was not detected by single cell RNA sequencing in stromal vascular fraction cells of fat depots from two and 8 weeks old mice. Moreover, *Grin1* was not detected by bulk RNA sequencing from pre- and mature brown immortalized adipocytes clones. However, low *Grin1* gene expression was detected in stromal vascular fraction from different fat depots of mice via qPCR. Interestingly, primary differentiated subcutaneous adipocytes show *Grin1* gene expression. However, pre-adipocytes were still present in culture after 8 days of differentiation. These data point that the stromal vascular fraction cells which express *Grin1* could be pre-adipocytes. The presence of GluN1 is also confirmed by western blot from WAT and BAT whole tissue lysates. NMDAR have been consistently shown to play various roles in several organs of the periphery. For example, cardio-myocytes express NMDAR. Activation of NMDAR in neonatal rat cardio-myocytes leads to oxidative stress and mitochondrial dysfunction leading to cell death (Gao et al. 2007). *In vivo*, agonizing of NMDAR can lead to myocardial contractile abnormalities (Moshal et al. 2008). NMDAR are also expressed in podocytes. Activation of NMDAR in podocytes leads to reactive oxygen species production and prolonged activation leads to apoptotic cell death (Kim, Anderson, and Dryer 2012). Moreover, agonizing of NMDAR aggravates oxidative stress and ischemia-reperfusion-induced acute kidney injury while blocking NMDAR reduces oxidative stress and attenuates ischemia-reperfusion-induced acute kidney injury (Pundir et al. 2013). Furthermore, in the stomach, NMDAR in parietal cells are involved in gastric acid inhibition while NMDAR in nerve cells of submucosal ganglia are involved in gastric acid stimulation (Golovynska et al. 2018). Additionally, a recent report show that NMDAR are expressed in pulmonary smooth muscle cells and modulate pulmonary vasoconstriction (Dong et al. 2021). Importantly, in the pancreas, which is tightly involved in glucose homeostasis, D-serine shows antidiabetic effects via potentiating insulin secretion via activation of β-cells NMDAR (Lockridge et al. 2021). Moreover, pancreatic NMDAR were shown to be possible drug targets for the treatment of diabetes (Marquard et al. 2015). Combination of an NMDAR antagonist with the drug sitagliptin (dipeptidyl peptidase inhibitor) showed stronger glucose lowering effect after an oral glucose tolerance test in diabetic individuals than sitagliptin alone (Marquard et al. 2016). *Grin1* is expressed in several organs in the periphery (Ma et al. 2020). However. We did not detect *Grin1* gene expression in mature adipocytes and the mouse model

Grin1$^{Adipo\text{-}KO}$ only have deletion of *Grin1* in differentiating adipocytes, expressing adiponectin, and not other progenitors cells or stromal vascular fraction cells. Surprisingly, Grin1$^{Adipo\text{-}KO}$ mice show lower body weight that is due to reduction in lean mass and not fat mass. The reason for this puzzling observation is unknown. However, Grin1$^{Adipo\text{-}KO}$ mice show no difference in glucose tolerance, insulin sensitivity and HbA1c levels in comparison to controls.

In this thesis, adipose tissue serine racemase is characterized as a novel regulator of subcutaneous fat beiging. This is of particular importance as BAT is not present in all adults. One study demonstrated that out of one thousand men and one thousand women only 3.1% of men and 7.5% of women had active BAT (Cypess et al. 2009). Another study demonstrated that 50% of adults had active BAT when subjected to cold for two hours (Matsushita et al. 2014). Moreover, BAT activity is inversely correlated to BMI (Cypess et al. 2009; Saito et al. 2009; van Marken Lichtenbelt et al. 2009; Zingaretti et al. 2009). Therefore, cold-induced thermogenesis is reduced in obese individuals (Vijgen et al. 2011; Wijers, Saris, and Lichtenbelt 2010). This reduction in cold-induced thermogenesis is also thought to be due increased insulation due to increased fat depots in obese individuals (Thyagarajan and Foster 2017; Vijgen et al. 2011). Additionally, BAT decreases with aging (Heaton 1972). Given that BAT is not found in all adults and BAT decreases with obesity and aging, beiging of WAT has promising therapeutic potential (Harms and Seale 2013; Peschechera and Eckel 2013; Qian, Huang, and Tang 2015; Vosselman, van Marken Lichtenbelt, and Schrauwen 2013; Wu, Cohen, and Spiegelman 2013). Induction of beiging ameliorates metabolic abnormalities and protect against diet induced obesity in rodents (Baskaran et al. 2016; Bi et al. 2014; Rachid et al. 2015). Moreover, Intermittent fasting and microbiota regulate beging (Li et al. 2017). Furthermore, under cold exposure, mast cells promote human adipose beiging (Finlin et al. 2019). However, chronic cold exposure is not a feasible therapy for obesity. Therefore, a complete knowledge of the molecular targets that regulate beiging will enable adipose beiging in humans under thermoneutrality. For this goal, several molecular targets have been demonstrated to regulate beiging. β-adrenergic receptors (Keipert and Jastroch 2014), bone morphogenetic protein 8b (Whittle et al. 2012), FGF21 (Abu-Odeh et al. 2021; Huang et al. 2017), PRDM-16 (Ohno et al. 2012) and Sirtuin 1 (Baskaran et al. 2017; Qiang, Wang, Kon, Zhao, Lee, Zhang, Rosenbaum, Zhao, Gu, et al. 2012) are all modulators of beiging. In this report, I show that serine racemase is another modulator of adipose tissue beiging and therefore, could be targeted and tested for therapeutic applications in humans. On the other hand, adipose tissue hypertrophy is associated with insulin resistance and glucose intolerance (Goossens 2017; Stenkula and Erlanson-Albertsson 2018). I show that serine racemase deletion in adipose depots causes adipose tissue hypertrophy without altering glucose homeostasis parameters. Furthermore, under HFD, serine racemase deletion in adipose tissues delays the onset of diet-induced glucose intolerance. Thus, adipose tissue serine racemase is a novel modulator of adipose hypertrophy and glucose homeostasis. Of note, adipose tissue regulates energy homeostasis via adipokines it secretes and via alterations in adipocyte metabolism (e.g. thermogenesis) (Rosen and Spiegelman 2006). Here, I show that adipose tissue serine racemase regulates whole body energy expenditure. Therefore, adipose serine racemase could be targeted and tested for improving metabolic parameters in humans.

4.2 Second generation telomerase deficient mice show reduction in body weight, intestinal fatty acid uptake gene expression and sexual dimorphism

Telomerase deficient mice are a valuable tool in the study of the effects of telomeres shortening. Mice lacking telomerase have shorter telomeres and telomeres get shorter with each generation. Phenotypes associated with telomeres dysfunction include embryonic mortality due to failure to close the neural tube, male and female infertility, severe intestinal atrophy, atrophy of the spleen and defective proliferation of lymphocytes, reduced angiogenesis, diminished proliferative potential of bone marrow stem cells and compromised germinal center function (Blasco 2005). On a C57BL6/129Sv/SJL mixed background telomerase (Terc) deficient mice can go up to the sixth generation while on C57BL6 pure background mice can go up to only the fourth generation (G4) (Blasco et al. 1997; Herrera et al. 1999; Lee et al. 1998; Rudolph et al. 1999). These drastic phenotypes seen in late generations of telomerase deficient mice are all due to telomere shortening and can be reversed via re-introduction of telomerase. For instance, introduction of one allele of Terc in G4 Terc KO mice results in detectable telomeres and prevents chromosomal instability and premature aging (Samper, Flores, and Blasco 2001). G4 pure C57BL6 Terc KO mice show reduced food intake that explains the reduction in body weight. This reduction in body weight could also be explained by the severe intestinal atrophy in G4 Terc KO. However, G4 Terc KO mice do not show reduction in body fat or energy expenditure (Kuhlow et al. 2010). Interestingly, these mice show impaired glucose tolerance that is due to impaired insulin secretion. This impaired insulin secretion is due to reduced pancreatic islet size and impaired β-cell regeneration (Kuhlow et al. 2010). However, one caveat of this study is that G4 Terc KO, as discussed above, show major abnormalities in several tissues. Therefore, the observed phenotype could be due to deterioration of the whole body and not due to a direct effect on glucose homeostasis. Third generation (G3) Terc KO mice have reduced life expectancy as well. They also show a reduction in body weight. However, G3 Terc KO mice, unlike G4 Terc KO mice, show improvement in both glucose tolerance and insulin sensitivity (Missios et al. 2014). G3 Terc KO mice show only slight intestinal atrophy and less severe phenotype than G4 Terc KO mice (Samper, Flores, and Blasco 2001). In this thesis, I show that G2 mice show reduction in body weight that is due to both reduction in fat mass and lean mass. This reduction in body weight is not due to reduction in food intake or increase in energy expenditure but rather due to a decrease in fatty acid absorption as evident by reduction in fatty acid uptake genes expression in small intestine enterocytes in both male and female G2 Terc KO mice. This reduction in fatty acid uptake is in line with the reduction in WAT weight and the reduction in the size of pgWAT adipocytes. The small intestine is the primarily region for nutrient absorption while the large intestine is responsible for water and electrolyte transport (Kiela and Ghishan 2016). Intestinal fatty acid absorption is a process likely mediated by protein-mediated transfer and diffusion (Abumrad and Davidson 2012). One of these proteins is CD36. CD36 is a scavenger receptor that recognize similar molecular patterns rather than specific epitopes. That´s why it is involved in phagocytosis and antigen presentation and not only in fatty acid uptake (Cifarelli and Abumrad 2018). CD36 is highly expressed on the apical membranes of enterocytes villi in the small intestine. Primary enterocytes isolated from small intestine of *Cd36*$^{-/-}$ mice show reduced fatty acid uptake (Cifarelli and Abumrad 2018). Moreover, *Cd36*$^{-/-}$ mice show reduced oleic acid uptake when refed for 30 min after a 6h fast (Schwartz et al. 2008). Other intestinal proteins like fatty acid transport protein (FATP) 2 and 4 and plasma membrane fatty acid binding protein (gene name *Got2*) also modulate fatty acid uptake (Black et al. 2016; Roepstorff et al. 2004; Stahl

et al. 1999). In the case of G2 Terc KO mice, *Cd36* along with all other genes involved in fatty acid uptake tested are downregulated regardless of the gender in the small intestine, strongly suggesting a decrease in fatty acid uptake. Interestingly, higher expression of inflammatory markers is detected in small intestine of G2 Terc KO mice. This could highlight an effect on immune homeostasis especially giving that G4 and G6 Terc KO mice show immune abnormalities.

One major finding of this thesis is that G2 Terc KO mice show sexual dimorphism. The first observation was that 10 weeks old male G2 Terc KO mice show reduction in body weight that is due to a reduction in lean mass while female G2 Terc KO mice do not. Moreover, in the small intestine of G2 Terc KO mice, female mice show downregulation of glucose uptake genes namely *Slc5a1* (*Sglt1*) and *Glut2* while male mice show the opposite with upregulation of *Glut2* gene expression and, insignificant, increase in *Slc5a1*. Under low glucose conditions SGLT1 is localized to the brush border membrane of enterocytes and GLUT2 to the basolateral membrane. However, under high glucose conditions both transporters localize to the brush border membrane and participate in absorption of glucose from the gut lumen (Gromova, Fetissov, and Gruzdkov 2021; Helliwell and Kellett 2002). These data point that female G2 Terc KO mice could have reduced intestinal glucose uptake while male G2 Terc KO mice could have augmented intestinal glucose uptake. In the kidney, more than 180g/day of glucose is filtered through the renal glomerulus and almost all of it is reabsorbed (Mather and Pollock 2011). SGLT2 reabsorbs 90% of glucose from the S1 segment of the renal proximal convoluted tubule while SGLT1 reabsorbs the remaining 10% from the S3 segment. Once glucose is reabsorbed into the tubular epithelial cells, it diffuses into the interstitium via the action of facultative transporters, GLUT1 and GLUT2 (Gromova, Fetissov, and Gruzdkov 2021; Helliwell and Kellett 2002; Mather and Pollock 2011). Female G2 Terc KO mice show downregulation of both *Slc5a1* and *Slc5a2* (*Sglt2*) indicating impairment in renal glucose reabsorption. On the other hand, male G2 Terc KO mice show downregulation of *Slc5a2* but an upregulation of *Slc5a1* gene expression. Since, we did not measure renal glucose reabsorption directly, we cannot hypothesize how these changes in *Slc5a1* and *Slc5a2* gene expression in kidneys of male G2 Terc KO mice will affect glucose reabsorption. The reason for this sexual dimorphism in gene expression in small intestine enterocytes and kidneys of G2 Terc KO mice is unknown. However, it is worth noting that there are gender differences in glucose homeostasis. For instance, males are more susceptible to impaired glucose tolerance and diabetes than females (Kautzky-Willer, Harreiter, and Pacini 2016; Menke et al. 2015; Xu et al. 2013) which could be at least be partly explained by hormonal-driven differences in microbiota (Gao et al. 2021). Furthermore, hyperinsulinaemic-euglycaemic clamps show that healthy women show higher insulin sensitivity than men (Tramunt et al. 2020). Interestingly, healthy women absorb less sucrose, and not glucose, than men (Ishii et al. 2016). Another example of sexual dimorphism in G2 Terc KO mice is that female G2 Terc KO mice show increased dark phase respiratory exchange ratio in comparison to controls while male G2 Terc KO mice do not. This indicates that female G2 Terc KO mice use more carbohydrates and less lipid than control mice. This finding is intriguing as men usually have higher respiratory exchange ratio and greater carbohydrate oxidation than women (Cano et al. 2021). In G2 Terc KO mice, the reason for this modulation of respiratory exchange ratio could be due to different availability of substrate due to differences in nutrient absorption between sexes. Interestingly, in female G2 Terc KO mice, increased fecal caloric content was observed with no significant differences in fecal FFA, triglycerides or glycerol levels. Therefore, one could hypothesize that the reason for this reduction in body weight is due malabsorption of intestinal fatty acid and glucose leading to increased fecal caloric content. This phenomenon coupled with decreased reabsorption of renal glucose could explain the decrease in body weight and fat mass. However, in male G2 Terc KO mice, no difference in fecal caloric content or food intake is observed.

Moreover, no difference in energy expenditure between male G2 Terc KO mice and controls is observed. Therefore, the reason for this reduction in body weight in male G2 Terc KO mice is not clear. One explanation for this is microbiota. Microbiota is known to regulate host glucose metabolism and is altered in pre-diabetic and diabetic states (Allin et al. 2018; Karlsson et al. 2013; Martin et al. 2019). Moreover, males and females show differences in their gut microbiota composition and their immune system (Fish 2008; Markle et al. 2013; Mueller et al. 2006; vom Steeg and Klein 2016). Therefore, an increase in fatty acids in the intestine of G2 Terc KO mice due to a lack of their uptake by enterocytes will result in a favorable environment for the growth of bacterial species consuming these fatty acids. This could lead to the consumption of these fatty acids and not their excretion in feces. Thus, no increase in fecal caloric intake will be observed. However, in this study, no microbiota data is presented to support or disprove this hypothesis. Another explanation for the discrepancies between genders is that, although men and women are born with similar telomere length, women show longer telomere length than men later in life (Gardner et al. 2014). Therefore, telomerase action could be different between the genders leading to variance in the rate of telomere elongation. An interesting paper also show that *Terc* plays a role in inflammation independent of telomerase by enhancing the expression and secretion of inflammatory cytokines (Liu et al. 2019). Moreover, overexpression of *Terc* in telomerase deficient cells alters the expression of hundreds of genes, many of which are involved in cellular immunity (Liu et al. 2019). Since, *Terc* plays a role in immunity and there are gender specific differences in immunity then this could explain the gender differences seen in G2 Terc KO mice.

Aging in humans is associated with an increase in fat mass (St-Onge 2005; St-Onge and Gallagher 2010; Study 2008). In this thesis, I show that aging, induced by telomerase deletion (telomere shortening), leads to a reduction in both fat and lean mass in mice. The reason for this discrepancy is unknown. However, rodents may exhibit reduced intestinal fatty acid uptake (Drozdowski and Thomson 2006) which is in line with our study showing that accelerated aging via telomerase deletion show reduced intestinal fatty acid uptake in mice. On the other hand, humans do not show reduction in fatty acid uptake with aging (Rémond et al. 2015) and this in part could explain the discrepancy between aged humans and rodents. Another important difference is that rodents have much longer telomeres than humans (Calado and Dumitriu 2013) and this complicates translation of the findings from rodents to humans. In line with this, telomerase deficiency is tolerated in mice for several generations while heterozygous telomerase mutations in humans result in physiological abnormalities (Calado and Dumitriu 2013). Nonetheless, I show that telomerase deletion in rodents modulate body weight and nutrients absorption. These data broaden the knowledge about telomeres in the regulation of aging and body weight with the future aim to develop therapies to delay or revert aging phenotypes (e.g. obesity and glucose intolerance).

5 Conclusion and perspectives

Beiging as a therapeutic strategy to increase energy expenditure and ameliorate metabolic abnormalities is a prominent topic. In this thesis, serine racemase has been shown, for the first time, to be expressed in stromal vascular fractions and adipocytes of fat depots. Moreover, this dissertation characterized serine racemase as a modulator of beiging in scWAT of mice. I also demonstrated that serine racemase in fat tissues is a novel modulator of whole body energy expenditure. A novel finding is that serine racemase is modulated by diet and its deletion in fat cells leads to adipose tissue hypertrophy. This could either be due to the reduction in energy expenditure or physiological effect of serine racemase deletion on adipocytes. In line with the cell autonomous effect of serine racemase deletion, *in vitro* differentiated subcutaneous adipocytes lacking serine racemase show increased adipogenesis and beiging gene expression. We also show that *Grin1,* which is the target of D-serine, is expressed in stromal vascular fraction of adipocytes and GluN1 (protein coded by *Grin1*) is expressed in whole fat tissue lysates. Pre-adipocytes could be one the cells expressing *Grin1.* Future experiments should aim to pinpoint which cells express *Grin1* in fat depots and what its physiological role in fat depots and whole body function. As serine racemase produces both D-serine and pyruvate, future investigations should examine whether the effects of serine racemase deletion are due to D-serine or pyruvate. The effects of D-serine production are thoroughly studied while pyruvate production by serine racemase is seldom studied. This is of importance especially given that serine racemase produces more pyruvate than D-serine and a role of pyruvate produced by serine racemase has been demonstrated in cancer cells.

Aging is the single largest risk factor for the development of many disease and for mortality. Obesity risk increases with aging. Telomeres shorten with aging and obesity and short telomeres are thought to play a role in the deterioration in tissue functionality seen with aging. In this dissertation, the effect of telomere shortening was studied in mice. Telomere shortening induced by telomerase deletion led to reduction in body weight that is due to reduction in both fat mass and lean mass. This reduction in body weight could be due to reduction in fatty acid uptake by intestinal enterocytes. In this dissertation, it was demonstrated, for the first time, that telomerase deletion affects sexes differently. With telomerase deletion, female mice do not show reduction in body weight early in life while male mice show reduction in body weight already at 10 weeks of age. Telomerase deletion also led female mice to have increased feces caloric content and altered substrate utilization in comparison to age-matched controls. Female mice with telomerase deletion show reduction in intestinal glucose uptake gene expression while males show the opposite. These many differences between the sexes could be due to differences in telomerase action between males and females. Future research should aim to investigate how sex interacts with telomerase or how sex hormones interact with telomerase, or even telomeres. This dissertation also demonstrated that moderate telomere shortening does not lead to intestinal atrophy.

All in all, obesity is an alarming health issue affecting the wellbeing of many individuals. Therefore, strategies to combat it are thought after. One such strategy is activation of thermogenic adipocytes to burn excess fat and ameliorate metabolic abnormalities. In this thesis, serine racemase has been shown to be a modulator of beiging and whole body energy expenditure. Therefore, it could be a promising candidate for combating obesity. A big risk factor for the development of obesity and many other disorders is aging. Therefore, understanding mechanisms leading to aging like telomere shortening is of crucial importance. Here, we show that telomere shortening affects body weight, nutrient acquisition and

shows sexual dimorphism. In this thesis, we extend on the knowledge of molecular targets modulating beiging, obesity and aging.

References

Abarca-Gómez, Leandra, Ziad A Abdeen, Zargar Abdul Hamid, Niveen M Abu-Rmeileh, Benjamin Acosta-Cazares, Cecilia Acuin, Robert J Adams, Wichai Aekplakorn, Kaosar Afsana, and Carlos A Aguilar-Salinas. 2017. 'Worldwide trends in body-mass index, underweight, overweight, and obesity from 1975 to 2016: a pooled analysis of 2416 population-based measurement studies in 128· 9 million children, adolescents, and adults', *The lancet*, 390: 2627-42.

Abdullah, Asnawi, Anna Peeters, Maximilian de Courten, and Johannes Stoelwinder. 2010. 'The magnitude of association between overweight and obesity and the risk of diabetes: a meta-analysis of prospective cohort studies', *Diabetes research and clinical practice*, 89: 309-19.

Ables, Gene P, Carmen E Perrone, David Orentreich, and Norman Orentreich. 2012. 'Methionine-restricted C57BL/6J mice are resistant to diet-induced obesity and insulin resistance but have low bone density', *PloS one*, 7: e51357.

Abu-Odeh, Mohammad, Yuan Zhang, Shannon M Reilly, Nima Ebadat, Omer Keinan, Joseph M Valentine, Maziar Hafezi-Bakhtiari, Hadeel Ashayer, Lana Mamoun, and Xin Zhou. 2021. 'FGF21 promotes thermogenic gene expression as an autocrine factor in adipocytes', *Cell Reports*, 35: 109331.

Abumrad, Nada A, and Nicholas O Davidson. 2012. 'Role of the gut in lipid homeostasis', *Physiological reviews*, 92: 1061-85.

Adaikalakoteswari, Antonysunil, Muthuswamy Balasubramanyam, Radhakrishnan Ravikumar, Raj Deepa, and Viswanathan Mohan. 2007. 'Association of telomere shortening with impaired glucose tolerance and diabetic macroangiopathy', *Atherosclerosis*, 195: 83-89.

Al Khaldi, Rasha, Olusegun Mojiminiyi, Fahd AlMulla, and Nabila Abdella. 2015. 'Associations of TERC single nucleotide polymorphisms with human leukocyte telomere length and the risk of type 2 diabetes mellitus', *PloS one*, 10: e0145721.

Allin, Kristine H, Valentina Tremaroli, Robert Caesar, Benjamin AH Jensen, Mads TF Damgaard, Martin I Bahl, Tine R Licht, Tue H Hansen, Trine Nielsen, and Thomas M Dantoft. 2018. 'Aberrant intestinal microbiota in individuals with prediabetes', *Diabetologia*, 61: 810-20.

Anstey, KJ, Nicolas Cherbuin, Marc Budge, and John Young. 2011. 'Body mass index in midlife and late-life as a risk factor for dementia: a meta-analysis of prospective studies', *Obesity Reviews*, 12: e426-e37.

Apovian, Caroline M., Louis J. Aronne, Daniel H. Bessesen, Marie E. McDonnell, M. Hassan Murad, Uberto Pagotto, Donna H. Ryan, and Christopher D. Still. 2015. 'Pharmacological Management of Obesity: An Endocrine Society Clinical Practice Guideline', *The Journal of Clinical Endocrinology & Metabolism*, 100: 342-62.

Aronne, Louis J, and Karen R Segal. 2003. 'Weight gain in the treatment of mood disorders', *Journal of Clinical Psychiatry*, 64: 22-29.

Assmann, Gerd, and Helmut Schulte. 1992. 'Role of triglycerides in coronary artery disease: lessons from the Prospective Cardiovascular Münster Study', *The American journal of cardiology*, 70: H10-H13.

Association, American Diabetes. 2012. 'Standards of medical care in diabetes--2012', *Diabetes Care*, 35: S11-S63.

Austin, Melissa A. 1991. 'Plasma triglyceride and coronary heart disease', *Arteriosclerosis and thrombosis: a journal of vascular biology*, 11: 2-14.

Bäckhed, Fredrik, Hao Ding, Ting Wang, Lora V. Hooper, Gou Young Koh, Andras Nagy, Clay F. Semenkovich, and Jeffrey I. Gordon. 2004. 'The gut microbiota as an environmental factor that regulates fat storage', *Proceedings of the National Academy of Sciences*, 101: 15718-23.

Bäckhed, Fredrik, Jill K. Manchester, Clay F. Semenkovich, and Jeffrey I. Gordon. 2007. 'Mechanisms underlying the resistance to diet-induced obesity in germ-free mice', *Proceedings of the National Academy of Sciences*, 104: 979-84.

Bajzer, Matej, and Randy J. Seeley. 2006. 'Obesity and gut flora', *Nature*, 444: 1009-10.

Balland, Eglantine, Weiyi Chen, Garron T Dodd, Gregory Conductier, Roberto Coppari, Tony Tiganis, and Michael A Cowley. 2019. 'Leptin signaling in the arcuate nucleus reduces insulin's capacity to suppress hepatic glucose production in obese mice', *Cell Reports*, 26: 346-55. e3.

Baskaran, Padmamalini, Vivek Krishnan, Kevin Fettel, Peng Gao, Zhiming Zhu, Jun Ren, and Baskaran Thyagarajan. 2017. 'TRPV1 activation counters diet-induced obesity through sirtuin-1 activation and PRDM-16 deacetylation in brown adipose tissue', *International Journal of Obesity*, 41: 739-49.

Baskaran, Padmamalini, Vivek Krishnan, Jun Ren, and Baskaran Thyagarajan. 2016. 'Capsaicin induces browning of white adipose tissue and counters obesity by activating TRPV1 channel-dependent mechanisms', *British journal of pharmacology*, 173: 2369-89.

Basu, Alo C, Guochuan E Tsai, Chun-Lei Ma, Jeffrey T Ehmsen, Asif K Mustafa, Liqun Han, Zhichun I Jiang, Michael A Benneyworth, Michael P Froimowitz, and Nicholas Lange. 2009. 'Targeted disruption of serine racemase affects glutamatergic neurotransmission and behavior', *Molecular psychiatry*, 14: 719-27.

Begum, Najma, KE Sussman, and B Draznin. 1992. 'Calcium-induced inhibition of phosphoserine phosphatase in insulin target cells is mediated by the phosphorylation and activation of inhibitor 1', *Journal of Biological Chemistry*, 267: 5959-63.

Bell, Joshua A, Mika Kivimaki, and Mark Hamer. 2014. 'Metabolically healthy obesity and risk of incident type 2 diabetes: a meta-analysis of prospective cohort studies', *Obesity Reviews*, 15: 504-15.

Benneyworth, Michael A, Yan Li, Alo C Basu, Vadim Y Bolshakov, and Joseph T Coyle. 2012. 'Cell selective conditional null mutations of serine racemase demonstrate a predominate localization in cortical glutamatergic neurons', *Cellular and molecular neurobiology*, 32: 613-24.

Bertea, Mariana, Markus F Rütti, Alaa Othman, Jaqueline Marti-Jaun, Martin Hersberger, Arnold von Eckardstein, and Thorsten Hornemann. 2010. 'Deoxysphingoid bases as plasma markers in diabetes mellitus', *Lipids in health and disease*, 9: 1-7.

Bervoets, Liene, Guy Massa, Wanda Guedens, Evelyne Louis, Jean-Paul Noben, and Peter Adriaensens. 2017. 'Metabolic profiling of type 1 diabetes mellitus in children and adolescents: a case–control study', *Diabetology & metabolic syndrome*, 9: 1-8.

Bi, Pengpeng, Tizhong Shan, Weiyi Liu, Feng Yue, Xin Yang, Xin-Rong Liang, Jinghua Wang, Jie Li, Nadia Carlesso, and Xiaoqi Liu. 2014. 'Inhibition of Notch signaling promotes browning of white adipose tissue and ameliorates obesity', *Nature medicine*, 20: 911-18.

Biswas, Dipsikha, Luke Duffley, and Thomas Pulinilkunnil. 2019. 'Role of branched-chain amino acid–catabolizing enzymes in intertissue signaling, metabolic remodeling, and energy homeostasis', *The FASEB Journal*, 33: 8711-31.

Black, Paul N, Constance Ahowesso, David Montefusco, Nipun Saini, and Concetta C DiRusso. 2016. 'Fatty acid transport proteins: targeting FATP2 as a gatekeeper involved in the transport of exogenous fatty acids', *Medchemcomm*, 7: 612-22.

Blasco, María A. 2005. 'Mice with bad ends: mouse models for the study of telomeres and telomerase in cancer and aging', *The EMBO journal*, 24: 1095-103.

Blasco, María A, Han-Woong Lee, M Prakash Hande, Enrique Samper, Peter M Lansdorp, Ronald A DePinho, and Carol W Greider. 1997. 'Telomere shortening and tumor formation by mouse cells lacking telomerase RNA', *Cell*, 91: 25-34.

Blondin, Denis P, Sébastien M Labbé, Hans C Tingelstad, Christophe Noll, Margaret Kunach, Serge Phoenix, Brigitte Guérin, Éric E Turcotte, André C Carpentier, and Denis Richard. 2014.

'Increased brown adipose tissue oxidative capacity in cold-acclimated humans', *The Journal of Clinical Endocrinology & Metabolism*, 99: E438-E46.

Blüher, Matthias. 2019. 'Obesity: global epidemiology and pathogenesis', *Nature Reviews Endocrinology*, 15: 288-98.

Boden, Guenther. 1997. 'Role of fatty acids in the pathogenesis of insulin resistance and NIDDM', *Diabetes*, 46: 3-10.

Bult, Marielle JF, Thijs van Dalen, and Alex F Muller. 2008. 'Surgical treatment of obesity', *European journal of endocrinology*, 158: 135-46.

Buxton, Jessica L, Robin G Walters, Sophie Visvikis-Siest, David Meyre, Philippe Froguel, and Alexandra IF Blakemore. 2011. 'Childhood obesity is associated with shorter leukocyte telomere length', *The Journal of Clinical Endocrinology & Metabolism*, 96: 1500-05.

Caballero, Benjamin. 2019. 'Humans against obesity: who will win?', *Advances in nutrition*, 10: S4-S9.

Calado, Rodrigo T, and Bogdan Dumitriu. 2013. "Telomere dynamics in mice and humans." In *Seminars in hematology*, 165-74. Elsevier.

Calle, Eugenia E, Carmen Rodriguez, Kimberly Walker-Thurmond, and Michael J Thun. 2003. 'Overweight, obesity, and mortality from cancer in a prospectively studied cohort of US adults', *New England Journal of Medicine*, 348: 1625-38.

Cano, Antonella, Lucia Ventura, Gianluca Martinez, Lucia Cugusi, Marcello Caria, Franca Deriu, and Andrea Manca. 2021. 'Analysis of sex-based differences in energy substrate utilization during moderate-intensity aerobic exercise', *European journal of applied physiology*: 1-42.

Castaño-Martinez, Teresa, Fabian Schumacher, Silke Schumacher, Bastian Kochlik, Daniela Weber, Tilman Grune, Ronald Biemann, Adrian McCann, Klaus Abraham, and Cornelia Weikert. 2019. 'Methionine restriction prevents onset of type 2 diabetes in NZO mice', *The FASEB Journal*, 33: 7092-102.

Cawley, John, Adam Biener, Chad Meyerhoefer, Yuchen Ding, Tracy Zvenyach, B Gabriel Smolarz, and Abhilasha Ramasamy. 2021. 'Direct medical costs of obesity in the United States and the most populous states', *Journal of Managed Care & Specialty Pharmacy*, 27: 354-66.

Cawley, John, and Chad Meyerhoefer. 2012. 'The medical care costs of obesity: an instrumental variables approach', *Journal of health economics*, 31: 219-30.

CDC. 2017. 'National diabetes statistics report, 2017', *Estimates of diabetes and its burden in the United States*.

Chang, Annette M., and Jeffrey B. Halter. 2003. 'Aging and insulin secretion', *American Journal of Physiology-Endocrinology and Metabolism*, 284: E7-E12.

Chechi, K., J. Nedergaard, and D. Richard. 2014. 'Brown adipose tissue as an anti-obesity tissue in humans', *Obesity Reviews*, 15: 92-106.

Chen, Geng, Baitang Ning, and Tieliu Shi. 2019. 'Single-Cell RNA-Seq Technologies and Related Computational Data Analysis', *Frontiers in Genetics*, 10.

Cheng, Long, Jingkang Wang, Hongyu Dai, Yuhui Duan, Yongcheng An, Lu Shi, Yinglan Lv, Huimin Li, Chen Wang, and Quantao Ma. 2021. 'Brown and beige adipose tissue: a novel therapeutic strategy for obesity and type 2 diabetes mellitus', *Adipocyte*, 10: 48-65.

Chia, Chee W, Josephine M Egan, and Luigi Ferrucci. 2018. 'Age-related changes in glucose metabolism, hyperglycemia, and cardiovascular risk', *Circulation research*, 123: 886-904.

Chondronikola, Maria, Elena Volpi, Elisabet Børsheim, Craig Porter, Palam Annamalai, Sven Enerbäck, Martin E Lidell, Manish K Saraf, Sebastien M Labbe, and Nicholas M Hurren. 2014. 'Brown adipose tissue improves whole-body glucose homeostasis and insulin sensitivity in humans', *Diabetes*, 63: 4089-99.

Chondronikola, Maria, Elena Volpi, Elisabet Børsheim, Craig Porter, Manish K Saraf, Palam Annamalai, Christina Yfanti, Tony Chao, Daniel Wong, and Kosaku Shinoda. 2016. 'Brown adipose tissue

activation is linked to distinct systemic effects on lipid metabolism in humans', *Cell Metabolism*, 23: 1200-06.

Christakis, Nicholas A, and James H Fowler. 2007. 'The spread of obesity in a large social network over 32 years', *New England Journal of Medicine*, 357: 370-79.

Cifarelli, Vincenza, and Nada A Abumrad. 2018. 'Intestinal CD36 and other key proteins of lipid utilization: role in absorption and gut homeostasis', *Comprehensive Physiology*, 8: 493.

Collaboration, NCD Risk Factor. 2016. 'Trends in adult body-mass index in 200 countries from 1975 to 2014: a pooled analysis of 1698 population-based measurement studies with 19· 2 million participants', *The lancet*, 387: 1377-96.

Collaborators, G. B. D. Risk Factors. 2016. 'Global, regional, and national comparative risk assessment of 79 behavioural, environmental and occupational, and metabolic risks or clusters of risks, 1990-2015: a systematic analysis for the Global Burden of Disease Study 2015', *Lancet (London, England)*, 388: 1659-724.

Collins, S., and R. S. Surwit. 2001. 'The beta-adrenergic receptors and the control of adipose tissue metabolism and thermogenesis', *Recent Prog Horm Res*, 56: 309-28.

Consultation, WHO Expert. 2004. 'Appropriate body-mass index for Asian populations and its implications for policy and intervention strategies', *Lancet (London, England)*, 363: 157-63.

Cramer, Emil. 1865. 'Ueber die bestandtheile der seide', *J Prakt Chem*, 96: 76-98.

Cruz, Kyria Jayanne Clímaco, Ana Raquel Soares de Oliveira, Jennifer Beatriz Silva Morais, Juliana Soares Severo, and Dilina do Nascimento Marreiro. 2017. 'Role of microRNAs on adipogenesis, chronic low-grade inflammation, and insulin resistance in obesity', *Nutrition*, 35: 28-35.

Cypess, Aaron M, Sanaz Lehman, Gethin Williams, Ilan Tal, Dean Rodman, Allison B Goldfine, Frank C Kuo, Edwin L Palmer, Yu-Hua Tseng, and Alessandro Doria. 2009. 'Identification and importance of brown adipose tissue in adult humans', *New England Journal of Medicine*, 360: 1509-17.

Darlington, Gretchen J., Sarah E. Ross, and Ormond A. MacDougald. 1998. 'The Role of C/EBP Genes in Adipocyte Differentiation*', *Journal of Biological Chemistry*, 273: 30057-60.

Davis, Cindy D. 2016. 'The gut microbiome and its role in obesity', *Nutrition Today*, 51: 167.

De Koning, Tom J, Keith Snell, Marinus Duran, Ruud Berger, Bwee-Tien Poll-The, and Robert Surtees. 2003. 'L-serine in disease and development', *Biochemical Journal*, 371: 653-61.

De Rooij, Susanne R, Rebecca C Painter, David IW Phillips, Clive Osmond, Robert PJ Michels, Ian F Godsland, Patrick MM Bossuyt, Otto P Bleker, and Tessa J Roseboom. 2006. 'Impaired insulin secretion after prenatal exposure to the Dutch famine', *Diabetes Care*, 29: 1897-901.

DeFronzo, Ralph A. 1981. 'Glucose intolerance and aging', *Diabetes Care*, 4: 493-501.

Deng, Aihua, and Scott C Thomson. 2009. 'Renal NMDA receptors independently stimulate proximal reabsorption and glomerular filtration', *American Journal of Physiology-Renal Physiology*, 296: F976-F82.

Deurenberg-Yap, M., G. Schmidt, W. A. van Staveren, and P. Deurenberg. 2000. 'The paradox of low body mass index and high body fat percentage among Chinese, Malays and Indians in Singapore', *International Journal of Obesity*, 24: 1011-17.

Deurenberg, P., M. Deurenberg-Yap, and S. Guricci. 2002. 'Asians are different from Caucasians and from each other in their body mass index/body fat per cent relationship', *Obesity Reviews*, 3: 141-46.

Discacciati, A, N Orsini, and A Wolk. 2012. 'Body mass index and incidence of localized and advanced prostate cancer—a dose–response meta-analysis of prospective studies', *Annals of oncology*, 23: 1665-71.

Dong, Yi Na, Fu-Chun Hsu, Cynthia J Koziol-White, Victoria Stepanova, Joseph Jude, Andrei Gritsiuta, Ryan Rue, Rosalind Mott, Douglas A Coulter, and Reynold A Panettieri. 2021. 'Functional NMDA receptors are expressed by human pulmonary artery smooth muscle cells', *Scientific Reports*, 11: 1-12.

Drábková, Petra, Jana Šanderová, Jakub Kovařík, and Roman KanĎár. 2015. 'An assay of selected serum amino acids in patients with type 2 diabetes mellitus', *Advances in Clinical and Experimental Medicine*, 24: 447-51.

Drozdowski, Laurie, and Alan BR Thomson. 2006. 'Aging and the intestine', *World journal of gastroenterology: WJG*, 12: 7578.

Dvorak, Roman V, Walter F DeNino, Philip A Ades, and Eric T Poehlman. 1999. 'Phenotypic characteristics associated with insulin resistance in metabolically obese but normal-weight young women', *Diabetes*, 48: 2210-14.

Eguchi, Jun, Xun Wang, Songtao Yu, Erin E Kershaw, Patricia C Chiu, Joanne Dushay, Jennifer L Estall, Ulf Klein, Eleftheria Maratos-Flier, and Evan D Rosen. 2011. 'Transcriptional control of adipose lipid handling by IRF4', *Cell Metabolism*, 13: 249-59.

Eijsbouts, AM, BJ Witteman, RG de Sevaux, JF Fennis, UJ van Haelst, AH Naber, and JB Jansen. 1995. 'Undefined malabsorption syndrome with villous atrophy successfully reversed by treatment with cyclosporine', *European journal of gastroenterology & hepatology*, 7: 803-06.

El-Hattab, Ayman W. 2016. 'Serine biosynthesis and transport defects', *Molecular genetics and metabolism*, 118: 153-59.

Fain, John N, Atul K Madan, M Lloyd Hiler, Paramjeet Cheema, and Suleiman W Bahouth. 2004. 'Comparison of the release of adipokines by adipose tissue, adipose tissue matrix, and adipocytes from visceral and subcutaneous abdominal adipose tissues of obese humans', *Endocrinology*, 145: 2273-82.

Felig, Philip, Errol Marliss, and George F Cahill Jr. 1969. 'Plasma amino acid levels and insulin secretion in obesity', *New England Journal of Medicine*, 281: 811-16.

Fenzl, Anna, and Florian W Kiefer. 2014. 'Brown adipose tissue and thermogenesis', *Hormone molecular biology and clinical investigation*, 19: 25-37.

Finlin, Brian S, Amy L Confides, Beibei Zhu, Mary C Boulanger, Hasiyet Memetimin, Kyle W Taylor, Zachary R Johnson, Philip M Westgate, Esther E Dupont-Versteegden, and Philip A Kern. 2019. 'Adipose tissue mast cells promote human adipose beiging in response to cold', *Scientific Reports*, 9: 1-10.

Fish, Eleanor N. 2008. 'The X-files in immunity: sex-based differences predispose immune responses', *Nature Reviews Immunology*, 8: 737-44.

Flint, Alan J, Frank B Hu, Robert J Glynn, Hervé Caspard, JoAnn E Manson, Walter C Willett, and Eric B Rimm. 2010. 'Excess weight and the risk of incident coronary heart disease among men and women', *Obesity*, 18: 377-83.

Foster, Gary. 2006. 'The behavioral approach to treating obesity', *American Heart Journal*, 151: 625-27.

Fox, Caroline S, Joseph M Massaro, Udo Hoffmann, Karla M Pou, Pal Maurovich-Horvat, Chun-Yu Liu, Ramachandran S Vasan, Joanne M Murabito, James B Meigs, and L Adrienne Cupples. 2007. 'Abdominal visceral and subcutaneous adipose tissue compartments: association with metabolic risk factors in the Framingham Heart Study', *Circulation*, 116: 39-48.

Fuchs, Sabine A, Ruud Berger, Leo WJ Klomp, and Tom J De Koning. 2005. 'D-amino acids in the central nervous system in health and disease', *Molecular genetics and metabolism*, 85: 168-80.

Gabbard, Carl. 2001. 'The Need for Quality Physical Education', *The Journal of School Nursing*, 17: 73-75.

Gangwisch, James E, Dolores Malaspina, Bernadette Boden-Albala, and Steven B Heymsfield. 2005. 'Inadequate sleep as a risk factor for obesity: analyses of the NHANES I', *Sleep*, 28: 1289-96.

Gao, Aibo, Junlei Su, Ruixin Liu, Shaoqian Zhao, Wen Li, Xiaoqiang Xu, Danjie Li, Juan Shi, Bin Gu, and Juan Zhang. 2021. 'Sexual dimorphism in glucose metabolism is shaped by androgen-driven gut microbiome', *Nature Communications*, 12: 1-14.

Gao, X, X Xu, J Pang, C Zhang, JM Ding, X Peng, Y Liu, and J Cao. 2007. 'NMDA receptor activation induces mitochondrial dysfunction, oxidative stress and apoptosis in cultured neonatal rat cardiomyocytes', *Physiological research*, 56: 559.

Gardner, Michael, David Bann, Laura Wiley, Rachel Cooper, Rebecca Hardy, Dorothea Nitsch, Carmen Martin-Ruiz, Paul Shiels, Avan Aihie Sayer, and Michelangela Barbieri. 2014. 'Gender and telomere length: systematic review and meta-analysis', *Experimental gerontology*, 51: 15-27.

Geserick, Mandy, Mandy Vogel, Ruth Gausche, Tobias Lipek, Ulrike Spielau, Eberhard Keller, Roland Pfäffle, Wieland Kiess, and Antje Körner. 2018. 'Acceleration of BMI in early childhood and risk of sustained obesity', *New England Journal of Medicine*.

Gesta, Stephane, Yu-Hua Tseng, and C Ronald Kahn. 2007. 'Developmental origin of fat: tracking obesity to its source', *Cell*, 131: 242-56.

Ghaben, Alexandra L, and Philipp E Scherer. 2019. 'Adipogenesis and metabolic health', *Nature reviews Molecular cell biology*, 20: 242-58.

Giesecke, Kajsa, Inger Magnusson, Marianne Ahlberg, Lars Hagenfeldt, and John Wahren. 1989. 'Protein and amino acid metabolism during early starvation as reflected by excretion of urea and methylhistidines', *Metabolism*, 38: 1196-200.

Glance, Laurent G, Yue Li, Turner M Osler, Dana B Mukamel, and Andrew W Dick. 2014. 'Impact of obesity on mortality and complications in trauma patients', *Annals of surgery*, 259: 576-81.

Glatt, Stephen J, Pamela Chayavichitsilp, Colin Depp, Nicholas J Schork, and Dilip V Jeste. 2007. 'Successful aging: from phenotype to genotype', *Biological psychiatry*, 62: 282-93.

Golovynska, Iuliia, Tatiana V Beregova, Tatiana M Falalyeyeva, Ludmila I Stepanova, Sergii Golovynskyi, Junle Qu, and Tymish Y Ohulchanskyy. 2018. 'Peripheral N-methyl-D-aspartate receptor localization and role in gastric acid secretion regulation: immunofluorescence and pharmacological studies', *Scientific Reports*, 8: 1-11.

Gómez-Hernández, Almudena, Nuria Beneit, Sabela Díaz-Castroverde, and Óscar Escribano. 2016. 'Differential role of adipose tissues in obesity and related metabolic and vascular complications', *International journal of endocrinology*, 2016.

Goodwin, Pamela J, Marguerite Ennis, Kathleen I Pritchard, Maureen E Trudeau, Jarley Koo, Yolanda Madarnas, Warren Hartwick, Barry Hoffman, and Nicky Hood. 2002. 'Fasting insulin and outcome in early-stage breast cancer: results of a prospective cohort study', *Journal of clinical oncology*, 20: 42-51.

Goossens, Gijs H. 2017. 'The metabolic phenotype in obesity: fat mass, body fat distribution, and adipose tissue function', *Obesity facts*, 10: 207-15.

Gordon, Tavia, William P Castelli, Marthana C Hjortland, William B Kannel, and Thomas R Dawber. 1977. 'High density lipoprotein as a protective factor against coronary heart disease: the Framingham Study', *The American journal of medicine*, 62: 707-14.

Gracz, A. D., B. J. Puthoff, and S. T. Magness. 2012. 'Identification, Isolation, and Culture of Intestinal Epithelial Stem Cells from Murine Intestine.' in Shree Ram Singh (ed.), *Somatic Stem Cells: Methods and Protocols* (Humana Press: Totowa, NJ).

Green, Cara L, and Dudley W Lamming. 2019. 'Regulation of metabolic health by essential dietary amino acids', *Mechanisms of ageing and development*, 177: 186-200.

Gromova, Lyudmila V, Serguei O Fetissov, and Andrey A Gruzdkov. 2021. 'Mechanisms of glucose absorption in the small intestine in health and metabolic diseases and their role in appetite regulation', *Nutrients*, 13: 2474.

Haack, Tobias B, Robert Kopajtich, Peter Freisinger, Thomas Wieland, Joanna Rorbach, Thomas J Nicholls, Enrico Baruffini, Anett Walther, Katharina Danhauser, and Franz A Zimmermann. 2013. 'ELAC2 mutations cause a mitochondrial RNA processing defect associated with hypertrophic cardiomyopathy', *The American Journal of Human Genetics*, 93: 211-23.

Haffner, Steven M, Eleuterio Ferrannini, Helen P Hazuda, and Michael P Stern. 1992. 'Clustering of cardiovascular risk factors in confirmed prehypertensive individuals', *Hypertension*, 20: 38-45.

Hansen, Kasper B., Feng Yi, Riley E. Perszyk, Hiro Furukawa, Lonnie P. Wollmuth, Alasdair J. Gibb, and Stephen F. Traynelis. 2018. 'Structure, function, and allosteric modulation of NMDA receptors', *Journal of General Physiology*, 150: 1081-105.

Harms, Matthew, and Patrick Seale. 2013. 'Brown and beige fat: development, function and therapeutic potential', *Nature medicine*, 19: 1252-63.

Heaton, JULIET M. 1972. 'The distribution of brown adipose tissue in the human', *Journal of anatomy*, 112: 35.

Helliwell, Philip A, and George L Kellett. 2002. 'The active and passive components of glucose absorption in rat jejunum under low and high perfusion stress', *The Journal of physiology*, 544: 579-89.

Herrera, Eloísa, Enrique Samper, Juan Martín-Caballero, Juana M Flores, Han-Woong Lee, and María A Blasco. 1999. 'Disease states associated with telomerase deficiency appear earlier in mice with short telomeres', *The EMBO journal*, 18: 2950-60.

Herz, Carsten T, and Florian W Kiefer. 2019. 'Adipose tissue browning in mice and humans', *Journal of Endocrinology*, 241: R97-R109.

Hogan-Cann, Adam D, and Christopher M Anderson. 2016. 'Physiological roles of non-neuronal NMDA receptors', *Trends in pharmacological sciences*, 37: 750-67.

Holm, Laurits J, and Karsten Buschard. 2019. 'L-serine: a neglected amino acid with a potential therapeutic role in diabetes', *Apmis*, 127: 655-59.

Holm, Laurits J, Martin Haupt-Jorgensen, Jesper Larsen, Jano D Giacobini, Mesut Bilgin, and Karsten Buschard. 2018. 'L-serine supplementation lowers diabetes incidence and improves blood glucose homeostasis in NOD mice', *PloS one*, 13: e0194414.

Hotamisligil, Gökhan S. 2006. 'Inflammation and metabolic disorders', *Nature*, 444: 860-67.

Hotamisligil, Gokhan S, Peter Arner, Jose F Caro, Richard L Atkinson, and Bruce M Spiegelman. 1995. 'Increased adipose tissue expression of tumor necrosis factor-alpha in human obesity and insulin resistance', *The Journal of Clinical Investigation*, 95: 2409-15.

Hotamisligil, Gökhan S, Adriane Budavari, David Murray, and Bruce M Spiegelman. 1994. 'Reduced tyrosine kinase activity of the insulin receptor in obesity-diabetes. Central role of tumor necrosis factor-alpha', *The Journal of Clinical Investigation*, 94: 1543-49.

Hruby, Adela, and Frank B Hu. 2015. 'The epidemiology of obesity: a big picture', *Pharmacoeconomics*, 33: 673-89.

Hsing, Ann W, Streamson Chua Jr, Yu-Tang Gao, Elisabeth Gentzschein, Lilly Chang, Jie Deng, and Frank Z Stanczyk. 2001. 'Prostate cancer risk and serum levels of insulin and leptin: a population-based study', *Journal of the National Cancer Institute*, 93: 783-89.

Huang, Zhe, Ling Zhong, Jimmy Tsz Hang Lee, Jialiang Zhang, Donghai Wu, Leiluo Geng, Yu Wang, Chi-Ming Wong, and Aimin Xu. 2017. 'The FGF21-CCL11 axis mediates beiging of white adipose tissues by coupling sympathetic nervous system to type 2 immunity', *Cell Metabolism*, 26: 493-508. e4.

Iqbal, Jahangir, and M Mahmood Hussain. 2009. 'Intestinal lipid absorption', *American Journal of Physiology-Endocrinology and Metabolism*, 296: E1183-E94.

Isanejad, Masoud, Andrea Z LaCroix, Cynthia A Thomson, Lesley Tinker, Joseph C Larson, Qibin Qi, Lihong Qi, Rhonda M Cooper-DeHoff, Lawrence S Phillips, and Ross L Prentice. 2017. 'Branched-chain amino acid, meat intake and risk of type 2 diabetes in the Women's Health Initiative', *British Journal of Nutrition*, 117: 1523-30.

Ishii, Y, F Shimizu, M Ogawa, T Takao, and A Takada. 2016. 'Gender differences in foods uptakes, glycemic index, BMI, and various plasma parameters between young men and women in Japan', *Integr Food Nutr Metab*, 3: 427-30.

Jensen, Michael D., Donna H. Ryan, Caroline M. Apovian, Jamy D. Ard, Anthony G. Comuzzie, Karen A. Donato, Frank B. Hu, Van S. Hubbard, John M. Jakicic, Robert F. Kushner, Catherine M. Loria, Barbara E. Millen, Cathy A. Nonas, F. Xavier Pi-Sunyer, June Stevens, Victor J. Stevens, Thomas A. Wadden, Bruce M. Wolfe, and Susan Z. Yanovski. 2014. '2013 AHA/ACC/TOS Guideline for the Management of Overweight and Obesity in Adults', *Circulation*, 129: S102-S38.

Jersin, Regine Å., Divya Sri Priyanka Tallapragada, André Madsen, Linn Skartveit, Even Fjære, Adrian McCann, Laurence Dyer, Aron Willems, Jan-Inge Bjune, Mona S. Bjune, Villy Våge, Hans Jørgen Nielsen, Håvard Luong Thorsen, Bjørn Gunnar Nedrebø, Christian Busch, Vidar M. Steen, Matthias Blüher, Peter Jacobson, Per-Arne Svensson, Johan Fernø, Mikael Rydén, Peter Arner, Ottar Nygård, Melina Claussnitzer, Ståle Ellingsen, Lise Madsen, Jørn V. Sagen, Gunnar Mellgren, and Simon N. Dankel. 2021. 'Role of the Neutral Amino Acid Transporter SLC7A10 in Adipocyte Lipid Storage, Obesity, and Insulin Resistance', *Diabetes*, 70: 680-95.

Jiang, Ying, Ying Zhang, Mengmeng Jin, Zhaoyan Gu, Yu Pei, and Ping Meng. 2015. 'Aged-related changes in body composition and association between body composition with bone mass density by body mass index in Chinese Han men over 50-year-old', *PloS one*, 10: e0130400.

Jura, Magdalena, and Leslie Kozak. 2016. 'Obesity and related consequences to ageing', *Age*, 38: 1-18.

Kam, Michelle LW, Trang TT Nguyen, and Joanne YY Ngeow. 2021. 'Telomere biology disorders', *NPJ genomic medicine*, 6: 1-13.

Kannel, William B, Tavia Gordon, and Dorsey Offutt. 1969. 'Left ventricular hypertrophy by electrocardiogram: prevalence, incidence, and mortality in the Framingham study', *Annals of internal medicine*, 71: 89-105.

Karlina, Ruth, Dominik Lutter, Viktorian Miok, David Fischer, Irem Altun, Theresa Schöttl, Kenji Schorpp, Andreas Israel, Cheryl Cero, and James W Johnson. 2021. 'Identification and characterization of distinct brown adipocyte subtypes in C57BL/6J mice', *Life science alliance*, 4.

Karlsson, Fredrik, Valentina Tremaroli, Jens Nielsen, and Fredrik Bäckhed. 2013. 'Assessing the human gut microbiota in metabolic diseases', *Diabetes*, 62: 3341-49.

Kautzky-Willer, Alexandra, Jürgen Harreiter, and Giovanni Pacini. 2016. 'Sex and gender differences in risk, pathophysiology and complications of type 2 diabetes mellitus', *Endocrine reviews*, 37: 278-316.

Kazak, Lawrence, Edward T. Chouchani, Gina Z. Lu, Mark P. Jedrychowski, Curtis J. Bare, Amir I. Mina, Manju Kumari, Song Zhang, Ivan Vuckovic, Dina Laznik-Bogoslavski, Petras Dzeja, Alexander S. Banks, Evan D. Rosen, and Bruce M. Spiegelman. 2017. 'Genetic Depletion of Adipocyte Creatine Metabolism Inhibits Diet-Induced Thermogenesis and Drives Obesity', *Cell Metabolism*, 26: 660-71.e3.

Keipert, Susanne, and Martin Jastroch. 2014. 'Brite/beige fat and UCP1—is it thermogenesis?', *Biochimica et Biophysica Acta (BBA)-Bioenergetics*, 1837: 1075-82.

Keith, Scott W, David T Redden, Peter T Katzmarzyk, Mary M Boggiano, Erin C Hanlon, Ruth M Benca, Douglas Ruden, Angelo Pietrobelli, Jamie L Barger, and KRothers Fontaine. 2006. 'Putative contributors to the secular increase in obesity: exploring the roads less traveled', *International Journal of Obesity*, 30: 1585-94.

Khalangot, Mykola D., Dmytro S. Krasnienkov, Valentina P. Chizhova, Oleg V. Korkushko, Valery B. Shatilo, Vitaly M. Kukharsky, Victor I. Kravchenko, Volodymyr A. Kovtun, Vitaly G. Guryanov, and Alexander M. Vaiserman. 2019. 'Additional Impact of Glucose Tolerance on Telomere Length in Persons With and Without Metabolic Syndrome in the Elderly Ukraine Population', *Frontiers in Endocrinology*, 10.

Kiela, Pawel R, and Fayez K Ghishan. 2016. 'Physiology of intestinal absorption and secretion', *Best practice & research Clinical gastroenterology*, 30: 145-59.

Kim, Eun Young, Marc Anderson, and Stuart E Dryer. 2012. 'Sustained activation of N-methyl-D-aspartate receptors in podoctyes leads to oxidative stress, mobilization of transient receptor potential canonical 6 channels, nuclear factor of activated T cells activation, and apoptotic cell death', *Molecular pharmacology*, 82: 728-37.

Kim, Sun H, Fahim Abbasi, and Gerald M Reaven. 2004. 'Impact of degree of obesity on surrogate estimates of insulin resistance', *Diabetes Care*, 27: 1998-2002.

Kimm, Sue Y.S., Nancy W. Glynn, Andrea M. Kriska, Bruce A. Barton, Shari S. Kronsberg, Stephen R. Daniels, Patricia B. Crawford, Zak I. Sabry, and Kiang Liu. 2002. 'Decline in Physical Activity in Black Girls and White Girls during Adolescence', *New England Journal of Medicine*, 347: 709-15.

Kissig, Megan, Suzanne N Shapira, and Patrick Seale. 2016. 'SnapShot: brown and beige adipose thermogenesis', *Cell*, 166: 258-58. e1.

Klingenspor, Martin. 2003. 'Cold-induced recruitment of brown adipose tissue thermogenesis', *Experimental physiology*, 88: 141-48.

Kodama, S, C Horikawa, K Fujihara, S Yoshizawa, Y Yachi, S Tanaka, N Ohara, S Matsunaga, T Yamada, and O Hanyu. 2014. 'Quantitative relationship between body weight gain in adulthood and incident type 2 diabetes: a meta-analysis', *Obesity Reviews*, 15: 202-14.

Koenen, Mascha, Michael A Hill, Paul Cohen, and James R Sowers. 2021. 'Obesity, adipose tissue and vascular dysfunction', *Circulation research*, 128: 951-68.

Kolterman, Orville G, J Insel, M Saekow, and JM Olefsky. 1980. 'Mechanisms of insulin resistance in human obesity: evidence for receptor and postreceptor defects', *The Journal of Clinical Investigation*, 65: 1272-84.

Kramer, Caroline K, Bernard Zinman, and Ravi Retnakaran. 2013. 'Are metabolically healthy overweight and obesity benign conditions? A systematic review and meta-analysis', *Annals of internal medicine*, 159: 758-69.

Kruger, J, HW Kohl III, and IJ Miles. 2007. 'Prevalence of regular physical activity among adults-United States, 2001 and 2005', *Morbidity and Mortality Weekly Report*, 56: 1209-12.

Kuhlow, Doreen, Simone Florian, Guido von Figura, Sandra Weimer, Nadja Schulz, Klaus J Petzke, Kim Zarse, Andreas FH Pfeiffer, K Lenhard Rudolph, and Michael Ristow. 2010. 'Telomerase deficiency impairs glucose metabolism and insulin secretion', *Aging (Albany NY)*, 2: 650.

Kuk, Jennifer L, Travis J Saunders, Lance E Davidson, and Robert Ross. 2009. 'Age-related changes in total and regional fat distribution', *Ageing research reviews*, 8: 339-48.

Kumar, Ashok. 2015. 'NMDA receptor function during senescence: implication on cognitive performance', *Frontiers in neuroscience*, 9: 473.

Langin, Dominique. 2006. 'Adipose tissue lipolysis as a metabolic pathway to define pharmacological strategies against obesity and the metabolic syndrome', *Pharmacological Research*, 53: 482-91.

LaRocca, Thomas J, Douglas R Seals, and Gary L Pierce. 2010. 'Leukocyte telomere length is preserved with aging in endurance exercise-trained adults and related to maximal aerobic capacity', *Mechanisms of ageing and development*, 131: 165-67.

Larsson, S. C., and A. Wolk. 2007a. 'Obesity and the risk of gallbladder cancer: a meta-analysis', *British Journal of Cancer*, 96: 1457-61.

Larsson, SC, and A Wolk. 2007b. 'Overweight, obesity and risk of liver cancer: a meta-analysis of cohort studies', *British Journal of Cancer*, 97: 1005-08.

Larsson, Susanna C, and Alicja Wolk. 2008. 'Overweight and obesity and incidence of leukemia: a meta-analysis of cohort studies', *International journal of cancer*, 122: 1418-21.

Lee, Han-Woong, Maria A Blasco, Geoffrey J Gottlieb, James W Horner, Carol W Greider, and Ronald A DePinho. 1998. 'Essential role of mouse telomerase in highly proliferative organs', *Nature*, 392: 569-74.

Levy, Michael Z, Richard C Allsopp, A Bruce Futcher, Carol W Greider, and Calvin B Harley. 1992. 'Telomere end-replication problem and cell aging', *Journal of molecular biology*, 225: 951-60.

Ley, Ruth E., Fredrik Bäckhed, Peter Turnbaugh, Catherine A. Lozupone, Robin D. Knight, and Jeffrey I. Gordon. 2005. 'Obesity alters gut microbial ecology', *Proceedings of the National Academy of Sciences*, 102: 11070-75.

Li, Guolin, Cen Xie, Siyu Lu, Robert G Nichols, Yuan Tian, Licen Li, Daxeshkumar Patel, Yinyan Ma, Chad N Brocker, and Tingting Yan. 2017. 'Intermittent fasting promotes white adipose browning and decreases obesity by shaping the gut microbiota', *Cell Metabolism*, 26: 672-85. e4.

Lichtenbelt, Wouter D, Joost W Vanhommerig, Nanda M Smulders, Jamie Drossaerts, Gerrit J Kemerink, Nicole D Bouvy, Patrick Schrauwen, and GJ Teule. 2009. 'Cold-activated brown adipose tissue in healthy men', *New England Journal of Medicine*, 360: 1500-08.

Lidell, M. E., M. J. Betz, and S. Enerbäck. 2014. 'Brown adipose tissue and its therapeutic potential', *Journal of Internal Medicine*, 276: 364-77.

Lim, Sharon, Jennifer Honek, Yuan Xue, Takahiro Seki, Ziquan Cao, Patrik Andersson, Xiaojuan Yang, Kayoko Hosaka, and Yihai Cao. 2012. 'Cold-induced activation of brown adipose tissue and adipose angiogenesis in mice', *Nature protocols*, 7: 606-15.

Liu, Haiying, Yiding Yang, Yuanlong Ge, Juanhong Liu, and Yong Zhao. 2019. 'TERC promotes cellular inflammatory response independent of telomerase', *Nucleic acids research*, 47: 8084-95.

Liu, Tao, Jia-jun Chen, Xiang-jun Bai, Guo-shou Zheng, and Wei Gao. 2013. 'The effect of obesity on outcomes in trauma patients: a meta-analysis', *Injury*, 44: 1145-52.

Lockridge, A. D., D. C. Baumann, B. Akhaphong, A. Abrenica, R. F. Miller, and E. U. Alejandro. 2016. 'Serine racemase is expressed in islets and contributes to the regulation of glucose homeostasis', *Islets*, 8: 195-206.

Lockridge, Amber, Eric Gustafson, Alicia Wong, Robert F Miller, and Emilyn U Alejandro. 2021. 'Acute D-serine co-agonism of β-Cell NMDA receptors potentiates glucose-stimulated insulin secretion and excitatory β-cell membrane activity', *Cells*, 10: 93.

López-Gonzales, Elena, Lisa Lehmann, Francisco Javier Ruiz-Ojeda, René Hernández-Bautista, Irem Altun, Yasuhiro Onogi, Ahmed Elagamy Khalil, Xue Liu, Andreas Israel, and Siegfried Ussar. 2022. 'L-Serine Supplementation Blunts Fasting-Induced Weight Regain by Increasing Brown Fat Thermogenesis', *Nutrients*, 14: 1922.

Love, Michael I, Wolfgang Huber, and Simon Anders. 2014. 'Moderated estimation of fold change and dispersion for RNA-seq data with DESeq2', *Genome biology*, 15: 1-21.

Low, Serena, Mien Chew Chin, Stefan Ma, Derrick Heng, and Mabel Deurenberg-Yap. 2009. 'Rationale for redefining obesity in Asians', *Annals Academy of Medicine Singapore*, 38: 66.

Lowell, Bradford B, Andreas Hamann, Joel A Lawitts, Jean Himms-Hagen, Bert B Boyer, Leslie P Kozak, and Jeffrey S Flier. 1993. 'Development of obesity in transgenic mice after genetic ablation of brown adipose tissue', *Nature*, 366: 740-42.

Lozano, Rafael, Mohsen Naghavi, Kyle Foreman, Stephen Lim, Kenji Shibuya, Victor Aboyans, Jerry Abraham, Timothy Adair, Rakesh Aggarwal, and Stephanie Y Ahn. 2012. 'Global and regional mortality from 235 causes of death for 20 age groups in 1990 and 2010: a systematic analysis for the Global Burden of Disease Study 2010', *The lancet*, 380: 2095-128.

Lu, Yuan, Kaveh Hajifathalian, Majid Ezzati, Mark Woodward, Eric B Rimm, Goodarz Danaei, and Catherine D'Este. 2014. 'Metabolic mediators of the eff ects of body-mass index, overweight, and obesity on coronary heart disease and stroke: a pooled analysis of 97 prospective cohorts with 1.8 million participants'.

Ma, Tianqi, Qingmei Cheng, Chen Chen, Ziqiang Luo, and Dandan Feng. 2020. 'Excessive activation of NMDA receptors in the pathogenesis of multiple peripheral organs via mitochondrial dysfunction, oxidative stress, and inflammation', *SN Comprehensive Clinical Medicine*, 2: 551-69.

Markle, Janet GM, Daniel N Frank, Steven Mortin-Toth, Charles E Robertson, Leah M Feazel, Ulrike Rolle-Kampczyk, Martin Von Bergen, Kathy D McCoy, Andrew J Macpherson, and Jayne S Danska. 2013. 'Sex differences in the gut microbiome drive hormone-dependent regulation of autoimmunity', *Science*, 339: 1084-88.

Marquard, Jan, Silke Otter, Alena Welters, Alin Stirban, Annelie Fischer, Jan Eglinger, Diran Herebian, Olaf Kletke, Maša Skelin Klemen, and Andraž Stožer. 2015. 'Characterization of pancreatic NMDA receptors as possible drug targets for diabetes treatment', *Nature medicine*, 21: 363-72.

Marquard, Jan, Alin Stirban, Freimut Schliess, Felix Sievers, Alena Welters, Silke Otter, Annelie Fischer, Stephan Wnendt, Thomas Meissner, and Tim Heise. 2016. 'Effects of dextromethorphan as add-on to sitagliptin on blood glucose and serum insulin concentrations in individuals with type 2 diabetes mellitus: a randomized, placebo-controlled, double-blinded, multiple crossover, single-dose clinical trial', *Diabetes, Obesity and Metabolism*, 18: 100-03.

Marti, A, B Berraondo, and JA Martinez. 1999. 'Leptin: physiological actions', *Journal of physiology and biochemistry*, 55: 43-49.

Martin, Alyce M., Julian M. Yabut, Jocelyn M. Choo, Amanda J. Page, Emily W. Sun, Claire F. Jessup, Steve L. Wesselingh, Waliul I. Khan, Geraint B. Rogers, Gregory R. Steinberg, and Damien J. Keating. 2019. 'The gut microbiome regulates host glucose homeostasis via peripheral serotonin', *Proceedings of the National Academy of Sciences*, 116: 19802-04.

Mather, Amanda, and Carol Pollock. 2011. 'Glucose handling by the kidney', *Kidney International*, 79: S1-S6.

Matsushita, M., T. Yoneshiro, S. Aita, T. Kameya, H. Sugie, and M. Saito. 2014. 'Impact of brown adipose tissue on body fatness and glucose metabolism in healthy humans', *International Journal of Obesity*, 38: 812-17.

Menke, Andy, Sarah Casagrande, Linda Geiss, and Catherine C Cowie. 2015. 'Prevalence of and trends in diabetes among adults in the United States, 1988-2012', *Jama*, 314: 1021-29.

Metcalf, JS, RA Dunlop, JT Powell, SA Banack, and PA Cox. 2018. 'L-serine: a naturally-occurring amino acid with therapeutic potential', *Neurotoxicity research*, 33: 213-21.

Mikkola, Tuija M, Minna K Salonen, Eero Kajantie, Hannu Kautiainen, and Johan G Eriksson. 2020. 'Associations of fat and lean body mass with circulating amino acids in older men and women', *The Journals of Gerontology: Series A*, 75: 885-91.

Minokoshi, Yasuhiko, C Ronald Kahn, and Barbara B Kahn. 2003. 'Tissue-specific ablation of the GLUT4 glucose transporter or the insulin receptor challenges assumptions about insulin action and glucose homeostasis', *Journal of Biological Chemistry*, 278: 33609-12.

Misra, Anoop, P Chowbey, BM Makkar, NK Vikram, JS Wasir, D Chadha, Shashank R Joshi, S Sadikot, R Gupta, and Seema Gulati. 2009. 'Consensus statement for diagnosis of obesity, abdominal obesity and the metabolic syndrome for Asian Indians and recommendations for physical activity, medical and surgical management', *Japi*, 57: 163-70.

Missios, Pavlos, Yuan Zhou, Luis Miguel Guachalla, Guido Von Figura, Andre Wegner, Sundaram Reddy Chakkarappan, Tina Binz, Anne Gompf, Götz Hartleben, and Martin D Burkhalter. 2014. 'Glucose substitution prolongs maintenance of energy homeostasis and lifespan of telomere dysfunctional mice', *Nature Communications*, 5: 1-13.

Miya, Kazushi, Ran Inoue, Yoshimi Takata, Manabu Abe, Rie Natsume, Kenji Sakimura, Kazuhisa Hongou, Toshio Miyawaki, and Hisashi Mori. 2008. 'Serine racemase is predominantly localized in neurons in mouse brain', *Journal of Comparative Neurology*, 510: 641-54.

Mokdad, Ali H, James S Marks, Donna F Stroup, and Julie L Gerberding. 2004. 'Actual causes of death in the United States, 2000', *Jama*, 291: 1238-45.

Monickaraj, Finny, Kuppan Gokulakrishnan, Paramasivam Prabu, Chandrakumar Sathishkumar, Ranjit Mohan Anjana, Janavikula Sankaran Rajkumar, Viswanathan Mohan, and Muthuswamy

Balasubramanyam. 2012. 'Convergence of adipocyte hypertrophy, telomere shortening and hypoadiponectinemia in obese subjects and in patients with type 2 diabetes', *Clinical biochemistry*, 45: 1432-38.

Montague, Carl T, and Stephen O'Rahilly. 2000. 'The perils of portliness: causes and consequences of visceral adiposity', *Diabetes*, 49: 883-88.

Montague, Carl T, Johannes B Prins, Louise Sanders, Janet E Digby, and Stephen O'Rahilly. 1997. 'Depot- and sex-specific differences in human leptin mRNA expression: implications for the control of regional fat distribution', *Diabetes*, 46: 342-47.

Montoro-Huguet, Miguel A, Blanca Belloc, and Manuel Domínguez-Cajal. 2021. 'Small and large intestine (I): malabsorption of nutrients', *Nutrients*, 13: 1254.

Moore, Lee E, Robin T Wilson, and Sharan L Campleman. 2005. 'Lifestyle factors, exposures, genetic susceptibility, and renal cell cancer risk: a review', *Cancer investigation*, 23: 240-55.

Morigny, Pauline, Jeremie Boucher, Peter Arner, and Dominique Langin. 2021. 'Lipid and glucose metabolism in white adipocytes: pathways, dysfunction and therapeutics', *Nature Reviews Endocrinology*, 17: 276-95.

Moshal, Karni S, Srinivas M Tipparaju, Thomas P Vacek, Munish Kumar, Mahavir Singh, Iluiana E Frank, Phani K Patibandla, Neetu Tyagi, Jayesh Rai, and Naira Metreveli. 2008. 'Mitochondrial matrix metalloproteinase activation decreases myocyte contractility in hyperhomocysteinemia', *American Journal of Physiology-Heart and Circulatory Physiology*, 295: H890-H97.

Motoshima, Hiroyuki, Xiangdong Wu, Madhur K Sinha, V Elise Hardy, Ernest L Rosato, Donna J Barbot, Francis E Rosato, and Barry J Goldstein. 2002. 'Differential regulation of adiponectin secretion from cultured human omental and subcutaneous adipocytes: effects of insulin and rosiglitazone', *The Journal of Clinical Endocrinology & Metabolism*, 87: 5662-67.

Mu, Huiling, and Carl-Erik Høy. 2004. 'The digestion of dietary triacylglycerols', *Progress in lipid research*, 43: 105-33.

Mueller, Susanne, Katiana Saunier, Christiana Hanisch, Elisabeth Norin, Livia Alm, Tore Midtvedt, Alberto Cresci, Stefania Silvi, Carla Orpianesi, and Maria Cristina Verdenelli. 2006. 'Differences in fecal microbiota in different European study populations in relation to age, gender, and country: a cross-sectional study', *Applied and environmental microbiology*, 72: 1027-33.

Müller, Constanze, Juliano R Fonseca, Theresa M Rock, Susanne Krauss-Etschmann, and Philippe Schmitt-Kopplin. 2014. 'Enantioseparation and selective detection of D-amino acids by ultra-high-performance liquid chromatography/mass spectrometry in analysis of complex biological samples', *Journal of Chromatography A*, 1324: 109-14.

Müller, Timo D., Matthias Blüher, Matthias H. Tschöp, and Richard D. DiMarchi. 2022. 'Anti-obesity drug discovery: advances and challenges', *Nature Reviews Drug Discovery*, 21: 201-23.

Muzik, Otto, Thomas J Mangner, William R Leonard, Ajay Kumar, James Janisse, and James G Granneman. 2013. '15O PET measurement of blood flow and oxygen consumption in cold-activated human brown fat', *Journal of Nuclear Medicine*, 54: 523-31.

Nakamura, Kazuhiro. 2011. 'Central circuitries for body temperature regulation and fever', *American journal of Physiology-Regulatory, integrative and comparative Physiology*, 301: R1207-R28.

Nakata, Masanori, Toshihiko Yada, Noriko Soejima, and Ikuro Maruyama. 1999. 'Leptin promotes aggregation of human platelets via the long form of its receptor', *Diabetes*, 48: 426-29.

Narayan, KM Venkat, James P Boyle, Theodore J Thompson, Edward W Gregg, and David F Williamson. 2007. 'Effect of BMI on lifetime risk for diabetes in the US', *Diabetes Care*, 30: 1562-66.

Nedergaard, Jan, and Barbara Cannon. 2014. 'The Browning of White Adipose Tissue: Some Burning Issues', *Cell Metabolism*, 20: 396-407.

Newgard, Christopher B, Jie An, James R Bain, Michael J Muehlbauer, Robert D Stevens, Lillian F Lien, Andrea M Haqq, Svati H Shah, Michelle Arlotto, and Cris A Slentz. 2009. 'A branched-chain

amino acid-related metabolic signature that differentiates obese and lean humans and contributes to insulin resistance', *Cell Metabolism*, 9: 311-26.

Nguyen, Thi Mong Diep. 2020. 'Adiponectin: role in physiology and pathophysiology', *International journal of preventive medicine*, 11.

Obradovic, Milan, Emina Sudar-Milovanovic, Sanja Soskic, Magbubah Essack, Swati Arya, Alan J Stewart, Takashi Gojobori, and Esma R Isenovic. 2021. 'Leptin and obesity: role and clinical implication', *Frontiers in Endocrinology*, 12: 585887.

Ohno, Haruya, Kosaku Shinoda, Bruce M Spiegelman, and Shingo Kajimura. 2012. 'PPARγ agonists induce a white-to-brown fat conversion through stabilization of PRDM16 protein', *Cell Metabolism*, 15: 395-404.

Ohshima, Kenji, Satoshi Nojima, Shinichiro Tahara, Masako Kurashige, Keisuke Kawasaki, Yumiko Hori, Moyu Taniguchi, Yutaka Umakoshi, Daisuke Okuzaki, and Naoki Wada. 2020. 'Serine racemase enhances growth of colorectal cancer by producing pyruvate from serine', *Nature Metabolism*, 2: 81-96.

Okunogbe, Adeyemi, Rachel Nugent, Garrison Spencer, Johanna Ralston, and John Wilding. 2021. 'Economic impacts of overweight and obesity: current and future estimates for eight countries', *BMJ global health*, 6: e006351.

Öngel, Melek Ece, Cennet Yıldız, Can Akpınaroğlu, Bayram Yilmaz, and Mustafa Özilgen. 2021. 'Why women may live longer than men do? A telomere-length regulated and diet-based entropic assessment', *Clinical Nutrition*, 40: 1186-91.

Orgeron, Manda L., Kirsten P. Stone, Desiree Wanders, Cory C. Cortez, Nancy T. van, and Thomas W. Gettys. 2014. 'Chapter Eleven - The Impact of Dietary Methionine Restriction on Biomarkers of Metabolic Health.' in Ya-Xiong Tao (ed.), *Progress in Molecular Biology and Translational Science* (Academic Press).

Otero-Díaz, Berenice, Marcela Rodríguez-Flores, Verónica Sánchez-Muñoz, Fernando Monraz-Preciado, Samuel Ordoñez-Ortega, Vicente Becerril-Elias, Guillermina Baay-Guzmán, Rodolfo Obando-Monge, Eduardo García-García, and Berenice Palacios-González. 2018. 'Exercise induces white adipose tissue browning across the weight spectrum in humans', *Frontiers in physiology*, 9: 1781.

Ouellet, Veronique, Annick Routhier-Labadie, William Bellemare, Lajmi Lakhal-Chaieb, Eric Turcotte, André C Carpentier, and Denis Richard. 2011. 'Outdoor temperature, age, sex, body mass index, and diabetic status determine the prevalence, mass, and glucose-uptake activity of 18F-FDG-detected BAT in humans', *The Journal of Clinical Endocrinology & Metabolism*, 96: 192-99.

Ozaki, Hironori, Ran Inoue, Takako Matsushima, Masakiyo Sasahara, Atsushi Hayashi, and Hisashi Mori. 2018. 'Serine racemase deletion attenuates neurodegeneration and microvascular damage in diabetic retinopathy', *PloS one*, 13: e0190864.

Palmer, Biff F, and Deborah J Clegg. 2015. 'The sexual dimorphism of obesity', *Molecular and cellular endocrinology*, 402: 113-19.

Pan, Wen-Harn, Katherine M Flegal, Hsing-Yi Chang, Wen-Ting Yeh, Chih-Jung Yeh, and Wen-Chung Lee. 2004. 'Body mass index and obesity-related metabolic disorders in Taiwanese and US whites and blacks: implications for definitions of overweight and obesity for Asians', *The American Journal of Clinical Nutrition*, 79: 31-39.

Parkin, DM, and L Boyd. 2011. '8. Cancers attributable to overweight and obesity in the UK in 2010', *British Journal of Cancer*, 105: S34-S37.

Paz-Filho, Gilberto, Claudio Mastronardi, Ma-Li Wong, and Julio Licinio. 2012. 'Leptin therapy, insulin sensitivity, and glucose homeostasis', *Indian journal of endocrinology and metabolism*, 16: S549.

Peeters, Anna, Jan J. Barendregt, Frans Willekens, Johan P. Mackenbach, Abdullah Al Mamun, and Luc Bonneux. 2003. 'Obesity in Adulthood and Its Consequences for Life Expectancy: A Life-Table Analysis', *Annals of internal medicine*, 138: 24-32.

Pérez, Coralia, Carmen Fernández-Galaz, Teresa Fernández-Agullo, Carmen Arribas, Antonio Andrés, Manuel Ros, and José M Carrascosa. 2004. 'Leptin impairs insulin signaling in rat adipocytes', *Diabetes*, 53: 347-53.

Persichetti, Agnese, Rosa Sciuto, Sandra Rea, Sabrina Basciani, Carla Lubrano, Stefania Mariani, Salvatore Ulisse, Italo Nofroni, Carlo Ludovico Maini, and Lucio Gnessi. 2013. 'Prevalence, mass, and glucose-uptake activity of 18F-FDG-detected brown adipose tissue in humans living in a temperate zone of Italy', *PloS one*, 8: e63391.

Peschechera, Alessandro, and Juergen Eckel. 2013. '"Browning" of adipose tissue–regulation and therapeutic perspectives', *Archives of physiology and biochemistry*, 119: 151-60.

Pfannenberg, Christina, Matthias K Werner, Sabine Ripkens, Irina Stef, Annette Deckert, Maria Schmadl, Matthias Reimold, Hans-Ulrich Häring, Claus D Claussen, and Norbert Stefan. 2010. 'Impact of age on the relationships of brown adipose tissue with sex and adiposity in humans', *Diabetes*, 59: 1789-93.

Phan, Cam T, and Patrick Tso. 2001. 'Intestinal lipid absorption and transport', *Frontiers in Bioscience-Landmark*, 6: 299-319.

PI-SUNYER, F. XAVIER. 1999. 'Comorbidities of overweight and obesity: current evidence and research issues', *Medicine & Science in Sports & Exercise*, 31: S602.

Podlevsky, Joshua D, Christopher J Bley, Rebecca V Omana, Xiaodong Qi, and Julian J-L Chen. 2007. 'The telomerase database', *Nucleic acids research*, 36: D339-D43.

Polednak, Anthony P. 2008. 'Estimating the number of US incident cancers attributable to obesity and the impact on temporal trends in incidence rates for obesity-related cancers', *Cancer detection and prevention*, 32: 190-99.

Poret, J. M., F. Souza-Smith, S. J. Marcell, D. A. Gaudet, T. H. Tzeng, H. D. Braymer, L. M. Harrison-Bernard, and S. D. Primeaux. 2018. 'High fat diet consumption differentially affects adipose tissue inflammation and adipocyte size in obesity-prone and obesity-resistant rats', *International Journal of Obesity*, 42: 535-41.

Prats-Puig, Anna, Francisco J Ortega, Josep M Mercader, José M Moreno-Navarrete, María Moreno, Nuria Bonet, Wifredo Ricart, Abel López-Bermejo, and José M Fernández-Real. 2013. 'Changes in circulating microRNAs are associated with childhood obesity', *The Journal of Clinical Endocrinology & Metabolism*, 98: E1655-E60.

Primeau, V, L Coderre, AD Karelis, M Brochu, ME Lavoie, V Messier, R Sladek, and R Rabasa-Lhoret. 2011. 'Characterizing the profile of obese patients who are metabolically healthy', *International Journal of Obesity*, 35: 971-81.

Pundir, Mandeep, Shiyana Arora, Tajpreet Kaur, Randhir Singh, and Amrit Pal Singh. 2013. 'Effect of modulating the allosteric sites of N-methyl-D-aspartate receptors in ischemia-reperfusion induced acute kidney injury', *journal of surgical research*, 183: 668-77.

Qian, Shuwen, Haiyan Huang, and Qiqun Tang. 2015. 'Brown and beige fat: the metabolic function, induction, and therapeutic potential', *Frontiers of medicine*, 9: 162-72.

Qiang, L, L Wang, N Kon, W Zhao, S Lee, Y Zhang, M Rosenbaum, Y Zhao, and W Gu. 2012. 'Farmer; Stephen, R.; Accili, D', *Brown Remodeling of White Adipose Tissue by SirT1-Dependent Deacetylation of Pparγ. Cell*, 150: 620-32.

Qiang, Li, Liheng Wang, Ning Kon, Wenhui Zhao, Sangkyu Lee, Yiying Zhang, Michael Rosenbaum, Yingming Zhao, Wei Gu, and Stephen R Farmer. 2012. 'Brown remodeling of white adipose tissue by SirT1-dependent deacetylation of Pparγ', *Cell*, 150: 620-32.

Rabiee, Atefeh. 2020. 'Beige fat maintenance; toward a sustained metabolic health', *Frontiers in Endocrinology*, 11: 634.

Rachid, Tamiris Lima, Aline Penna-de-Carvalho, Isabele Bringhenti, Marcia B Aguila, Carlos A Mandarim-de-Lacerda, and Vanessa Souza-Mello. 2015. 'Fenofibrate (PPARalpha agonist) induces beige cell formation in subcutaneous white adipose tissue from diet-induced male obese mice', *Molecular and cellular endocrinology*, 402: 86-94.

Raiko, Juho, Teemu Saari, Nobu Kudomi, Tuula Tolvanen, Vesa Oikonen, Jarmo Teuho, Hannu T Sipilä, Nina Savisto, Riitta Parkkola, and Pirjo Nuutila. 2016. 'Human brown adipose tissue [15O] O2 PET imaging in the presence and absence of cold stimulus', *European Journal of Nuclear Medicine and Molecular Imaging*, 43: 1878-86.

Raji, Cyrus A, April J Ho, Neelroop N Parikshak, James T Becker, Oscar L Lopez, Lewis H Kuller, Xue Hua, Alex D Leow, Arthur W Toga, and Paul M Thompson. 2010. 'Brain structure and obesity', *Human brain mapping*, 31: 353-64.

Reaven, Gerald M. 1988. 'Role of insulin resistance in human disease', *Diabetes*, 37: 1595-607.

Reaven, Gerald M, Clarie Hollenbeck, Chii-Yang Jeng, Min Shung Wu, and Yii-Der Ida Chen. 1988. 'Measurement of plasma glucose, free fatty acid, lactate, and insulin for 24 h in patients with NIDDM', *Diabetes*, 37: 1020-24.

Reid, Michael A., Annamarie E. Allen, Shiyu Liu, Maria V. Liberti, Pei Liu, Xiaojing Liu, Ziwei Dai, Xia Gao, Qian Wang, Ying Liu, Luhua Lai, and Jason W. Locasale. 2018. 'Serine synthesis through PHGDH coordinates nucleotide levels by maintaining central carbon metabolism', *Nature Communications*, 9: 5442.

Reilly, John J, and Joanna Kelly. 2011. 'Long-term impact of overweight and obesity in childhood and adolescence on morbidity and premature mortality in adulthood: systematic review', *International Journal of Obesity*, 35: 891-98.

Reinert, Kaela RS, Eli K Po'e, and Shari L Barkin. 2013. 'The relationship between executive function and obesity in children and adolescents: a systematic literature review', *Journal of obesity*, 2013.

Rémond, Didier, Danit R Shahar, Doreen Gille, Paula Pinto, Josefa Kachal, Marie-Agnès Peyron, Claudia Nunes Dos Santos, Barbara Walther, Alessandra Bordoni, and Didier Dupont. 2015. 'Understanding the gastrointestinal tract of the elderly to develop dietary solutions that prevent malnutrition', *Oncotarget*, 6: 13858.

Révész, Dóra, Yuri Milaneschi, Josine E. Verhoeven, Jue Lin, and Brenda W. J. H. Penninx. 2015. 'Longitudinal Associations Between Metabolic Syndrome Components and Telomere Shortening', *The Journal of Clinical Endocrinology & Metabolism*, 100: 3050-59.

Reynisdottir, Signy, Michèle Dauzats, Anders Thörne, and Dominique Langin. 1997. 'Comparison of hormone-sensitive lipase activity in visceral and subcutaneous human adipose tissue', *The Journal of Clinical Endocrinology & Metabolism*, 82: 4162-66.

Ridaura, Vanessa K., Jeremiah J. Faith, Federico E. Rey, Jiye Cheng, Alexis E. Duncan, Andrew L. Kau, Nicholas W. Griffin, Vincent Lombard, Bernard Henrissat, James R. Bain, Michael J. Muehlbauer, Olga Ilkayeva, Clay F. Semenkovich, Katsuhiko Funai, David K. Hayashi, Barbara J. Lyle, Margaret C. Martini, Luke K. Ursell, Jose C. Clemente, William Van Treuren, William A. Walters, Rob Knight, Christopher B. Newgard, Andrew C. Heath, and Jeffrey I. Gordon. 2013. 'Gut Microbiota from Twins Discordant for Obesity Modulate Metabolism in Mice', *Science*, 341: 1241214.

Roden, Michael, Thomas B Price, Gianluca Perseghin, Kitt Falk Petersen, Douglas L Rothman, Gary W Cline, and Gerald I Shulman. 1996. 'Mechanism of free fatty acid-induced insulin resistance in humans', *The Journal of Clinical Investigation*, 97: 2859-65.

Roepstorff, C, J Wulff Helge, B Vistisen, and B Kiens. 2004. 'Studies of plasma membrane fatty acid-binding protein and other lipid-binding proteins in human skeletal muscle', *Proceedings of the Nutrition Society*, 63: 239-44.

Roglic, Gojka. 2016. 'WHO Global report on diabetes: A summary', *International Journal of Noncommunicable Diseases*, 1: 3.

Rokholm, Benjamin, Jennifer Lyn Baker, and Thorkild Ingvor A Sørensen. 2010. 'The levelling off of the obesity epidemic since the year 1999–a review of evidence and perspectives', *Obesity Reviews*, 11: 835-46.

Rolls, Barbara J. 2003. 'The Supersizing of America: Portion Size and the Obesity Epidemic', *Nutrition Today*, 38: 42-53.

Rosen, Evan D, Pasha Sarraf, Amy E Troy, Gary Bradwin, Kathryn Moore, David S Milstone, Bruce M Spiegelman, and Richard M Mortensen. 1999. 'PPARγ is required for the differentiation of adipose tissue in vivo and in vitro', *Molecular cell*, 4: 611-17.

Rosen, Evan D, and Bruce M Spiegelman. 2006. 'Adipocytes as regulators of energy balance and glucose homeostasis', *Nature*, 444: 847-53.

Rosen, Howard. 2014. 'Is obesity a disease or a behavior abnormality? Did the AMA get it right?', *Missouri medicine*, 111: 104.

Ruderman, Neil B, Stephen H Schneider, and Peter Berchtold. 1981. 'The "metabolically-obese," normal-weight individual', *The American Journal of Clinical Nutrition*, 34: 1617-21.

Ruderman, Neil, Donald Chisholm, Xavier Pi-Sunyer, and Stephen Schneider. 1998. 'The metabolically obese, normal-weight individual revisited', *Diabetes*, 47: 699-713.

Rudolph, Karl Lenhard, Sandy Chang, Han-Woong Lee, Maria Blasco, Geoffrey J Gottlieb, Carol Greider, and Ronald A DePinho. 1999. 'Longevity, stress response, and cancer in aging telomerase-deficient mice', *Cell*, 96: 701-12.

Ryo, Miwa, Tadashi Nakamura, Shinji Kihara, Masahiro Kumada, Satomi Shibazaki, Mihoko Takahashi, Masaki Nagai, Yuji Matsuzawa, and Tohru Funahashi. 2004. 'Adiponectin as a biomarker of the metabolic syndrome', *Circulation journal*, 68: 975-81.

Saito, Masayuki, Mami Matsushita, Takeshi Yoneshiro, and Yuko Okamatsu-Ogura. 2020. 'Brown Adipose Tissue, Diet-Induced Thermogenesis, and Thermogenic Food Ingredients: From Mice to Men', *Frontiers in Endocrinology*, 11.

Saito, Masayuki, Yuko Okamatsu-Ogura, Mami Matsushita, Kumiko Watanabe, Takeshi Yoneshiro, Junko Nio-Kobayashi, Toshihiko Iwanaga, Masao Miyagawa, Toshimitsu Kameya, and Kunihiro Nakada. 2009. 'High incidence of metabolically active brown adipose tissue in healthy adult humans: effects of cold exposure and adiposity', *Diabetes*, 58: 1526-31.

Samper, Enrique, Juana M Flores, and María A Blasco. 2001. 'Restoration of telomerase activity rescues chromosomal instability and premature aging in Terc−/− mice with short telomeres', *EMBO reports*, 2: 800-07.

Santomauro, AT, Guenther Boden, ME Silva, Dalva M Rocha, Rosa F Santos, MJ Ursich, Paula G Strassmann, and Bernardo L Wajchenberg. 1999. 'Overnight lowering of free fatty acids with Acipimox improves insulin resistance and glucose tolerance in obese diabetic and nondiabetic subjects', *Diabetes*, 48: 1836-41.

Saretzki, Gabriele. 2018. 'Telomeres, telomerase and ageing', *Biochemistry and Cell Biology of Ageing: Part I Biomedical Science*: 221-308.

Sasabe, Jumpei, and Masataka Suzuki. 2018. 'Distinctive roles of d-amino acids in the homochiral world: chirality of amino acids modulates mammalian physiology and pathology', *The Keio journal of medicine*.

Schoettl, Theresa, Ingrid P Fischer, and Siegfried Ussar. 2018. 'Heterogeneity of adipose tissue in development and metabolic function', *Journal of Experimental Biology*, 221: jeb162958.

Schwartz, Gary J, Jin Fu, Giuseppe Astarita, Xiaosong Li, Silvana Gaetani, Patrizia Campolongo, Vincenzo Cuomo, and Daniele Piomelli. 2008. 'The lipid messenger OEA links dietary fat intake to satiety', *Cell Metabolism*, 8: 281-88.

Shai, Iris, Rui Jiang, JoAnn E. Manson, Meir J. Stampfer, Walter C. Willett, Graham A. Colditz, and Frank B. Hu. 2006. 'Ethnicity, Obesity, and Risk of Type 2 Diabetes in Women: A 20-year follow-up study', *Diabetes Care*, 29: 1585-90.

Sharma, Shaligram, Taylor Dixon, Sean Jung, Emily C Graff, Laura A Forney, Thomas W Gettys, and Desiree Wanders. 2019. 'Dietary methionine restriction reduces inflammation independent of FGF21 action', *Obesity*, 27: 1305-13.

Siersbæk, Rasmus, Ronni Nielsen, and Susanne Mandrup. 2010. 'PPARγ in adipocyte differentiation and metabolism – Novel insights from genome-wide studies', *FEBS Letters*, 584: 3242-49.

Silventoinen, K., B. Rokholm, J. Kaprio, and T. I. A. Sørensen. 2010. 'The genetic and environmental influences on childhood obesity: a systematic review of twin and adoption studies', *International Journal of Obesity*, 34: 29-40.

Snehalatha, Chamukuttan, Bheekamchand Mukesh, Mary Simon, Vijay Viswanathan, Steven M Haffner, and Ambady Ramachandran. 2003. 'Plasma adiponectin is an independent predictor of type 2 diabetes in Asian Indians', *Diabetes Care*, 26: 3226-29.

Spiegel, Karine, Esra Tasali, Plamen Penev, and Eve Van Cauter. 2004. 'Brief communication: sleep curtailment in healthy young men is associated with decreased leptin levels, elevated ghrelin levels, and increased hunger and appetite', *Annals of internal medicine*, 141: 846-50.

Spring, Shelby, Arashdeep Singh, Rizaldy C Zapata, Prasanth K Chelikani, and Adel Pezeshki. 2019. 'Methionine restriction partly recapitulates the sympathetically mediated enhanced energy expenditure induced by total amino acid restriction in rats', *Nutrients*, 11: 707.

St-Onge, Marie-Pierre. 2005. 'Relationship between body composition changes and changes in physical function and metabolic risk factors in aging', *Current Opinion in Clinical Nutrition & Metabolic Care*, 8: 523-28.

St-Onge, Marie-Pierre, and Dympna Gallagher. 2010. 'Body composition changes with aging: the cause or the result of alterations in metabolic rate and macronutrient oxidation?', *Nutrition*, 26: 152-55.

Stahl, Andreas, David J Hirsch, Ruth E Gimeno, Sandhya Punreddy, Pei Ge, Nicki Watson, Shraddha Patel, Mariana Kotler, Alejandra Raimondi, and Louis A Tartaglia. 1999. 'Identification of the major intestinal fatty acid transport protein', *Molecular cell*, 4: 299-308.

Stamler, Rose, Jeremiah Stamler, Wallace F Riedlinger, George Algera, and Richard H Roberts. 1978. 'Weight and blood pressure: findings in hypertension screening of 1 million Americans', *Jama*, 240: 1607-10.

Stefan, Norbert, Konstantinos Kantartzis, Jürgen Machann, Fritz Schick, Claus Thamer, Kilian Rittig, Bernd Balletshofer, Fausto Machicao, Andreas Fritsche, and Hans-Ulrich Häring. 2008. 'Identification and characterization of metabolically benign obesity in humans', *Archives of internal medicine*, 168: 1609-16.

Stenkula, Karin G, and Charlotte Erlanson-Albertsson. 2018. 'Adipose cell size: importance in health and disease', *American journal of Physiology-Regulatory, integrative and comparative Physiology*, 315: R284-R95.

Study, Florey Adelaide Male Aging. 2008. 'Lifestyle factors associated with age-related differences in body composition: the Florey Adelaide Male Aging Study', *The American Journal of Clinical Nutrition*, 88: 95-104.

Stunkard, Albert J, Thorkild IA Sørensen, Craig Hanis, Thomas W Teasdale, Ranajit Chakraborty, William J Schull, and Fini Schulsinger. 1986. 'An adoption study of human obesity', *New England Journal of Medicine*, 314: 193-98.

Stunkard, Albert J., Jennifer R. Harris, Nancy L. Pedersen, and Gerald E. McClearn. 1990. 'The Body-Mass Index of Twins Who Have Been Reared Apart', *New England Journal of Medicine*, 322: 1483-87.

Suwandhi, Lisa, Irem Altun, Ruth Karlina, Viktorian Miok, Tobias Wiedemann, David Fischer, Thomas Walzthoeni, Christina Lindner, Anika Böttcher, and Silke S Heinzmann. 2021. 'Asc-1 regulates white versus beige adipocyte fate in a subcutaneous stromal cell population', *Nature Communications*, 12: 1-12.

Suwandhi, Lisa, Simone Hausmann, Alexander Braun, Tim Gruber, Silke S Heinzmann, Eric JC Gálvez, Achim Buck, Beata Legutko, Andreas Israel, and Annette Feuchtinger. 2018. 'Chronic d-serine supplementation impairs insulin secretion', *Molecular metabolism*, 16: 191-202.

Tak, Young Jin, and Sang Yeoup Lee. 2021. 'Long-term efficacy and safety of anti-obesity treatment: where do we stand?', *Current obesity reports*, 10: 14-30.

Takano, Mayuko, Rieko Nishihara, Naoyuki Sugano, Kazuma Matsumoto, Yutaka Yamada, Masatoshi Takane, Yoshiaki Fujisaki, and Koichi Ito. 2010. 'The effect of systemic anti-tumor necrosis factor-alpha treatment on Porphyromonas gingivalis infection in type 2 diabetic mice', *Archives of Oral Biology*, 55: 379-84.

Tam, Bjorn T, Jose A Morais, and Sylvia Santosa. 2020. 'Obesity and ageing: Two sides of the same coin', *Obesity Reviews*, 21: e12991.

Thaker, Vidhu V. 2017. 'Genetic and epigenetic causes of obesity', *Adolescent medicine: state of the art reviews*, 28: 379.

Thon, Mina, Toru Hosoi, and Koichiro Ozawa. 2016. 'Possible integrative actions of leptin and insulin signaling in the hypothalamus targeting energy homeostasis', *Frontiers in Endocrinology*, 7: 138.

Thyagarajan, Baskaran, and Michelle T Foster. 2017. 'Beiging of white adipose tissue as a therapeutic strategy for weight loss in humans', *Hormone molecular biology and clinical investigation*, 31.

Tobi, Elmar W, LH Lumey, Rudolf P Talens, Dennis Kremer, Hein Putter, Aryeh D Stein, P Eline Slagboom, and Bastiaan T Heijmans. 2009. 'DNA methylation differences after exposure to prenatal famine are common and timing-and sex-specific', *Human molecular genetics*, 18: 4046-53.

Tramunt, Blandine, Sarra Smati, Naia Grandgeorge, Françoise Lenfant, Jean-François Arnal, Alexandra Montagner, and Pierre Gourdy. 2020. 'Sex differences in metabolic regulation and diabetes susceptibility', *Diabetologia*, 63: 453-61.

Tremmel, Maximilian, Ulf-G Gerdtham, Peter M Nilsson, and Sanjib Saha. 2017. 'Economic burden of obesity: a systematic literature review', *International journal of environmental research and public health*, 14: 435.

Tsien, Joe Z, Patricio T Huerta, and Susumu Tonegawa. 1996. 'The essential role of hippocampal CA1 NMDA receptor–dependent synaptic plasticity in spatial memory', *Cell*, 87: 1327-38.

Turnbaugh, Peter J., Ruth E. Ley, Michael A. Mahowald, Vincent Magrini, Elaine R. Mardis, and Jeffrey I. Gordon. 2006. 'An obesity-associated gut microbiome with increased capacity for energy harvest', *Nature*, 444: 1027-31.

Turner, Kara J, Vimal Vasu, and Darren K Griffin. 2019. 'Telomere biology and human phenotype', *Cells*, 8: 73.

Ussar, Siegfried, Kevin Y Lee, Simon N Dankel, Jeremie Boucher, Max-Felix Haering, Andre Kleinridders, Thomas Thomou, Ruidan Xue, Yazmin Macotela, and Aaron M Cypess. 2014. 'ASC-1, PAT2, and P2RX5 are cell surface markers for white, beige, and brown adipocytes', *Science translational medicine*, 6: 247ra103-247ra103.

Vainio, Harri, and Franca Bianchini. 2002. *Weight control and physical activity* (Iarc).

Valdes, Ann M, Toby Andrew, Jeffery P Gardner, Masayuki Kimura, E Oelsner, Lynn F Cherkas, Abraham Aviv, and Tim D Spector. 2005. 'Obesity, cigarette smoking, and telomere length in women', *The lancet*, 366: 662-64.

van der Lans, Anouk AJJ, Joris Hoeks, Boudewijn Brans, Guy HEJ Vijgen, Mariëlle GW Visser, Maarten J Vosselman, Jan Hansen, Johanna A Jörgensen, Jun Wu, and Felix M Mottaghy. 2013. 'Cold

acclimation recruits human brown fat and increases nonshivering thermogenesis', *The Journal of Clinical Investigation*, 123: 3395-403.

van Marken Lichtenbelt, Wouter D, Joost W Vanhommerig, Nanda M Smulders, Jamie MAFL Drossaerts, Gerrit J Kemerink, Nicole D Bouvy, Patrick Schrauwen, and GJ Jaap Teule. 2009. 'Cold-activated brown adipose tissue in healthy men', *New England Journal of Medicine*, 360: 1500-08.

Vangipurapu, Jagadish, Alena Stancáková, Ulf Smith, Johanna Kuusisto, and Markku Laakso. 2019. 'Nine amino acids are associated with decreased insulin secretion and elevated glucose levels in a 7.4-year follow-up study of 5,181 Finnish men', *Diabetes*, 68: 1353-58.

Vijg, Jan, and Judith Campisi. 2008. 'Puzzles, promises and a cure for ageing', *Nature*, 454: 1065-71.

Vijgen, Guy HEJ, Nicole D Bouvy, GJ Jaap Teule, Boudewijn Brans, Patrick Schrauwen, and Wouter D van Marken Lichtenbelt. 2011. 'Brown adipose tissue in morbidly obese subjects', *PloS one*, 6: e17247.

Virtanen, Kirsi A, Martin E Lidell, Janne Orava, Mikael Heglind, Rickard Westergren, Tarja Niemi, Markku Taittonen, Jukka Laine, Nina-Johanna Savisto, and Sven Enerbäck. 2009. 'Functional brown adipose tissue in healthy adults', *New England Journal of Medicine*, 360: 1518-25.

Vitali, A, I Murano, MC Zingaretti, A Frontini, D Ricquier, and S Cinti. 2012. 'The adipose organ of obesity-prone C57BL/6J mice is composed of mixed white and brown adipocytes', *Journal of lipid research*, 53: 619-29.

vom Steeg, Landon G, and Sabra L Klein. 2016. 'SeXX matters in infectious disease pathogenesis', *PLoS pathogens*, 12: e1005374.

Vosselman, Maarten J, Wouter D van Marken Lichtenbelt, and Patrick Schrauwen. 2013. 'Energy dissipation in brown adipose tissue: from mice to men', *Molecular and cellular endocrinology*, 379: 43-50.

Wajchenberg, Bernardo Leo. 2000. 'Subcutaneous and visceral adipose tissue: their relation to the metabolic syndrome', *Endocrine reviews*, 21: 697-738.

Wang, Jianfei, Xu Dong, Li Cao, Yangyang Sun, Yu Qiu, Yi Zhang, Ruoqiong Cao, Mihai Covasa, and Li Zhong. 2016. 'Association between telomere length and diabetes mellitus: A meta-analysis', *Journal of International Medical Research*, 44: 1156-73.

Wang, Thomas J, Martin G Larson, Ramachandran S Vasan, Susan Cheng, Eugene P Rhee, Elizabeth McCabe, Gregory D Lewis, Caroline S Fox, Paul F Jacques, and Céline Fernandez. 2011. 'Metabolite profiles and the risk of developing diabetes', *Nature medicine*, 17: 448-53.

Wen, Chi Pang, Ting Yuan David Cheng, Shan Pou Tsai, Hui Ting Chan, Hui Ling Hsu, Chih Cheng Hsu, and Michael P. Eriksen. 2009. 'Are Asians at greater mortality risks for being overweight than Caucasians? Redefining obesity for Asians', *Public Health Nutrition*, 12: 497-506.

Whittle, Andrew J, Stefania Carobbio, Luís Martins, Marc Slawik, Elayne Hondares, María Jesús Vázquez, Donald Morgan, Robert I Csikasz, Rosalía Gallego, and Sergio Rodriguez-Cuenca. 2012. 'BMP8B increases brown adipose tissue thermogenesis through both central and peripheral actions', *Cell*, 149: 871-85.

WHO. 2021. 'Obesity and overweight', Accessed August 25, 2022. https://www.who.int/news-room/fact-sheets/detail/obesity-and-overweight.

Wijers, Sander LJ, Wim HM Saris, and Wouter D van Marken Lichtenbelt. 2010. 'Cold-induced adaptive thermogenesis in lean and obese', *Obesity*, 18: 1092-99.

Winkler, Gábor, Sándor Kiss, László Keszthelyi, Zoltán Sápi, Iván Ory, Ferenc Salamon, Margit Kovács, Péter Vargha, Orsolya Szekeres, and Gábor Speer. 2003. 'Expression of tumor necrosis factor (TNF)-a protein in the subcutaneous and visceral adipose tissue in correlation with adipocyte cell volume, serum TNF-a, soluble serum TNF-receptor-2 concentrations and C-peptide level', *Eur J Endocrinol*, 149: 129-35.

Wolin, Kathleen Y., Kenneth Carson, and Graham A. Colditz. 2010. 'Obesity and Cancer', *The Oncologist*, 15: 556-65.

Wolosker, Herman, Seth Blackshaw, and Solomon H Snyder. 1999. 'Serine racemase: a glial enzyme synthesizing D serine to regulate glutamate N methyl D aspartate neurotransmission', *Proceedings of the National Academy of Sciences*, 96: 13409-14.

Wolosker, Herman, and Hisashi Mori. 2012. 'Serine racemase: an unconventional enzyme for an unconventional transmitter', *Amino acids*, 43: 1895-904.

Wolosker, Herman, Kevin N Sheth, Masaaki Takahashi, Jean-Pierre Mothet, Roscoe O Brady Jr, Christopher D Ferris, and Solomon H Snyder. 1999. 'Purification of serine racemase: biosynthesis of the neuromodulator D-serine', *Proceedings of the National Academy of Sciences*, 96: 721-25.

Wright, Suzanne M., and Louis J. Aronne. 2012. 'Causes of obesity', *Abdominal Radiology*, 37: 730-32.

Wu, Guoqing, Yanan Wang, Yuhui Yang, Yonghui Shi, Jin Sun, Yunchong Xu, Tingyu Luo, and Guowei Le. 2019. 'Dietary Methionine Restriction Upregulates Endogenous H2S via miR-328-3p: A Potential Mechanism to Improve Liver Protein Metabolism Efficiency in a Mouse Model of High-fat-diet-induced Obesity', *Molecular nutrition & food research*, 63: 1800735.

Wu, Guoyao. 2009. 'Amino acids: metabolism, functions, and nutrition', *Amino acids*, 37: 1-17.

Wu, Jun, Paul Cohen, and Bruce M Spiegelman. 2013. 'Adaptive thermogenesis in adipocytes: is beige the new brown?', *Genes & development*, 27: 234-50.

Wu, Zhidan, Evan D Rosen, Regina Brun, Stefanie Hauser, Guillaume Adelmant, Amy E Troy, Catherine McKeon, Gretchen J Darlington, and Bruce M Spiegelman. 1999. 'Cross-regulation of C/EBPα and PPARγ controls the transcriptional pathway of adipogenesis and insulin sensitivity', *Molecular cell*, 3: 151-58.

Xu, Yu, Limin Wang, Jiang He, Yufang Bi, Mian Li, Tiange Wang, Linhong Wang, Yong Jiang, Meng Dai, and Jieli Lu. 2013. 'Prevalence and control of diabetes in Chinese adults', *Jama*, 310: 948-59.

Xu, Yuncong, Yuhui Yang, Jin Sun, Yuanyuan Zhang, Tingyu Luo, Bowen Li, Yuge Jiang, Yonghui Shi, and Guowei Le. 2019. 'Dietary methionine restriction ameliorates the impairment of learning and memory function induced by obesity in mice', *Food & function*, 10: 1411-25.

Yamamoto, Yukihiro, Hiroshi Hirose, Ikuo Saito, Kanako Nishikai, and Takao Saruta. 2004. 'Adiponectin, an adipocyte-derived protein, predicts future insulin resistance: two-year follow-up study in Japanese population', *The Journal of Clinical Endocrinology & Metabolism*, 89: 87-90.

Yazdani-Biuki, B, H Stelzl, HP Brezinschek, J Hermann, T Mueller, P Krippl, W Graninger, and TC Wascher. 2004. 'Improvement of insulin sensitivity in insulin resistant subjects during prolonged treatment with the anti-TNF-alpha antibody infliximab', *European journal of clinical investigation*, 34: 641-42.

Yoneshiro, Takeshi, Sayuri Aita, Mami Matsushita, Takashi Kayahara, Toshimitsu Kameya, Yuko Kawai, Toshihiko Iwanaga, and Masayuki Saito. 2013. 'Recruited brown adipose tissue as an antiobesity agent in humans', *The Journal of Clinical Investigation*, 123: 3404-08.

Yoneshiro, Takeshi, Sayuri Aita, Mami Matsushita, Yuko Okamatsu-Ogura, Toshimitsu Kameya, Yuko Kawai, Masao Miyagawa, Masayuki Tsujisaki, and Masayuki Saito. 2011. 'Age-related decrease in cold-activated brown adipose tissue and accumulation of body fat in healthy humans', *Obesity*, 19: 1755-60.

Young, James B., Elizabeth Saville, Nancy J. Rothwell, Michael J. Stock, and Lewis Landsberg. 1982. 'Effect of Diet and Cold Exposure on Norepinephrine Turnover in Brown Adipose Tissue of the Rat', *The Journal of Clinical Investigation*, 69: 1061-71.

Young, Katherine M, Clive M Gray, and Linda-Gail Bekker. 2013. 'Is obesity a risk factor for vaccine non-responsiveness?', *PloS one*, 8: e82779.

Yu, Junjie, Fei Xiao, Yajie Guo, Jiali Deng, Bin Liu, Qian Zhang, Kai Li, Chunxia Wang, Shanghai Chen, and Feifan Guo. 2014. 'Hepatic Phosphoserine Aminotransferase 1 Regulates Insulin Sensitivity in Mice via Tribbles Homolog 3', *Diabetes*, 64: 1591-602.

Zhang, Qiongyi, Muhammad Khairul Ramlee, Reinhard Brunmeir, Claudio J Villanueva, Daniel Halperin, and Feng Xu. 2012. 'Dynamic and distinct histone modifications modulate the expression of key adipogenesis regulatory genes', *Cell cycle*, 11: 4310-22.

Zhang, Qiongyue, Hongying Ye, Qing Miao, Zhaoyun Zhang, Yi Wang, Xiaoming Zhu, Shuo Zhang, Chuantao Zuo, Zhengwei Zhang, and Zhemin Huang. 2013. 'Differences in the metabolic status of healthy adults with and without active brown adipose tissue', *Wiener klinische Wochenschrift*, 125: 687-95.

Zheng, Yan, Yanping Li, Qibin Qi, Adela Hruby, JoAnn E Manson, Walter C Willett, Brian M Wolpin, Frank B Hu, and Lu Qi. 2016. 'Cumulative consumption of branched-chain amino acids and incidence of type 2 diabetes', *International journal of epidemiology*, 45: 1482-92.

Ziegler, Thomas R., Concepción Fernández-Estívariz, Li H. Gu, Michael W. Fried, and Lorraine M. Leader. 2003. 'Severe villus atrophy and chronic malabsorption induced by azathioprine', *Gastroenterology*, 124: 1950-57.

Zingaretti, Maria Cristina, Francesca Crosta, Alessandra Vitali, Mario Guerrieri, Andrea Frontini, Barbara Cannon, Jan Nedergaard, and Saverio Cinti. 2009. 'The presence of UCP1 demonstrates that metabolically active adipose tissue in the neck of adult humans truly represents brown adipose tissue', *The FASEB Journal*, 23: 3113-20.

Zoico, Elena, Sofia Rubele, Annamaria De Caro, Nicole Nori, Gloria Mazzali, Francesco Fantin, Andrea Rossi, and Mauro Zamboni. 2019. 'Brown and beige adipose tissue and aging', *Frontiers in Endocrinology*, 10: 368.

Acknowledgements

First of all I would like to thank God, the creator of everything, for giving me the health and energy to do my PhD and for making this way possible for me.

I would like to thank my family for supporting me all these years

I would like to thank Dr. Siegfried Ussar for giving me this opportunity to do my PhD in his lab and for supporting and guiding me all these years.

I would like to thank all members of the Ussar group especially Dr. Yasuhiro Onogi, Dr. Rene Hernandez-Bautista and Andreas Israel for teaching and helping me during my PhD. I would also like to thank Xue Liu for letting me work with her on one of her projects and helping me with it.

I would like to thank all members of the institute of Diabetes and Obesity for creating a great scientific atmosphere.

Publications and presentations

Publications:

Onogi, Yasuhiro*, **Ahmed Elagamy Mohamed Mahmoud Khalil***, and Siegfried Ussar. "Identification and characterization of adipose surface epitopes." *Biochemical Journal* 477, no. 13 (2020): 2509-2541.

Suwandhi, Lisa, Irem Altun, Ruth Karlina, Viktorian Miok, Tobias Wiedemann, David Fischer, Thomas Walzthoeni, **Ahmed Elagamy Mohamed Mahmoud Khalil** et al. "Asc-1 regulates white versus beige adipocyte fate in a subcutaneous stromal cell population." *Nature communications* 12, no. 1 (2021): 1-12.

López-Gonzales, Elena, Lisa Lehmann, Francisco Javier Ruiz-Ojeda, René Hernández-Bautista, Irem Altun, Yasuhiro Onogi, **Ahmed Elagamy Khalil**, Xue Liu, Andreas Israel, and Siegfried Ussar. "L-Serine Supplementation Blunts Fasting-Induced Weight Regain by Increasing Brown Fat Thermogenesis." *Nutrients* 14, no. 9 (2022): 1922.

*Equal contribution

Poster presentation and conference publication:

Ahmed Elagamy Khalil, Xue Liu and Siegfried Ussar “Telomere shortening improves insulin sensitivity in mice” Zoomforward 22 Congress on Obesity, Maastricht, Netherlands, May 4-7, 2022

Ahmed Elagamy Khalil, Xue Liu and Siegfried Ussar “Telomere shortening improves insulin sensitivity in mice” Avcilar T: Late-Breaking Abstracts for ECO2022. Obes Facts 2022;15(suppl 1):241-286. doi: 10.1159/000524649